[Papers in Palaeontology, Vol. 10, Part 6, 2024, e1604]

Theropod dinosaur diversity of the lower English Wealden: analysis of a tooth-based fauna from the Wadhurst Clay Formation (Lower Cretaceous: Valanginian) via phylogenetic, discriminant and machine learning methods

by CHRIS T. BARKER[1,2,*], LUCY HANDFORD[3], DARREN NAISH[2], SIMON WILLS[4], CHRISTOPHE HENDRICKX[5], PHIL HADLAND[6], DAVE BROCKHURST[7] *and* NEIL J. GOSTLING[1,2,*]

[1]Institute for Life Sciences, University of Southampton, Southampton, UK; ctb1g14@soton.ac.uk, n.j.gostling@soton.ac.uk
[2]School of Biological Sciences, Faculty of Environment and Life Sciences, University of Southampton, Southampton, UK
[3]Department of Archaeology, University of York, York, UK
[4]Fossil Reptiles, Amphibians and Birds Section, Natural History Museum, Cromwell Road, South Kensington, London, UK
[5]Unidad Ejecutora Lillo, CONICET-Fundación Miguel Lillo, Miguel Lillo 251, San Miguel de Tucumán 4000, Tucumán, Argentina
[6]Hastings Museum and Art Gallery, Hastings, UK
[7]8 Crowmere Avenue, Bexhill-on-Sea, East Sussex TN40 2BA, UK
*Corresponding authors

Typescript received 17 June 2024; accepted in revised form 15 October 2024

Abstract: The Lower Cretaceous Wealden Supergroup of southern England yields a diverse assemblage of theropod dinosaurs, its taxa being represented by fragments in addition to some of the most informative associated skeletons of the European Mesozoic. Spinosaurids, neovenatorid allosauroids, tyrannosauroids and dromaeosaurids are among reported Wealden Supergroup clades. However, the majority of relevant specimens are from the Barremian Upper Weald Clay and Wessex formations, and theropod diversity in the older Berriasian–Valanginian Hastings Group has remained poorly known, the fragmentary specimens reported thus far remaining enigmatic both in terms of phylogenetic affinities and sometimes provenance. A better understanding would be welcome given the paucity of Berriasian–Valanginian dinosaurs worldwide. Here, we describe an assemblage of Hastings Group theropod teeth from the Valanginian Wadhurst Clay Formation, mostly collected from the Ashdown Brickworks locality near Bexhill, East Sussex. These teeth were assessed using phylogenetic, discriminant and machine learning analyses and were found to include members of Spinosauridae, Tyrannosauroidea and Dromaeosauridae, in addition to others that remain of uncertain affinity within Coelurosauria. The taxa appear distinct from those already known from Wealden Supergroup strata: the spinosaurid cannot be referred to *Baryonyx* or the tyrannosauroid to *Eotyrannus*, for example, but we have not named new taxa at this time. Combined with other findings in the Wadhurst Clay Formation, our study indicates that Valanginian theropod diversity was comparable to that of younger Wealden Supergroup units, implying that the 'characteristic' theropod components of Wealden faunas were established early in the deposition of this famous geological succession.

Key words: theropod, Wealden Supergroup, phylogenetics, machine learning, dinosaur, Cretaceous.

THE fossiliferous Lower Cretaceous (Berriasian–Aptian) Wealden Supergroup of southern England is a rich and globally important source of dinosaur remains (Benton & Spencer 1995; Martill & Naish 2001; Naish & Martill 2007, 2008; Batten 2011a; Lomax & Tamura 2014; Austen & Batten 2018). Strata are deposited in two neighbouring sub-basins (Fig. 1A, B): the Weald sub-basin of England's southeast, which includes the temporally extensive (Berriasian–Aptian) outcrops of the Hastings and Weald Clay groups, and the Wessex sub-basin of southern England, which contains the Wealden Group, the Barremian–lower Aptian strata of which are exposed in Dorset and the Isle of Wight (Hopson *et al.* 2008; Batten 2011b; Radley & Allen 2012a, 2012b).

Several historically notable theropod dinosaurs are known from the Wealden Supergroup but fossils of the clade are generally rare, and our understanding of their diversity across the whole of the succession is patchy (Naish 2011). Few specimens are represented by articulated skeletons, many lack accurate locality or horizon data, and complicated taxonomic histories compound their study (Benton & Spencer 1995; Naish & Martill 2007;

doi: 10.1002/spp2.1604

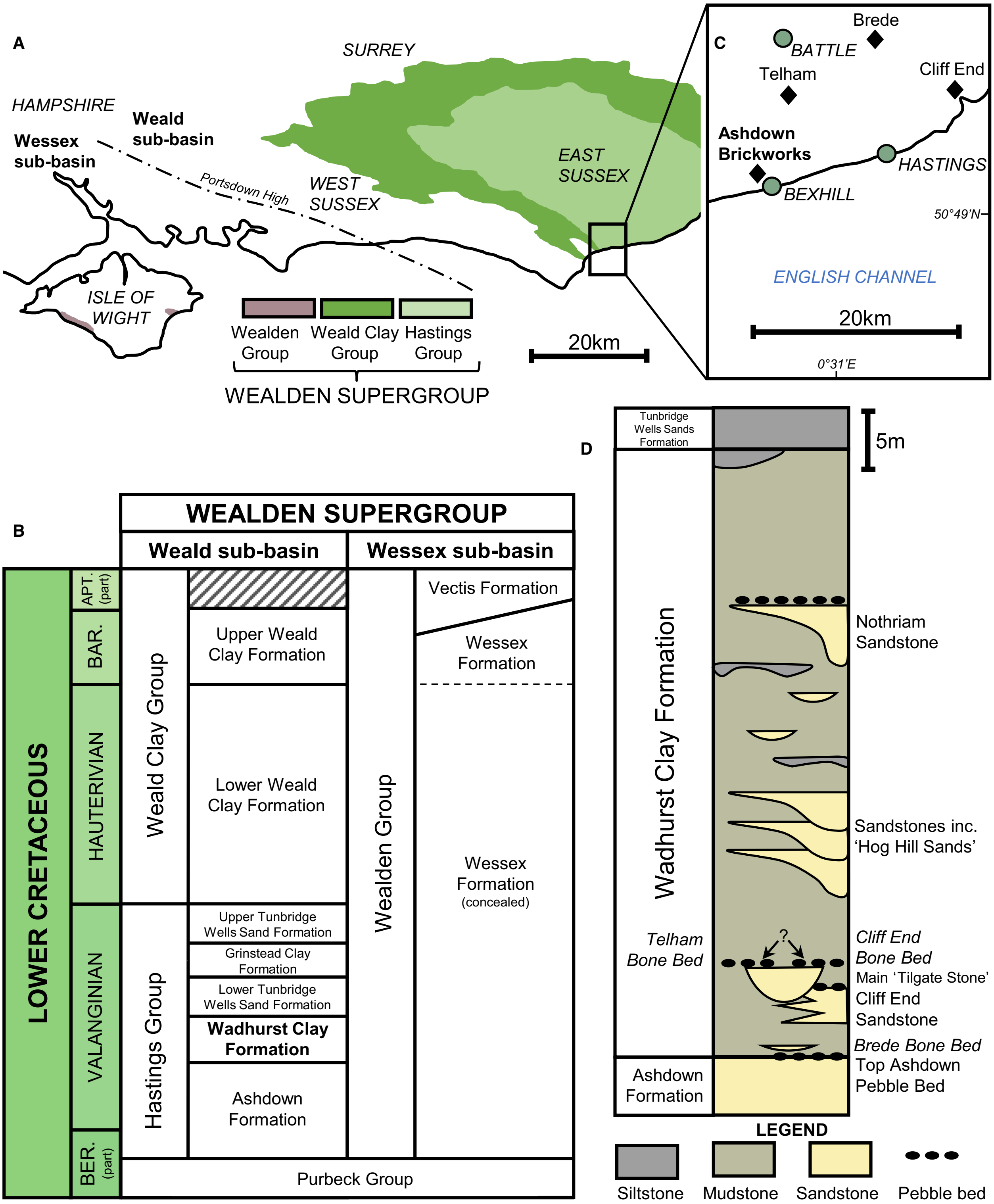

FIG. 1. Simplified geology of the Wealden Supergroup, with emphasis on the Wadhurst Clay Formation. A, schematic map of the Wealden Supergroup outcrop in the Wessex and Weald sub-basins, based on Sweetman (2013). B, simplified stratigraphy of the Wealden Supergroup, based on Batten (2011a) and Austen & Batten (2018). C, location of various sites mentioned in the text, based on Benton & Spencer (1995). D, simplified stratigraphy of the Wadhurst Clay Formation, based on Lake & Shepard-Thorn (1987) and Radley & Allen (2012a).

Naish 2011). Hindering interpretation is that treatments of the topic are either selective in terms of which taxa and material are discussed (Benton & Spencer 1995; Blows 1998): they are typically biased toward the Isle of Wight's Wealden Group (Insole & Hutt 1994; Naish *et al.* 2001; Naish 2011), or were published prior to establishment of the refined stratigraphic terminology now in use (Weishampel *et al.* 2004).

Much of our understanding of Wealden theropods is based on data from the highly fossiliferous Barremian exposures of the Wessex Formation (and to a lesser extent, Vectis Formation) of the Isle of Wight (Naish 2011; Lomax & Tamura 2014). This preserves a tetanuran-dominated fauna including spinosaurids (Martill & Hutt 1996; Barker *et al.* 2021, 2022), allosauroids (Hutt *et al.* 1996; Brusatte *et al.* 2008), and tyrannosauroid (Hutt *et al.* 2001; Naish & Cau 2022) and maniraptoran (Sweetman 2004; Longrich *et al.* 2022) coelurosaurs. Additional taxa of uncertain affinities are also known (Benson *et al.* 2009; Naish 2011).

In comparison, the theropods of the Weald sub-basin are less well understood. Named taxa from the Upper Weald Clay Formation include the iconic spinosaurid *Baryonyx walkeri* of Surrey (Charig & Milner 1986, 1997) and the indeterminate maniraptoran '*Wyleyia valdensis*' of West Sussex (Harrison & Walker 1973), a *nomen dubium* for which the proposed avialan affinities have been disputed (Naish & Martill 2007). Taxa from the older Hastings Group are also enigmatic, and include the possible allosauroid *Altispinax dunkeri*, recovered from an unknown locality near Battle, East Sussex (von Huene 1923; Maisch 2016), and *Valdoraptor oweni* from West Sussex (Lydekker 1889; Olshevsky 1991), a taxon suggested to be of allosauroid (Naish & Martill 2007; Naish 2011), ornithomimosaurian (Allain *et al.* 2014) or indeterminate neotetanuran (Naish 2011) affinities that probably originated from the Grinstead Clay Formation (Valanginian) (Naish 2011). Elsewhere, various isolated teeth and skeletal elements have been referred to the wastebasket taxon '*Megalosaurus dunkeri*' (Lydekker 1888, 1890; Naish 2011; Carrano *et al.* 2012). The affinities of these remains are unclear but they may represent a taxon or taxa related to non-megalosaurid tetanurans from the Lower Cretaceous (Hendrickx *et al.* 2015b) or a non-coelurosaurian tetanuran more specifically (Ősi *et al.* 2010; Naish 2011). The Hastings Group has also yielded teeth referred to '*Suchosaurus cultridens*': these were originally identified as crocodilian (Owen 1840–1845; Buffetaut 2010) but represent a baryonychine-type spinosaurid (Milner 2003; Buffetaut 2007, 2010; Mateus *et al.* 2011; Naish 2011; Carrano *et al.* 2012), the precise phylogenetic position and taxonomy of which is not yet resolved. Further finds of note include indeterminate tetanurans (Naish 1999), allosauroids (Naish 2003) and spinosaurids (Barker *et al.* 2023) from undetermined stratigraphic positions in the Hastings Group, and small maniraptorans from the Wadhurst Clay Formation near Bexhill, East Sussex (e.g. BEXHM 2008.14.1; see below) (Austen *et al.* 2010; Naish & Sweetman 2011).

Isolated theropod teeth, which can be found throughout the Weald sub-basin, are of importance for our understanding of theropod diversity in the absence of more complete remains (Smith *et al.* 2005; Brusatte *et al.* 2007; Hendrickx *et al.* 2015a, 2019, 2020, 2024; Meso *et al.* 2024). However, the accurate referral of isolated teeth to specific clades is often problematic and compounded by issues relating to homoplasy and insufficiently detailed accounts (Currie *et al.* 1990; Smith *et al.* 2005; Hendrickx *et al.* 2015a, 2019, 2024). Nevertheless, recent works have used the morphological variability of theropod teeth to generate comprehensive datasets and methods to aid in their identification (Hendrickx & Mateus 2014; Hendrickx *et al.* 2015b, 2020, 2024; Young *et al.* 2019; Meso *et al.* 2021b, 2024; Wills *et al.* 2021; Juarez *et al.* 2023; Chowchuvech *et al.* 2024; Delcourt *et al.* 2024; Isasmendi *et al.* 2024; Ribeiro *et al.* 2024).

Here, we use phylogenetic, discriminant and machine learning analyses to examine theropod teeth recovered from the Valanginian Wadhurst Clay Formation, a fossiliferous section of the Hastings Group, with particular emphasis on specimens collected from well-documented horizons located in the exposed strata at the Ashdown Brickworks near Bexhill-on-Sea (East Sussex; Fig. 1C). This dental sample is significant because the Valanginian is a poorly sampled interval in global dinosaur evolution, with limited localities largely biased towards western Europe (Weishampel *et al.* 2004; Csiki-Sava *et al.* 2016). Previous reports have suggested the potential presence of allosauroids, *Baryonyx*-like spinosaurids, velociraptorine dromaeosaurids, and specimens of undetermined affinities in the Wadhurst Clay Formation (see below); however, these have yet to be assessed using rigorous analytical techniques. This work aims to explore these previous referrals using the combined approach mentioned above, and to provide an updated interpretation of theropod diversity in the lower, lesser-known units of the Wealden Supergroup.

Institutional abbreviations. BEXHM, Bexhill Museum, Bexhill-on-Sea, UK; HASMG, Hastings Museum and Art Gellery, Hastings, UK; IWCMS, Isle of Wight County Museum Services, Sandown, Isle of Wight, UK; MCNA, Museo de Ciencias Naturales y Antropologicas (J. C. Moyano) de Mendoza, Mendoza, Argentina; NHMUK, Natural History Museum, London, UK; XMDFEC, Xixia Museum of Dinosaur Fossil Eggs of China, Xixia, China.

Terminology abbreviations. ADM, number of denticles per millimetre at the midpoint of the mesial carina; AL, apical length; CA, crown angle; CBL, crown base length; CBR, crown–base ratio; CBW, crown base width; CH, crown height; CHR, crown–height ratio; DAVG, average distal denticle density; DC, distocentral denticle density; DDL, distal denticle length; DHR, distal denticle height ratio; LAF, number of labial flutes; LIF, number of lingual flutes; MCL, mid-crown length; MCR, mid-crown ratio; MCW, mid-crown width; MDH, mesial denticle height; MDL, mesial denticle length; MDW, mesial denticle width; MHR, mesial denticle height ratio; MSL, mesial serrated carina length; PDM, number of denticles per millimetre at the midpoint of the distal carina.

GEOLOGICAL & PALAEONTOLOGICAL CONTEXT

Geological context

The Wadhurst Clay Formation is a fossiliferous Valanginian unit of the Hastings Group (Fig. 1B) and its extensive outcrop comprises both coastal and inland exposures (Fig. 1C) (Gallois & Edmunds 1965; Lake & Shepard-Thorn 1987; Batten & Austen 2011). Vertebrate remains, including a variety of theropod teeth, are relatively common, especially from the poorly sorted, coarse-grained 'bone beds' found throughout the succession (Allen 1949; Lake & Shepard-Thorn 1987). Quarries have also provided a valuable source of fossils from distinguishable Wadhurst Clay horizons (Topley 1875; Batten & Austen 2011; Austen & Batten 2018; Turmine-Juhel *et al.* 2019).

The Wadhurst Clay Formation is predominately mudstone dominated, and its subordinate lithologies include sandstone, siltstone, conglomerate, siderite mudstone and shelly limestone (Fig. 1D) (Lake & Shepard-Thorn 1987; Batten 2011b; Radley & Allen 2012a). These are dated to the early to early late Valanginian and are collectively interpreted as fresh to slightly brackish water lagoonal deposits (Allen 1975; Lake & Shepard-Thorn 1987; Hopson *et al.* 2008; Radley & Allen 2012a). Akinlotan (2015) considered the depositional environment analogous to that of the Niger delta.

The Ashdown Brickworks (TQ 720095) is located northwest of Bexhill, East Sussex (Fig. 1C). Two pits are present at the site: the southerly Crowborough Pit (exposing the Tunbridge Wells Sand Formation) and the northerly Pevensey Pit (with outcrops of the upper Wadhurst Clay Formation capped by the lower part of the Tunbridge Wells Sand Formation). These are separated by the west–east-running Whydown Fault (Austen *et al.* 2010; Naish & Sweetman 2011; Turmine-Juhel *et al.* 2019). The BEXHM specimens analysed herein were recovered from bonebeds in the Wadhurst Clay Formation exposed in the Pevensey Pit.

In the Pevensey Pit, the Wadhurst Clay Formation is locally subdivided into three units (Fig. 2), with a middle sandstone unit known as the Northiam Sandstone (2–3 m) interposed between a pair of upper (*c.* 10 m) and lower (*c.* 30 m) clay layers (Turmine-Juhel *et al.* 2019). These argillaceous units include five discrete bone beds, which are summarized here in ascending order (Austen *et al.* 2010; Naish & Sweetman 2011; Turmine-Juhel *et al.* 2019):

1. The 'Iguanodont Bed': a green clay up to 1 m thick, preserving two ornithopod specimens referred to *Hypselospinus fittoni* by Austen & Austen (2016).
2. The 'Turtle Bed': a 5–30 mm bonebed located 4 m above the Iguanodont Bed and 8–9 m below the base of the Northiam Sandstone, which mainly preserves the remains of turtles, crocodyliforms and fish.
3. The 'Conglomerate Bed': a 50–60-mm-thick bonebed comprising a matrix-supported conglomerate with clasts of clay ironstone and bone fragments (2–40 mm), in a medium-grained mature quartz and grey clay matrix. It lies *c.* 4 m below the base of the Northiam Sandstone and is lithologically similar to the Telham Bonebed described by Allen (1949). It is the main source of fossil material, including a diverse fauna consisting of microvertebrate remains and larger bones. Remains from this conglomeratic bed, as well as those from the Turtle Bed, are invariably polished and can be substantially abraded because of aqueous transport (Naish & Sweetman 2011). An intermittent black band, some 20 mm thick, is located 30–40 cm above the Conglomerate Bed and has produced theropod remains. Immediately above this band is an intermittent 10-cm-thick siltstone that contains pterosaur material.
4. An unnamed bone-bearing horizon, mentioned by Hayward (1996), located 2.3 m above the Northiam Sandstone.
5. The '*Polacanthus* bed': a 45–60-cm-thick unit located 11–12 m above the Northiam Sandstone, from which partial ankylosaur and *Hypselospinus* skeletons have been recovered alongside associated theropod teeth. The ankylosaur was previously referred to *Polacanthus* (Blows & Honeysett 2014) but is best considered an indeterminate nodosaurid (Raven *et al.* 2020). The bed is now largely inaccessible due to plant overgrowth.

Theropod remains from the Wadhurst Clay Formation

The theropod record from the Wadhurst Clay Formation of the Ashdown Brickworks includes isolated teeth

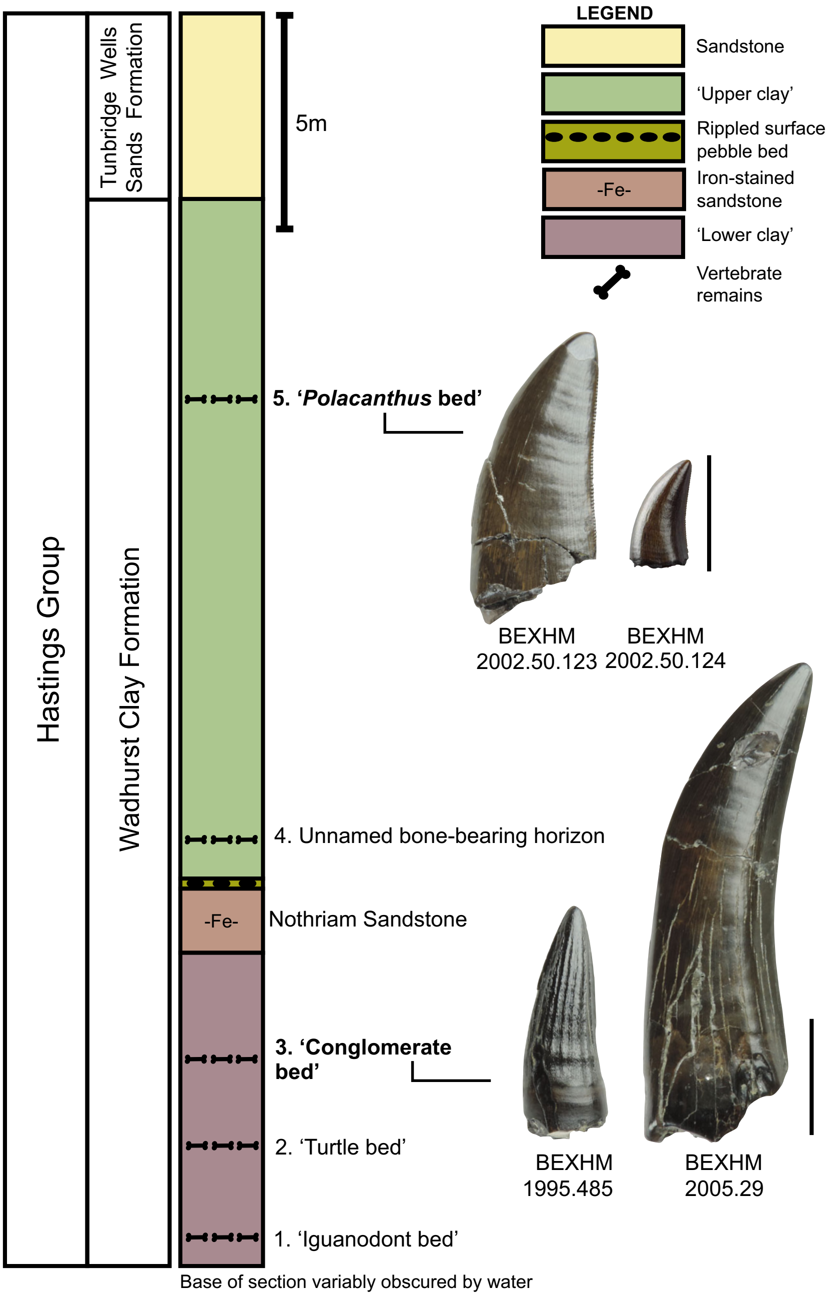

FIG. 2. Lithological log of the Pevensey Pit at Ashdown Brickworks, highlighting the position of the Wadhurst Clay Formation bone-beds and specimens studied herein. Based on Naish & Sweetman (2011) and Turmine-Juhel *et al.* (2019). Scale bars represent 10 mm.

provisionally referred to indeterminate allosauroids (e.g. BEXHM 2002.50.123, 2005.29), dromaeosaurids (e.g. BEXHM 2002.50.124, 2021.146.1–2), indeterminate 'carnosaurs' (BEXHM 2013.9) and the spinosaurid cf. *Baryonyx* (BEXHM 1995.485). Some of these teeth were documented in brief by Charig & Milner (1997), Austen *et al.* (2010) and Naish & Sweetman (2011). Additional teeth referred to *Baryonyx* sp. (BEXHM 2019.49.251, 253) and a possible allosauroid (BEXHM 2019.49.252) were more recently described from this locality (Turmine-Juhel *et al.* 2019). The aforementioned remains of tiny maniraptorans, which show similarities to oviraptorosaurs and avialans, were also found at this locality (Austen *et al.* 2010; Naish & Sweetman 2011), and new material was recently accessioned from the Conglomerate Bed more specifically (BEXHM 2024.23.1–2).

Elsewhere, the Telham Bone Bed (located in the now obscured Black Horse Quarry, near Battle in East Sussex; Fig. 1C) is the most likely source for specimens accessioned under 'Battle' or 'Telham' (Benton & Spencer 1995;

Radley & Allen 2012a). Detrital petrography and stratigraphic context support a correlation between the inland Telham Bone Bed and the coastal Cliff End Bone Bed located east of Hastings (Lake & Shepard-Thorn 1987; Radley & Allen 2012a). The latter is known for its microvertebrate remains, although reptile material is rare (Patterson 1966) and many specimens collected in its vicinity lack good stratigraphic data (Benton & Spencer 1995). Theropod finds from both localities include vertebrae and teeth referred to '*Megalosaurus dunkeri*' and '*Megalosaurus* sp.' (e.g. NHMUK PV R 2846) (Benton & Spencer 1995), while recently discovered teeth with provisional spinosaurid (BEXHM 2023.97.3) and dromaeosaurid (BEXHM 2024.22.3) affinities are likely to have originated from the Cliff End Bone Bed (or the layer immediately above it).

Theropod finds from the Brede Bone Bed (Brede, East Sussex; Fig. 1C) include teeth referred to '*Suchosaurus*' (e.g. NHMUK PV R 4415) (Allen 1949; Benton & Spencer 1995). The bone bed was best accessed at the Hare Farm Lane locality near Brede (Benton & Spencer 1995), but is today overgrown (Radley & Allen 2012a).

Finally, various Wadhurst Clay Formation theropod teeth are located in the Natural History Museum (London), including material referred to '*Suchosaurus*' (e.g. NHHMUK PV R 4414, 4416), the dromaeosaurid *Nuthetes* sp. (e.g. NHMUK PV R 4413), and indeterminate theropods previously referred to '*Megalosaurus dunkeri*' (e.g. NHMUK PV R 37629, 37 630). In keeping with previous comments, the precise stratigraphic origins of these specimens are often unclear.

MATERIAL & METHOD

Material

Five isolated teeth from the Wadhurst Clay Formation were examined first hand: BEXHM 1995.485 (morphotype I), BEXHM 2002.50.123 (morphotype II), BEXHM 2002.50.124 (morphotype III), BEXHM 2005.29 (morphotype IV) and NHMUK PV R37630 (morphotype V) (Fig. 3). All BEXHM specimens were recovered from the Pevensey Pit (Fig. 2).

BEXHM 1995.485 was accessioned as a *Baryonyx* tooth and was discussed in brief by Charig & Milner (1997). They referred it to *Baryonyx* under the mistyped accession number 'BEXHM 1993.485' (the latter number is in fact attributed to a palaeolithic hand axe; J. Porter pers. comm. 2022) (Barker *et al.* 2023), and was recovered from the Conglomerate Bed. BEXHM 2002.50.123 and 2005.29 were accessioned as indeterminate allosauroids, while BEXHM 2002.50.124 was accessioned as a dromaeosaurid. All were figured in brief in Austen *et al.* (2010), where BEXHM 2002.50.124 is referred to a velociraptorine dromaeosaurid more specifically. BEXHM 2002.50.123 and 124 were unearthed from the *Polacanthus* Bed and associated with the aforementioned skeletal remains of *Hypselospinus* and an ankylosaur. BEXHM 2005.29 was recovered from the Conglomerate Bed.

FIG. 3. Theropod teeth from the Wadhurst Clay Formation. A, BEXHM 1995.485 (morphotype I). B, BEXHM 2002.50.123 (morphotype II). C, BEXHM 2002.50.124 (morphotype III). D, BEXHM 2005.29 (morphotype IV). E, NHMUK PV R37630 (morphotype V). A, C–E, lingual; B, labial view. Scale bar represents 10 mm.

NHMUK PV R37630 is part of the Dawson Collection (1884), having been collected from an unknown stratum around the vicinity of Hastings (Sussex). It was previously accessioned under the catalogue number 'R604' and as belonging to the *nomen dubium* '*Megalosaurus dunkeri*'. It is currently accessioned as Theropoda indet. (https://data.nhm.ac.uk/dataset/collection-specimens/resource/05ff2255-c38a-40c9-b657-4ccb55ab2feb/record/9433926).

Terminology

Terminology on anatomical orientation follows Smith & Dodson (2003) and Hendrickx *et al.* (2015a), and anatomical and morphometric terms follow Smith *et al.* (2005) and Hendrickx *et al.* (2015a). The calculation method pertaining to the denticle size density index (DSDI), initially described in Hendrickx *et al.* (2015a), follows the updated recommendations set out in Hendrickx *et al.* (2020), whereby the mesiocentral denticle density (i.e. number of mesial denticles per unit distance at the mid-crown; MC) is measured at two-thirds crown height in specimens with apically restricted mesial carina. Phylogenetic definitions follow Hendrickx *et al.* (2020) and references therein.

Computed tomography

Given that parts of NHMUK PV R 37630 are obscured by glue, the specimen was underwent micro-computed tomography scanning (μ-CT) at the μ-VIS X-Ray Imaging Centre, University of Southampton (UK), using a custom 225/450 kVp Hutch dual source walk-in micro-focus CT system (Nikon Metrology). Peak voltage and current were set at 180 kV and 184 μA, respectively. A total of 3143 projections were collected over a 360° rotation, averaging 4 frames per projection with a 134 ms exposure time per frame. Voxel dimensions were 29.81 μm.

Measurements

Specimens were examined first hand using a DinoLite (AM4113TL) digital microscope. Measurements were taken using a digital calliper as well as the measuring tools provided in the Dinocapture 2.0 software (v.1.5.48.A). A full list of measurements is provided in Barker *et al.* (2024).

BEXHM 2002.50.123 is broken in its basal portion such that the cervix cannot be distinguished, rendering it difficult to gather various morphometric characters and affecting subordinate measures (e.g. MC length and width). In order to still include the specimen in our sample, we used a semi-quantitative approach to account for the basal damage: we assumed that the relatively more complete mesiobasal region approximates the level of the cervix, and derived our crown base width (CBW) measure from this. With the specimen positioned in lateral view, a 90° vertex was realized by drawing a horizontal line from the basalmost preserved mesial region and a vertical line that followed the basal portion of the distal carina in FIJI (Schindelin *et al.* 2012), and their intersection serving as the approximate position of the distal cervix. The length of the horizontal line thus equated the crown base length (CBL), and the position of the vertex enabled crown height (CH) to be estimated.

Additionally, due to the small size of BEXHM 2002.50.124, characters relating to denticle measurements per 5 mm were taken over 1 mm and subsequently multiplied by 5.

Phylogenetic analysis

The phylogenetic analysis follows the methodology detailed by Hendrickx *et al.* (2020) and was conducted using the programme TNT (v1.6) (Goloboff & Morales 2023). The specimens were separately added to dentition-based datasets focused on non-avian theropods and containing operational taxonomic units (OTUs) scored in matrices used by Meso *et al.* (2021a). These matrices are themselves based on those of Hendrickx & Mateus (2014) and their subsequent modifications by Young *et al.* (2019) and Hendrickx *et al.* (2020), and include a whole dentition matrix (146 characters) and a subsidiary crown-only matrix (91 characters).

The Wadhurst Clay Formation teeth were scored as lateral teeth (see specimen descriptions for morphological support for these positional inferences). Given that the conidont crown BEXHM 1995.485 has been previously referred to *Baryonyx*, and that spinosaurid teeth can be difficult to position within the tooth row (Hendrickx *et al.* 2015a), we follow the probabilistic positional inference used by Barker *et al.* (2023) in view of the supernumerary lateral dentition of early spinosaurids. We additionally score the '*Suchosaurus cultridens*' holotype (NHMUK PV R36536) for analyses involving the morphotype I specimen (BEXHM 1995.485).

Four analyses were undertaken per morphotype. First, a constrained analysis containing all Wadhurst Clay Formation morphotypes I–V (and also including the newly scored '*Suchosaurus*' holotype OTU; 113 OTUs in total) was conducted such that a preliminary phylogenetic hypothesis existed for each specimen. This constrained analysis is based on a backbone topology following a phylogenetic consensus described in Hendrickx *et al.* (2020) and implemented using the positive constraints command (*force* +), with the morphotypes of interest set as floating OTUs (the additional OTU '*Suchosaurus*' was also set as a floating OTU when relevant). The second and third analyses examined each morphotype separately, using the whole dentition matrix with and without constraints, respectively (108 OTUs total; 109 OTUs for the analysis of morphotype I). Finally, the fourth analysis involved each morphotype analysed seperately in an unconstrained search of the crown-only matrix (103 OTUs total; 104 OTUs for the analysis of morphotype I).

The search strategy for all three analyses involved a combination of the tree-search algorithms including Wagner trees, TBR (tree bisection and reconnection) branch swapping, sectorial searches, Ratchet (perturbation phase stopped after 20 substitutions) and Tree Fusing (5 rounds), until 100 hits of the same minimum tree length were obtained. Once the best trees were recovered, an additional round of TBR branch swapping was conducted (the TNT command used is *xmult = hits 100 rss fuse 5 ratchet 20* followed by the *bb* command). In the unconstrained analyses, wildcard taxa were identified using the *iterPCR* procedure (Pol & Escapa 2009; Goloboff & Szumik 2015), and Bremer supports were used to assess the nodal support of the resulting reduced consensus trees. The resulting topologies are available in Barker *et al.* (2024).

Regarding character scores, two minor comments are required: for NHMUK PV R37630, Character (Ch.) 88

TABLE 1. Measurements (in mm) used in the discriminant and machine learning analyses (see text for further details).

	CBL	CBW	CH	AL	MCL	MCW	MSL
BEXHM 1995.485	7.31	5.72	15.95	15.72	5.35	3.91	?
BEXHM 2002.50.123	11.23	7.08	24.51	26.22	9.23	5.29	13.46
BEXHM 2002.50.124	5.08	2.83	9.16	9.88	3.95	2.01	4.2
BEXHM 2005.29	12.9	6.06	33.75	36.72	10.59	4.72	25.86
NHMUKPVR37630	7.03	4.3	15.8	16.86	5.87	3.02	8.98

	LAF + 1	LIF + 1	CA	MDL	DDL	ADM	PDM
BEXHM 1995.485	8	10	78.42	0.188	0.145	?	8
BEXHM 2002.50.123	–	–	68.81	0.28	0.305	?	3
BEXHM 2002.50.124	–	–	66.82	?	0.215	8	5
BEXHM 2005.29	–	–	66.64	0.225	0.27	3.5	3.5
NHMUKPVR37630	–	–	69.5	0.177	0.306	4	4

Note that various measurements (e.g. CBL, CBW, CH) for BEXHM 2002.50.123 are estimates, which impact the collection of subsidiary measurements (e.g. MCL, MCW; see also main text). A full list of measurements is available in Barker *et al.* (2024).
Abbreviations: –, inapplicable; ?, missing due to damage; ADM, number of denticles per millimetre at the midpoint of the mesial carina; AL, apical length; CA, crown angle; CBL, crown base length; CBW, crown base width; CH, crown height; DDL, distal denticle length; LAF, number of labial flutes; LIF, number of lingual flutes; MCL, mid-crown length; MCW, mid-crown width; MDL, mesial denticle length; MSL, mesial serrated carina length; PDM, number of denticles per millimetre at the midpoint of the distal carina.

(number of denticles at two-thirds crown height) was measured over 1 mm (5 denticles present) and multiplied by 5 due to the close proximity of this portion to the damaged section of carina, which prevented measurements over the prescribed 5 mm. For BEXHM 2002.50.123, Ch. 90 was inferred based on available denticle count.

Discriminant function analysis

To predict their optimal classifications within ‘family-level’ groupings based on quantitative data (Table 1), the Wadhurst Clay Formation specimens were added to comprehensive published datasets of theropod teeth (Hendrickx *et al.* 2020) and assessed using discriminant function analysis (DFA) in Past4 (Hammer *et al.* 2001). Here, they were treated as unknown taxa and classified at genus or clade levels. The specimens replaced the ‘*Aerosteon*’ tooth MCNA-PV-3137 examined in Hendrickx *et al.* (2020). The analyses followed the protocol detailed by Young *et al.* (2019) and implemented in Hendrickx *et al.* (2020). All variables were log-transformed to normalize the quantitative variables, a log (x + 1) correction was applied to LAF (the number of labial flutes) and LIF (the number of lingual flutes) to account for the absence of fluted enamel, and an arbitrary value of 100 denticles per 5 mm was used for unserrated carinae (see Young *et al.* (2019) regarding justification of the latter modification).

The five Wadhurst Clay Formation specimens were added to different iterations of various datasets, being analysed together as well as individually. The whole dataset was constructed based on 1334 teeth belonging to 89 taxa (84 species and five indeterminate taxa) separated into 20 clades or paraphyletic groups measured for 12 variables (CBL, CBW, CH, AL, MCL, MCW, MSL, LAF, LIF, CA, MDL, DDL; Table 1). Due to inconsistencies between authors when measuring dinosaur tooth crowns (Hendrickx *et al.* 2020), additional analyses were conducted on a reduced (‘personal’) dataset restricted to measurements previously taken by a single author using a consistent measuring protocol. This reduced dataset consists of 593 teeth belonging to 72 theropod taxa separated into 20 monophyletic or paraphyletic groups.

Given that the ziphodont morphotypes II (BEXHM 2002.50.123) and IV (BEXHM 2005.29) have a CH in excess of 20 mm, and that morphotypes III (BEXHM 2002.50.124) and V (NHMUK PV R37630) have CH smaller than 20 mm, these specimens were added to subsidiary datasets consisting solely of large (i.e. CH > 20 mm) and small (i.e. CH < 20 mm) teeth, respectively. The former dataset included teeth extracted from the whole dataset (725 crowns) and the personal dataset (399 crowns) based on single author measurements. The latter dataset was extracted from the whole dataset and included 703 crowns. Finally, the teeth underwent additional rounds of clade- and genus-level analyses, using modified versions of the aforementioned datasets when the absence of denticles was considered inapplicable (no denticles = ‘?’).

While ziphodont teeth typically overlap in terms of morphospace occupation and are difficult to distinguish quantitatively (Hendrickx *et al.* 2015b), the conidont teeth of spinosaurids appear distinct at higher taxonomic levels and have high reclassification rates (Barker *et al.* 2023). As a result, the conidont morphotype I (BEXHM 1995.485) was added to the spinosaurid-only datasets used in the DFAs implemented in Barker *et al.* (2023), themselves based on data extracted from the Hendrickx *et al.* (2020) files described above. Two principal datasets were collated: one consisting of all spinosaurid specimens, and the other excluding *nomina dubia* (represented by singular specimens). These analyses follow Hendrickx *et al.* (2015b) in using two versions of the aforementioned spinosaurid-only datasets: one incorporates all morphometric variables of interest (n = 35) and the other excludes all ratio variables (see Barker *et al.* (2023) for further information regarding dataset construction). Variables were not log-transformed. Morphotype I replaced the specimen XMDFEC V10010 in the full spinosaurid dataset, given that the latter cannot be referred to Spinosauridae (Katsuhiro & Yoshikazu 2017; Buffetaut *et al.* 2019; Soto *et al.* 2020; Barker *et al.* 2023).

The full results from these analyses are presented in Barker *et al.* (2024).

Machine learning analysis

The machine learning analysis follows the methodology described by Wills *et al.* (2021). Two published theropod tooth measurement datasets (Hendrickx *et al.* 2020; Wills *et al.* 2023) were used as the training data, to which the Wadhurst Clay Formation specimens were added. Analyses were run on each training dataset independently, with the data split into 20 clades or paraphyletic groups for the Hendrickx *et al.* (2020) data and 25 clades for the Wills *et al.* (2023) data. For the analysis using the Hendrickx *et al.* (2020) training data, six variables were used to create the models (CBL, CBW, CH, AL, MDL, DDL), while five variables were used for the Wills *et al.* (2023) data (CBL, CBW, CH, ADM, PDM) (Table 1). All variables were log transformed (log x + 1), centred and scaled. Any cases with missing values were removed from the Hendrickx *et al.* (2020) data prior to training the machine learning models, leaving 717 complete cases from an original total of 1335. The Wills *et al.* (2023) data contained only complete cases, a total of 1715 specimens. The original training data were split into two in an 80:20 ratio: a training set to train and generate the models, and a testing set to assess the accuracy of the models. The split was conducted to preserve the class distributions of the original data. The testing set provides an unbiased assessment of model accuracy because these data are not used in model building. Three different classification models were generated, using 10-fold cross-validation, from the training data split: a mixture discriminant analysis (MDA) model; a random forests (RF) model; and a C5.0 decision tree model. The C5.0 algorithm can utilize data points containing missing values and therefore this model was generated without removing missing data. The RF and MDA models used the data with missing values removed. The accuracy of each individual model was assessed by first classifying data from the testing set before classifying the Wadhurst Clay Formation specimens. All machine learning analyses were performed using R version 4.3.2 (R Core Team 2023) in RStudio 2022.02.1 (R Studio Team 2023), with the Caret package v6.0-94 (Kuhn 2008) used for model generation and analysis. For specific classification models we used the R packages mda (Hastie *et al.* 2020), randomForest v4.7-1.1 (Liaw & Wiener 2002) and C5.0 (Kuhn *et al.* 2018). Details of the protocol and training data are available in Barker *et al.* (2024).

RESULTS

Phylogenetic, discriminant & machine learning analyses: preliminary comments

The constrained analysis of the whole dentition dataset including all five Wadhurst Clay Formation morphotypes produces 12 trees (tree length (TL) = 1329; consistency index (CI) = 0.196; retention index (RI) = 0.465), with no additional trees found by the subsequent TBR search (Fig. 4). Morphotype 1 (BEXHM 1995.485) was positioned alongside ‘*Suchosaurus*’ in a polytomous Spinosauridae, outside of Baryonychinae + Spinosaurinae. Morphotype II (BEXHM 2002.50.123) was recovered within a polytomous Tyrannosauroidea, occupying an early-diverging position in that clade. Morphotype III (BEXHM 2002.50.124) and morphotype V (NHMUK PV R37630) were both found in an unresolved dromaeosaurid clade, and morphotype IV (BEXHM 2005.29) was positioned at the base of the megalosauroid clade Piatnitzkysauridae.

The clade-level discriminant analyses of the whole (Fig. 5A; principal component (PC)1 = 50.02%, PC2 = 19.8%; reclassification rate (RR) = 61.02%) and personal (Fig. 5B; PC1 = 57.08%, PC2 = 21.9%; RR = 61.09%) datasets, as well as the versions in which the absence of denticles was considered inapplicable (whole dataset: PC1 = 50.21%, PC2 = 19.03%; personal dataset: PC1 = 54.24%, PC2 = 22.94%; RR = 59.36% in both cases) were consistent in their classifications of morphotypes I and II: the former was classified as a spinosaurid and the latter a non-megalosaurian megalosauroid. Morphotype III was classified as a noasaurid in three of the four results, differing only in the analysis of the personal dataset (absence of denticles = ?), in which it was found to be a dromaeosaurid. Similarly, morphotype V

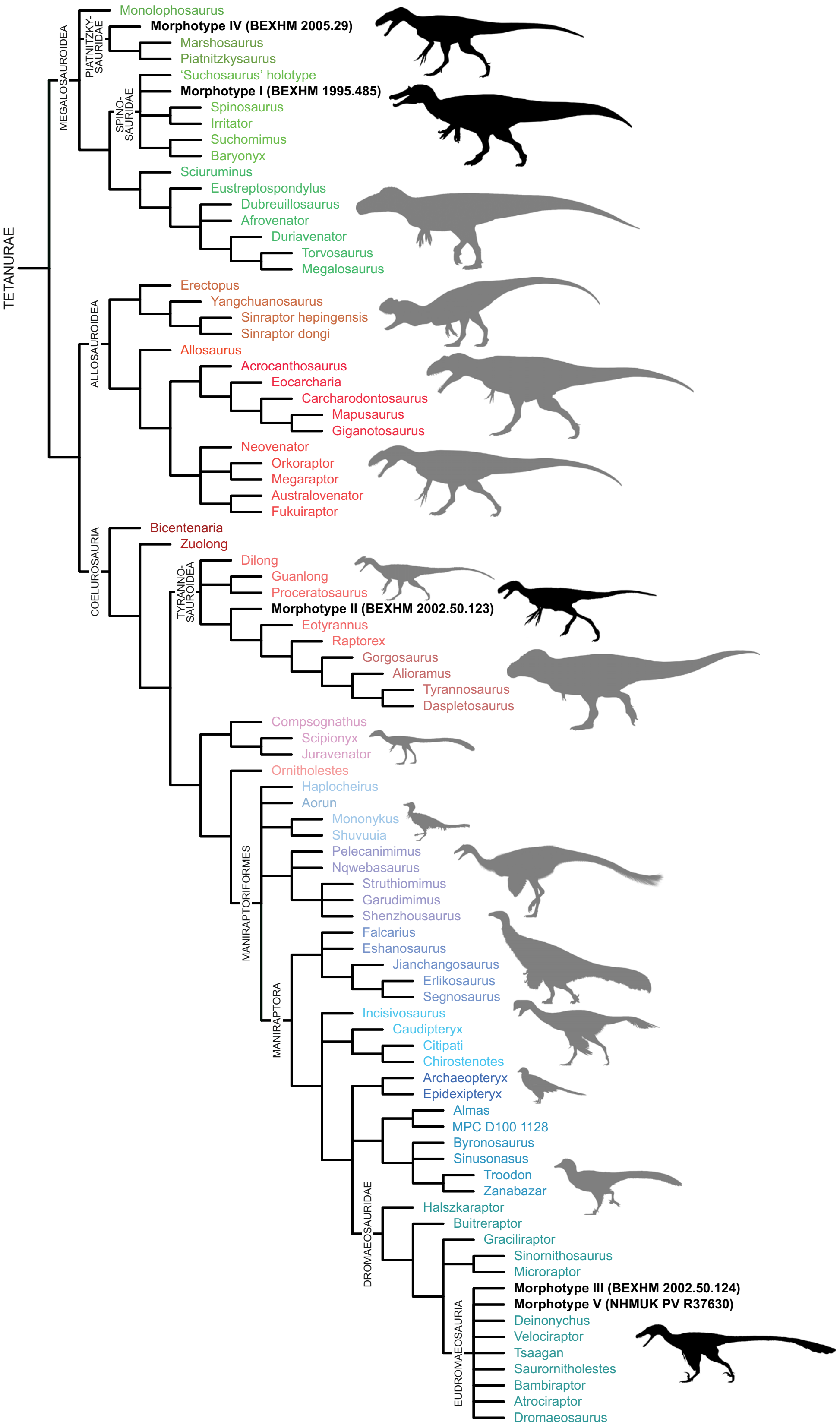
TETANURAE
MEGALOSAUROIDEA
PIATNITZKYSAURIDAE
Monolophosaurus
Morphotype IV (BEXHM 2005.29)
Marshosaurus
Piatnitzkysaurus
SPINOSAURIDAE
'Suchosaurus' holotype
Morphotype I (BEXHM 1995.485)
Spinosaurus
Irritator
Suchomimus
Baryonyx
Sciuruminus
Eustreptospondylus
Dubreuillosaurus
Afrovenator
Duriavenator
Torvosaurus
Megalosaurus
ALLOSAUROIDEA
Erectopus
Yangchuanosaurus
Sinraptor hepingensis
Sinraptor dongi
Allosaurus
Acrocanthosaurus
Eocarcharia
Carcharodontosaurus
Mapusaurus
Giganotosaurus
Neovenator
Orkoraptor
Megaraptor
Australovenator
Fukuiraptor
COELUROSAURIA
Bicentenaria
Zuolong
TYRANNOSAUROIDEA
Dilong
Guanlong
Proceratosaurus
Morphotype II (BEXHM 2002.50.123)
Eotyrannus
Raptorex
Gorgosaurus
Alioramus
Tyrannosaurus
Daspletosaurus
Compsognathus
Scipionyx
Juravenator
Ornitholestes
MANIRAPTORIFORMES
Haplocheirus
Aorun
Mononykus
Shuvuuia
Pelecanimimus
Nqwebasaurus
Struthiomimus
Garudimimus
Shenzhousaurus
MANIRAPTORA
Falcarius
Eshanosaurus
Jianchangosaurus
Erlikosaurus
Segnosaurus
Incisivosaurus
Caudipteryx
Citipati
Chirostenotes
Archaeopteryx
Epidexipteryx
Almas
MPC D100 1128
Byronosaurus
Sinusonasus
Troodon
Zanabazar
DROMAEOSAURIDAE
Halszkaraptor
Buitreraptor
Graciliraptor
Sinornithosaurus
Microraptor
EUDROMAEOSAURIA
Morphotype III (BEXHM 2002.50.124)
Morphotype V (NHMUK PV R37630)
Deinonychus
Velociraptor
Tsaagan
Saurornitholestes
Bambiraptor
Atrociraptor
Dromaeosaurus

FIG. 4. Phylogenetic affinities of the five theropod dental morphotypes from the Wadhurst Clay Formation of southern England. Strict consensus tree from the 12 most parsimonious trees (CI = 0.196; RI = 0.465), focusing on Tetanurae. Black silhouettes representative of the dental morphotypes based on this result (but see Systematic palaeontology for further discussion). Silhouette images from PhyloPic (https://www.phylopic.org/): Alessio Ciaffi (Spinosauridae CC BY 4.0), Ivan Iofrida (Oviraptorosauria CC BY 4.0), Jack Mayer Wood (Tyrannosauridae CC BY 3.0), Jagged Fang Designs (Megalosauridae CC0 1.0, Metriacanthosauridae CC0 1.0, Ornithomimosauria CC BY 4.0), John Conway (Compsognathidae CC0 1.0), Matt Martyniuk (Archaeopterygidae CC BY 3.0), Scott Hartman (Carcharodontosauridae, Dromaeosauridae, Neovenatoridae, non-tyrannosaurid Tyrannosauroidea, Piatnitzkysauridae, Proceratosauridae all CC BY-NC-SA 3.0), Tasman Dixon (Alvarezsauridae CC BY 4.0, Troodontidae CC0 1.0) and Walter Vladimir (Therizinosauria CC BY 3.0). For full details, see Table S1.

was classified as a noasaurid in the analyses of the whole dataset, and as a dromaeosaurid in those examining the personal datasets. Morphotype IV was variably classified as a metriacanthosaurid (whole dataset), a non-megalosaurian megalosauroid (whole and personal datasets in which absence of denticles = ?), and a megalosaurid (personal dataset).

We assessed the accuracies of the machine learning models by running each model against the test dataset to produce accuracies of: 82.9% (MDA), 84.8% (C50) and 87.2% (RF) for the Hendrickx *et al.* (2020) training data; and 82.6% (MDA), 82.1% (C50) and 85.6% (RF) for the Wills *et al.* (2023) training data (see Barker *et al.* 2024). Results pertaining to specific morphotypes are discussed below.

Morphotype I

The results of the constrained tree search on the whole dentition matrix returned two trees (TL = 1313; CI = 0.199; RI = 0.46), with no additional trees found in the subsequent TBR search. BEXHM 1995.485 was recovered within a polytomous Spinosauridae, positioned outside the Baryonychinae + Spinosaurinae clade alongside '*Suchosaurus*' (Fig. 6A). Spinosauridae is supported by 25 synapomorphies, of which 10 are present in BEXHM 1995.485 (Fig. 7): weakly labiolingually compressed crown (CBR > 0.75; Ch. 70:2), slightly concave distal margin (Ch. 72:1), subcircular basal cross-section (Ch. 76:0), 30 or more mid-crown denticles per 5 mm on the distal carina (Ch. 89:0), horizontally subrectangular denticles on the mesial carina at two-thirds crown height (Ch. 95:2), sporadic change in denticle size (Ch. 97:1), flutes present on both labial and lingual surfaces (Ch. 111:2), deeply veined enamel texture that strongly curves basally towards the carinae (Ch. 121:3, Ch. 122:1) and transverse undulations present on the root base (Ch. 145:1).

The unconstrained analyses of the whole dentition dataset recovered 160 trees (TL = 1068; CI = 0.244; RI = 0.586), with 2160 trees found following the additional round of TBR. The strict consensus generated a large polytomy containing all non-outgroup OTUs; BEXHM 1995.485 was again recovered within Spinosauridae and the clade assumed the same ingroup topology as recovered by the constrained analysis of this same dataset. However, BEXHM 1995.485 acted as a wildcard taxon along with 35 other OTUs (including all other spinosaurid OTUs). As a result, a reduced consensus was not attempted.

The analysis of the crown-only dataset found 212 trees (TL = 646; CI = 0.248; RI = 0.630), with 3000 trees (overflow) recovered following the additional round of TBR. The strict consensus produced a substantial polytomy containing all non-outgroup OTUs, some of which were organized in clades not corresponding to those identified in other studies. Spinosauridae, however, was recognizable within this polytomy: it was polytomous, included BEXHM 1995.485, and possessed the same topology as described above. BEXHM 1995.485 was one of 66 wildcard taxa (including all other spinosaurid OTUs) uncovered by the *iterPCR* procedure, and a reduced consensus was, again, not subsequently attempted.

The DFA consistently supports a spinosaurid affinity for BEXHM 1995.485 (Fig. 6B). The clade-level DFAs of the whole and personal datasets (regardless of whether the absence of denticles was considered inapplicable or not) all identified the specimen as a spinosaurid (PC1 range = 50.2–57.1%, PC2 range = 19.04–22.94%), while the taxon-level analyses of these same datasets classified BEXHM 1995.485 as belonging to *Suchomimus* (PC1 range = 41.05–42.87%, PC2 range = 17.08–25.65%). When the spinosaurid-only datasets were examined, BEXHM 1995.485 was either classified as belonging to *Suchomimus* (PC1 range = 71.81–81.92%, PC2 range = 15.56–17.43%) or *Baryonyx* (PC1 range = 58.3–84.14%, PC2 range = 15.04–28.61%). The reclassification rates using the whole and personal datasets were low throughout (clade level analyses, 59.36–62.07%; taxon level analyses, 59.37–63.74%) but those focusing on the spinosaurid-only datasets were consistently high: the referral of BEXHM 1995.485 to *Baryonyx* and to *Suchomimus* yielded reclassification rates of 100% and 98.18–98.28%, respectively.

The machine learning analysis (Table 2) recovered BEXHM 1995.485 as a spinosaurid for both the RF and

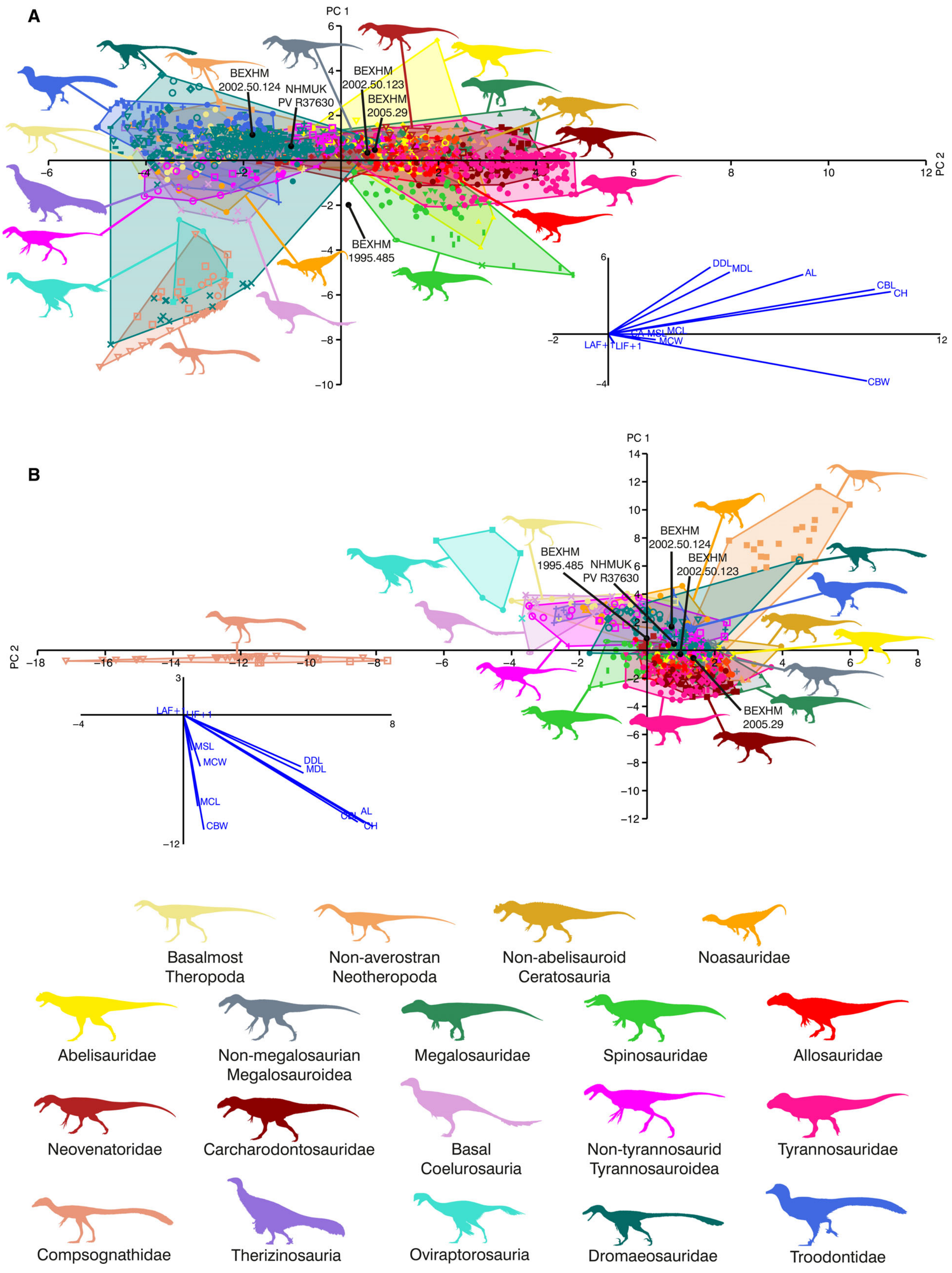
A
PC 1
PC 2
BEXHM 2002.50.124
NHMUK PV R37630
BEXHM 2002.50.123
BEXHM 2005.29
BEXHM 1995.485
DDL
MDL
AL
CBL
CH
MSL
MCL
MCW
LAF+1
LIF+1
CBW
B
PC 1
PC 2
BEXHM 1995.485
NHMUK PV R37630
BEXHM 2002.50.124
BEXHM 2002.50.123
BEXHM 2005.29
Basalmost Theropoda
Non-averostran Neotheropoda
Non-abelisauroid Ceratosauria
Noasauridae
Abelisauridae
Non-megalosaurian Megalosauroidea
Megalosauridae
Spinosauridae
Allosauridae
Neovenatoridae
Carcharodontosauridae
Basal Coelurosauria
Non-tyrannosaurid Tyrannosauroidea
Tyrannosauridae
Compsognathidae
Therizinosauria
Oviraptorosauria
Dromaeosauridae
Troodontidae

FIG. 5. Dispersion plots of the discriminant analyses of the five theropod dental morphotypes from the Wadhurst Clay Formation of southern England. Results based on: A, whole dataset; B, personal datasets. *Abbreviations*: AL, apical length; CA, crown angle; CBL, crown base length; CBW, crown base width; CH, crown height; DDL, distal denticle length; LAF, number of labial flutes; LIF, number of lingual flutes; MCL, mid-crown length; MCW, mid-crown width; MDL, mesial denticle length; MSL, mesial serrated carina length. Silhouette images from PhyloPic (https://www.phylopic.org/): Alessio Ciaffi (Spinosauridae CC BY 4.0); Ivan Iofrida (Oviraptorosauria CC BY 4.0); Jack Mayer Wood (Tyrannosauridae CC BY 3.0); Jagged Fang Designs (Megalosauridae CC0 1.0); John Conway (Compsognathidae CC0 1.0); Matt Martyniuk (Basal Coelurosauria CC BY 3.0); Scott Hartman (Abelisauridae, basalmost Theropoda, Carcharodontosauridae, Dromaeosauridae, Neovenatoridae, non-abelisauroid Ceratosauria all CC BY-NC-SA 3.0, non-averostran Neotheropoda CC BY 3.0, non-megalosaurian Megalosauroidea, non-tyrannosaurid Tyrannosauroidea both CC BY-NC-SA 3.0); Tasman Dixon (Allosauridae CC0 1.0, Noasauridae CC BY 4.0, Troodontidae CC0 1.0); Walter Vladimir (Therizinosauria CC BY 3.0). For full details, see Table S1.

MDA models using the Hendrickx *et al.* (2020) data and as a baryonychine spinosaurid for the MDA model using the Wills *et al.* (2023) data. In both cases the MDA analysis returned the highest posterior probabilities from the models ($p = 0.77$–0.99). The C5.0 model consistently classified this tooth within Dromaeosauridae, as did the RF model using the Wills *et al.* (2023) data. The posterior probabilities in all of these cases are, however, lower than the spinosaurid classification.

Morphotype II

The constrained phylogenetic analysis of the whole dentition dataset recovered 1 tree (TL = 1308; CI = 0.199; RI = 0.456), as did the additional round of TBR. The strict consensus placed BEXHM 2002.50.123 within Tyrannosauroidea. Specifically, the specimen is recovered as the earliest-diverging member of a lineage that also contains *Eotyrannus* + Tyrannosauridae (Fig. 6C). This relationship is supported by a single synapomorphy: 9–15 distal mid-crown denticles (Ch. 89:2; Fig. 8).

The unconstrained analysis of this same dataset initially found 163 trees (TL = 1063; CI = 0.245; RI = 0.584), with 2100 trees found following the additional round of TBR. The strict consensus is poorly resolved in general, featuring few recognizable clades, and BEXHM 2002.50.123 was recovered at the base of a polytomy composed mostly of single OTUs. The *iterPCR* procedure found 37 wildcard OTUs, and the reduced consensus following their pruning resulted in BEXHM 2002.50.123 being positioned at the base of a polytomous tyrannosauroid-dominated clade that also included the ceratosaur *Masiakasaurus* and dromaeosaurid *Halszkaraptor*. The position of BEXHM 2002.50.123 within this moderately robust clade (Bremer support value = 2) is supported by four synapomorphies, one of which is present in BEXHM 2002.50.123: asymmetrical crown in distal view (Ch. 87:1).

The analysis of the crown-only dataset returned 218 trees (TL = 640; CI = 0.248; RI = 0.628), with 3000 trees (overflow) recovered following TBR. All OTUs bar the outgroup formed a polytomy with few recognizable clades (e.g. Spinosauridae). BEXHM 2002.50.123 was positioned as one of multiple single OTUs at the base of this polytomy. BEXHM 2002.50.123 was one of 73 wildcard OTUs found by the *iterPCR* procedure, and as such a reduced consensus was not attempted.

The DFA mainly recovered a megalosauroid or dromaeosaurid signal for the classification of BEXHM 2002.50.123 (Fig. 6D). At the clade level, the specimen was consistently classified as a non-megalosauran megalosauroid using the whole and personal datasets, regardless of whether the absence of denticles was considered inapplicable (PC1 range = 50.21–57.1%, PC2 range = 19.04–22.94%). When analyses were restricted to datasets focusing on large teeth, the clade-level analyses consistently recovered BEXHM 2002.50.123 as a dromaeosaurid (PC1 range = 37.95–56.14%, PC2 range = 27.68–30.84%). Reclassification rates were low throughout, ranging between 58.4% and 61.99%. At the taxon level, analyses of the whole datasets classified BEXHM 2002.50.123 as an unnamed dromaeosaurid, regardless of whether the absence of denticles was considered inapplicable (PC1 = 42.86%, PC2 = 17.08%) or not (PC1 = 41.04%, PC2 = 21.56%). Analyses of the personal datasets, as well as the versions of the whole and personal datasets restricted to large teeth, classified BEXHM 2002.50.123 as the piatnitzkysaurid *Piatnitzkysaurus* (PC1 range = 35.5–54.25%, PC2 range = 18.44–27.82%). Reclassification rates for this classification are also low, ranging between 57.46% and 63.74%.

The highest posterior probability from the machine learning analysis (Table 2) came from the C5.0 classifier, which recovered BEXHM 2002.50.123 as a tyrannosaurid with a posterior probability of 0.61. The machine learning recovered a megalosauroid or even spinosaurid signal from a number of the models, albeit with consistently low ($p < 0.40$) posterior probabilities. In each of these cases, however, the next highest posterior probability indicates a tyrannosaurid affinity.

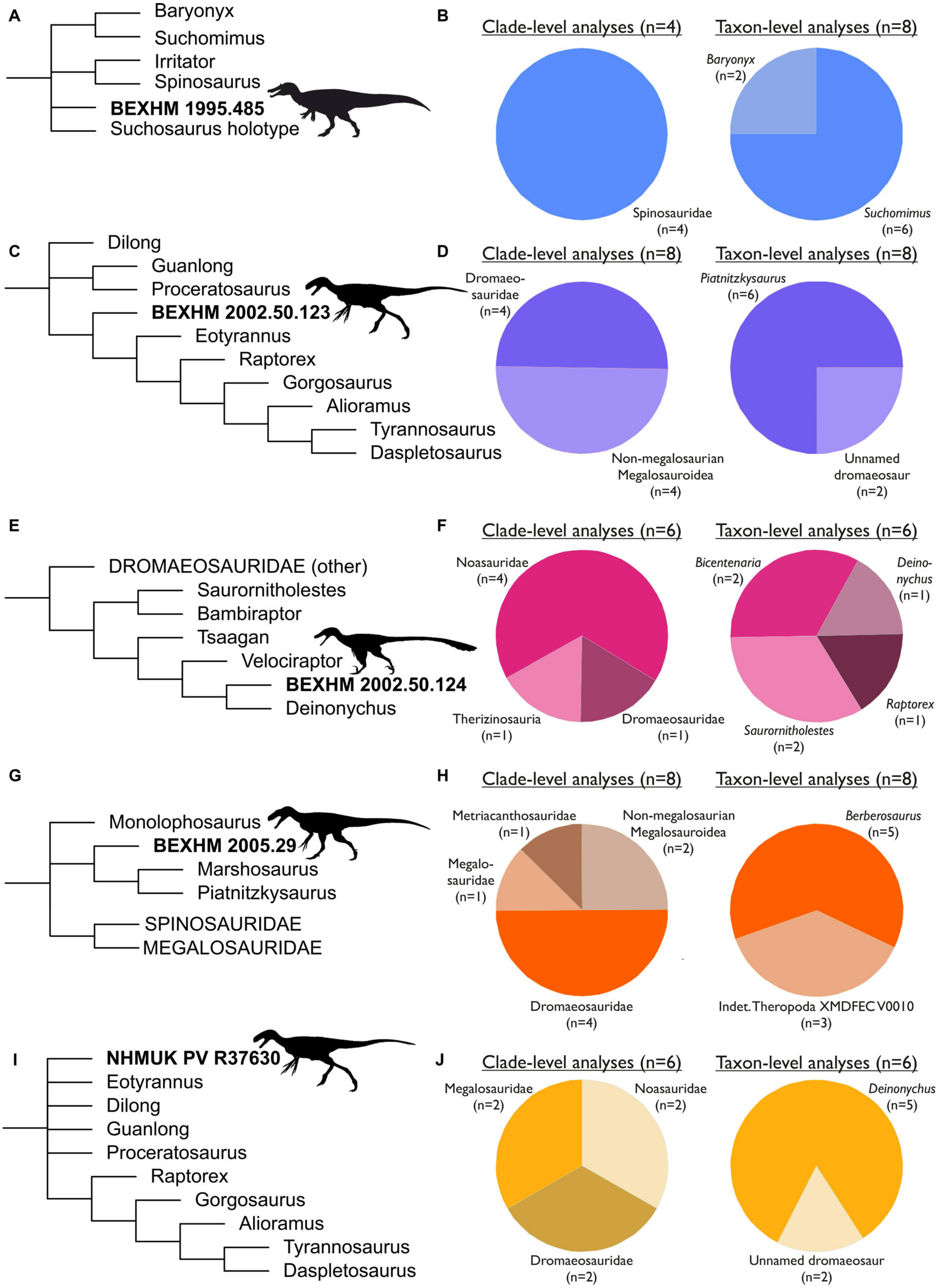
A
Baryonyx
Suchomimus
Irritator
Spinosaurus
BEXHM 1995.485
Suchosaurus holotype
B
Clade-level analyses (n=4)
Taxon-level analyses (n=8)
Spinosauridae (n=4)
Baryonyx (n=2)
Suchomimus (n=6)
C
Dilong
Guanlong
Proceratosaurus
BEXHM 2002.50.123
Eotyrannus
Raptorex
Gorgosaurus
Alioramus
Tyrannosaurus
Daspletosaurus
D
Clade-level analyses (n=8)
Taxon-level analyses (n=8)
Dromaeo-sauridae (n=4)
Non-megalosaurian Megalosauroidea (n=4)
Piatnitzkysaurus (n=6)
Unnamed dromaeosaur (n=2)
E
DROMAEOSAURIDAE (other)
Saurornitholestes
Bambiraptor
Tsaagan
Velociraptor
BEXHM 2002.50.124
Deinonychus
F
Clade-level analyses (n=6)
Taxon-level analyses (n=6)
Noasauridae (n=4)
Therizinosauria (n=1)
Dromaeosauridae (n=1)
Bicentenaria (n=2)
Deino-nychus (n=1)
Raptorex (n=1)
Saurornitholestes (n=2)
G
Monolophosaurus
BEXHM 2005.29
Marshosaurus
Piatnitzkysaurus
SPINOSAURIDAE
MEGALOSAURIDAE
H
Clade-level analyses (n=8)
Taxon-level analyses (n=8)
Metriacanthosauridae (n=1)
Non-megalosaurian Megalosauroidea (n=2)
Megalo-sauridae (n=1)
Dromaeosauridae (n=4)
Berberosaurus (n=5)
Indet. Theropoda XMDFEC V0010 (n=3)
I
NHMUK PV R37630
Eotyrannus
Dilong
Guanlong
Proceratosaurus
Raptorex
Gorgosaurus
Alioramus
Tyrannosaurus
Daspletosaurus
J
Clade-level analyses (n=6)
Taxon-level analyses (n=6)
Megalosauridae (n=2)
Noasauridae (n=2)
Dromaeosauridae (n=2)
Deinonychus (n=5)
Unnamed dromaeosaur (n=2)

FIG. 6. Summary of results. Strict consensus trees from the constrained phylogenetic analyses (A, C, E, G, I) and results of the discriminant analyses (B, D, F, H, J) for the Wadhurst Clay Formation theropod dental morphotypes I–V. Specimens were analysed separately. A–B, morphotype I (BEXHM 1995.485). C–D, morphotype II (BEXHM 2002.50.123). E–F, morphotype III (BEXHM 2002.50.124). G–H, morphotype IV (BEXHM 2005.29). I–J, morphotype V (NHMUK PV R37630). See Barker *et al.* (2024) for full results. Silhouette images from PhyloPic (https://www.phylopic.org/): Alessio Ciaffi (Spinosauridae CC BY 4.0); Scott Hartman (Dromaeosauridae, non-tyrannosaurid Tyrannosauroidea, Piatnitzkysauridae all CC BY-NC-SA 3.0). For full details, see Table S1.

Morphotype III

The constrained phylogenetic analysis of the whole dentition dataset recovered 1 tree (TL = 1311; CI = 0.198; RI = 0.457), with no additional trees recovered following the round of TBR. BEXHM 2002.50.124 was recovered as the sister taxon to *Deinonychus* (Fig. 6E), a topology supported by two synapomorphies: subrectangular mesial denticles with flattened external margins (Ch. 93:1) and broad interdenticular spaces between distal mid-crown denticles (Ch. 107:1; Fig. 9). Dromaeosauridae is supported by three synapomorphies, one of which is present in BEXHM 2002.50.124: lack of constriction between the root and crown (Ch. 67:0; the other two synapomorphies relate to mesial (Ch. 45:3) and root (Ch. 146:0) characters).

The unconstrained analysis of this dataset found 148 trees (TL = 1066; CI = 0.244; RI = 0.583); 1080 trees were recovered following the subsequent round of TBR, and the strict consensus of these produced a large, poorly resolved polytomy with few recognizable clades. BEXHM 2002.50.124 was one of several OTUs forming singular branches within this polytomy. The *iterPCR* process produced 39 wildcard OTUs. The reduced consensus recovered BEXHM 2002.50.124 in a weakly supported (Bremer support value = 1), polytomous clade alongside the dromaeosaurids *Deinonychus*, *Saurornitholestes* and a clade containing *Atrociraptor* and *Dromaeosaurus*. This topology is supported by three synapomorphies, one of which concerns lateral dentition: short, poorly developed interdenticular sulci between mid-crown denticles (Ch. 109:1; the mesial characters are Ch. 3:0 and Ch. 59:1).

The unconstrained analysis of the crown-only dataset returned 231 trees (TL = 644; CI = 0.247; RI = 0.626), with 99 999 trees (overflow) recovered following the additional round of TBR. All non-outgroup OTUs are collapsed into a large polytomy in the strict consensus, many of which (including BEXHM 2002.50.124) fail to form clades. Indeed, few recognizable clades are observed within the polytomy (e.g. Spinosauridae, Abelisauridae). BEXHM 2002.50.124 was one of 62 wildcard OTUs found by the *iterPCR* procedure, and as such a reduced consensus was also not attempted.

The results of the DFA offered conflicting classifications for BEXHM 2002.50.124 (Fig. 6F). The clade-level analyses of the whole datasets, regardless of whether the absence of denticles was considered inapplicable or not, classified the specimen as a noasaurid (whole dataset: PC1 = 51.02%, PC2 = 19.8%; whole dataset [no denticles=?]: PC1 = 50.21%, PC2 = 19.04%). At the taxon level, the specimen grouped with the dromaeosaurid *Deinonychus* (whole dataset: PC1 = 41.05%, PC2 = 21.55%) or the tyrannosauroid *Raptorex* (whole dataset [no denticles =?]: PC1 = 42.88%, PC2 = 17.07%). Reclassification rates are, however, low in both the clade- and taxon-level analyses, ranging between 59.37% and 61.99%. The analyses of the personal datasets were less consistent at the clade level, again grouping BEXHM 2002.50.124 with noasaurids (PC1 = 57.08%, PC2 = 21.9%) or among dromaeosaurids when the absence of denticles was considered inapplicable (PC1 = 54.26, PC2 = 22.94%). However, the taxon-level analyses of both personal datasets classified the specimen as the dromaeosaurid *Saurornitholestes* (‘My dataset’: PC1 = 41.07%, PC2 = 24.72%; ‘My dataset [no denticles=?]’: PC1 = 41.4%, PC2 = 25.66%). As above, the reclassification rates are low, ranging between 59.19% and 63.74%.

The DFA of the whole dataset focusing on small teeth also recovered mixed signals with limited support. At the clade level, BEXHM 2002.50.124 was classified as a noasaurid (PC1 = 31.15%, PC2 = 20.99%) or, when the absence of denticles was considered inapplicable, part of Therizinosauria (PC1 = 29.9%, PC2 = 21.97%). At the taxon level, BEXHM 2002.50.124 was classified as the early-diverging coelurosaurian *Bicentenaria*, regardless of whether denticles were considered applicable (PC1 = 36.63%, PC2 = 19.7%) or not (PC1 = 30.36%, PC2 = 20.5%). Reclassification rates were generally low, ranging between 62.02% and 67.99%.

The machine learning unambiguously classified BEXHM 2002.50.124 in Dromaeosauridae with posterior probabilities >0.99 in four out of six models (Table 2). The RF and MDA models developed against the Hendrickx *et al.* (2020) data refused to classify this specimen.

Morphotype IV

The constrained analysis of the whole dentition dataset recovered 1 tree (TL = 1314; CI = 0.198; RI = 0.456),

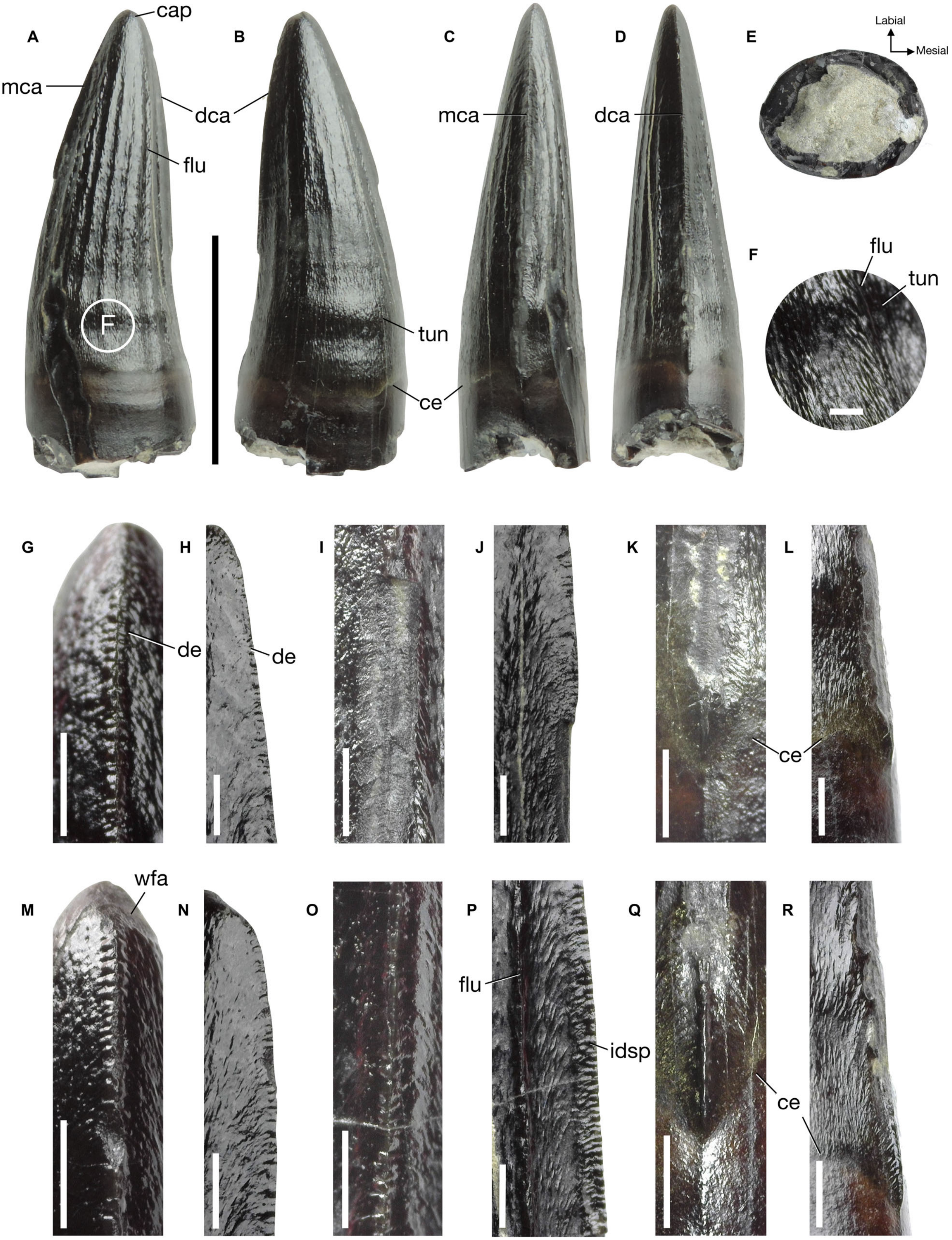
A
B
C
D
E
cap
mca
dca
flu
dca
mca
dca
Labial
Mesial
F
F
flu
tun
tun
ce
ce
G
H
I
J
K
L
de
de
ce
M
N
O
P
Q
R
wfa
flu
idsp
ce

FIG. 7. Morphotype I (BEXHM 1995.485) in: A, lingual; B, labial; C, mesial; D, distal; E, basal view. F, close-up of the enamel texture. G–H, apical portion of the mesial carina in: G, mesial; H, labial view. I–J, mid-crown portion of the mesial carina in: I, mesial; J, labial view. K–L, basal portion of the mesial carina in: K, mesial; L, labial view. M–N, apical portion of the distal carina in: M, distal; N, lingual view. O–P, mid-crown portion of the distal carina in; O, distal; P, lingual view. Q–R, basal portion of the distal carina in: Q, distal; R, lingual view. *Abbreviations*: cap, crown apex; ce, cervix; dca, distal carina; de, denticle; flu, flute; idsp, interdenticular space; mca, mesial carina; tun, transverse undulation; wfa, wear facet. Scale bars represent: 10 mm (A–E); 0.5 mm (F); 1 mm (G–R).

TABLE 2. Classification of the Wadhurst Clay Formation theropod tooth morphotypes I–V based on the machine learning analyses.

	Hendrickx *et al.* (2020) training data		
	Prediction and posterior probability		
	C5.0	Random forest	Mixture discriminant analysis
Morphotype I (BEXHM 1995.485)	Dromaeosauridae (0.67)	Spinosauridae (0.23)	Spinosauridae (0.99)
Morphotype II (BEXHM 2002.50.123)	Tyrannosauridae (0.61)	Non-megalosaurian Megalosauroidea (0.37)	Non-megalosaurian Megalosauroidea (0.39)
Morphotype III (BEXHM 2002.50.124)	Dromaeosauridae (1.0)	N/A	N/A
Morphotype IV (BEXHM 2005.29)	Non-megalosaurian Megalosauroidea (0.61)	Non-megalosaurian Megalosauroidea (0.30)	Spinosauridae (0.44)
Morphotype V (NHMUK PV R37630)	Dromaeosauridae (0.77)	Dromaeosauridae (0.55)	Dromaeosauridae (0.90)
	Wills *et al.* (2023) training data		
Morphotype I (BEXHM 1995.485)	Dromaeosauridae (0.71)	Dromaeosauridae (0.58)	Baryonychinae (0.77)
Morphotype II (BEXHM 2002.50.123)	Spinosauridae (0.28)	N/A	N/A
Morphotype III (BEXHM 2002.50.124)	Dromaeosauridae (1.0)	Dromaeosauridae (0.99)	Dromaeosauridae (1.0)
Morphotype IV (BEXHM 2005.29)	Tyrannosauroidea (0.37)	Dromaeosauridae (0.41)	Baryonychinae (0.51)
Morphotype V (NHMUK PV R37630)	Dromaeosauridae (0.75)	Dromaeosauridae (0.91)	Dromaeosauridae (1.0)

Numbers in parentheses represent the posterior probabilities.

with no additional trees found following the round of TBR. BEXHM 2005.29 was positioned at the base of Piatnitzkysauridae within a polytomous Megalosauroidea (Fig. 6G), a topology supported by three characters: distal denticles larger than mesial ones (DSDI > 1.2; Ch. 105: 2) and pronounced, closely packed transverse undulations (Ch. 113:2, Ch. 114: 1; Fig. 10). The unconstrained search of this dataset recovered 117 trees (TL = 1069; CI = 0.243; RI = 0.582), with 660 trees found following the additional round of TBR. The strict consensus collapsed all non-outgroup OTUs into a large polytomy, with few forming recognizable clades (e.g. Spinosauridae). BEXHM 2005.29 was one of several OTUs outside of any of the recovered clades. A total of 38 wildcard OTUs were identified via the *iterPCR* procedure, and their pruning produced a reduced consensus that placed BEXHM 2005.29 at the base of a polytomous clade containing ceratosaur, piatnitzkysaurid, dromaeosaurid, tyrannosauroid and megaraptoran OTUs.

The unconstrained analysis of the crown-only matrix recovered 162 trees (TL = 645; CI = 0.247; RI = 0.626), with 6210 trees found following the round of TBR. The strict consensus recovered a relatively well-resolved tree containing few natural clades (e.g. spinosaurids, abelisaurids). BEXHM 2005.29 was positioned at the base of a clade containing a mix of early-diverging neotheropods, ceratosaurs, megalosaurids, carcharodontosaurids and spinosaurids. The *iterPCR* identified 8 wildcard OTUs, and their pruning did not affect the placement of BEXHM 2005.29, which is weakly supported (Bremer support value = 1).

The results of the discriminant analyses (Fig. 6H) classified BEXHM 2005.29 as a metriacanthosaurid allosauroid when using the whole dataset (PC1 = 51.01%,

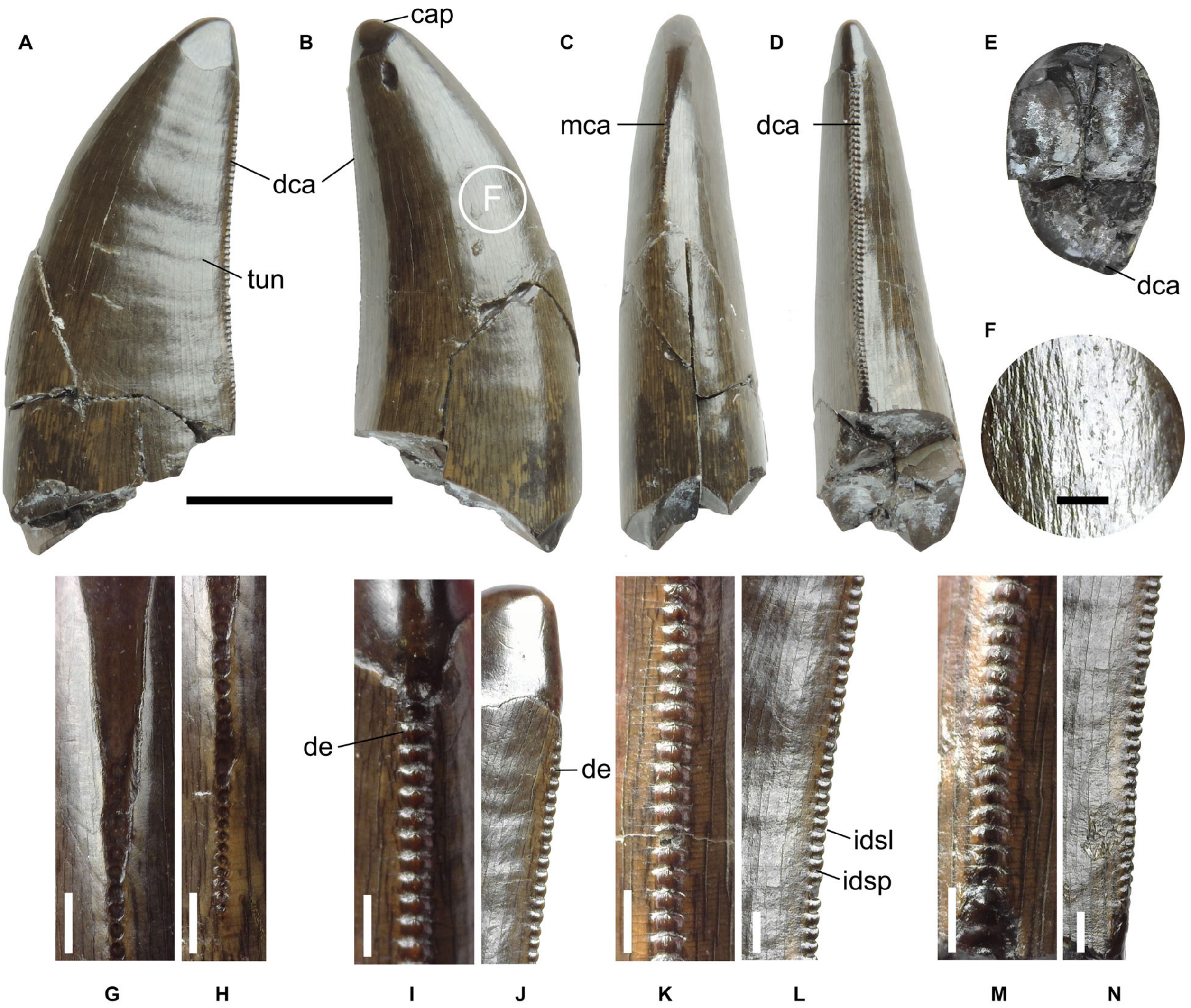

FIG. 8. Morphotype II (BEXHM 2002.50.123) in: A, labial; B, lingual; C, mesial; D, distal; E, basal view. F, close-up of the enamel texture. G–H, mesial carina in mesial view, showing the remnants of the apicocentral preserved denticles (G) and the basal extent of the carina (H). I–J, apical portion of the distal carina in: I, distal; J, labial view. K–L, mid-crown portion of the distal carina in: K, distal; L, labial view. M–N, basalmost preserved portion of the distal carina in: M, distal; N, labial view. *Abbreviations*: cap, crown apex; dca, distal carina; de, denticle; idsl; interdenticular slit; idsp, interdenticular space; mca, mesial carina; tun, transverse undulation. Scale bars represent: 10 mm (A–E); 0.5 mm (F); 1 mm (G–N).

PC2 = 19.8%), or among Megalosauroidea when analysing the whole dentition dataset when the absence of serrations was considered inapplicable (PC1 = 50.21%, PC2 = 10.04%), as well as both iterations of the personal dataset (PC1 = 54.27–57.1%; 21.9–22.94%). The datasets focusing on large teeth consistently classified the specimen as a dromaeosaurid, including both the whole and personal datasets and the versions in which the absence of serrations was considered inapplicable (PC1 = 37.95–56.15%, PC2 = 23.97–30.84%). Only a single unpublished dromaeosaurid specimen was included in these large-teeth-only datasets, known from mesial dentition and originating from the Cenomanian Ulansuhai Formation of Inner Mongolia (Hendrickx *et al.* 2015b). Reclassification rates recovered by the clade-level analyses are low throughout, ranging between 58.4% and 62.07%.

Taxon-level analyses of the whole datasets, including iterations in which the absence of serrations was considered inapplicable and those limited to large teeth only, classified BEXHM 2005.29 as *Berberosaurus* (identified as a non-abelisaurid ceratosaurian in the context of these analyses; PC1 = 35.5–42.86%, PC2 = 17.09–27.82%). The taxon-level analysis of the personal dataset also classified

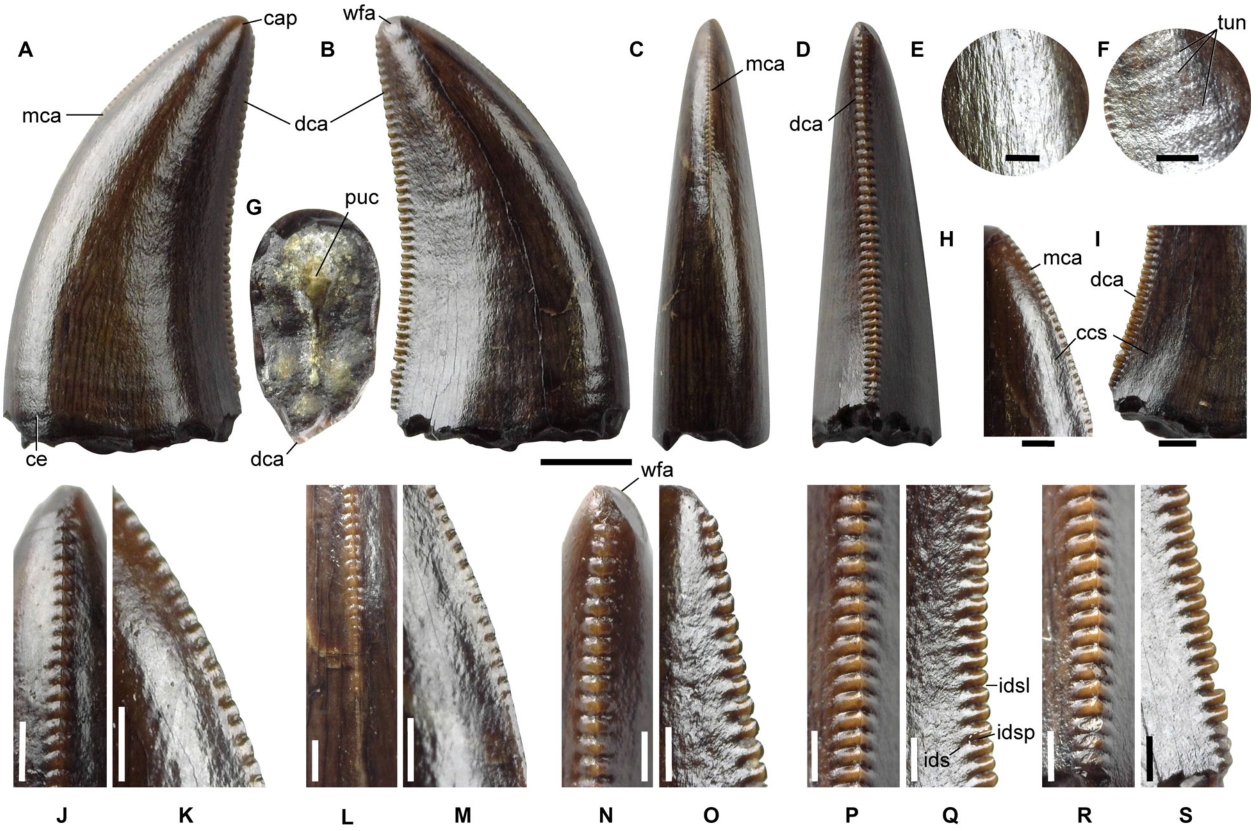

FIG. 9. Morphotype III (BEXHM 2002.50.124) in: A, lingual; B, labial; C, mesial; D, distal view. E–F, close-up of the: E, enamel texture; F, transverse undulations. G, specimen in basal view. H–I, close-up of the concave surfaces along the: H, mesial; I, distal labial carina. J–K, apical portion of the mesial carina in: J, mesial; K, labial view. L–M, basalmost portion of the mesial carina in: L, mesial; M, labial view. N–O, apical portion of the distal carina in: N, distal; O, lingual view. P–Q, mid-crown portion of the distal carina in: P, distal; Q, lingual view. R–S, basalmost portion of the preserved distal carina in: R, distal; S, lingual view. *Abbreviations*: cap, crown apex; ccs, concave surface; dca, distal carina; ids, interdenticular sulci; idsl, interdenticular slit; idsp, interdenticular space; mca, mesial carina; puc, pulp cavity; tun, transverse undulation; wfa, wear facet. Scale bars represent: 2 mm (A–D, G); 0.5 mm (E, H, J–S); 1 mm (F, I).

BEXHM 2005.29 as *Berberosaurus* (PC1 = 57.1%, PC2 = 21.9%), whereas the version for which the absence of serrations was considered inapplicable, as well as the iterations of the personal dataset focusing on large teeth only, classified the specimen as cf. Baryonychinae (PC1 = 41.4–54.26%, PC2 = 18.44–25.67%). The latter is based on XMDFEC V0010, which was initially considered to be a late-surviving baryonychine (Hone *et al.* 2010) but found in subsequent analyses to be outside of Spinosauridae altogether (Katsuhiro & Yoshikazu 2017; Buffetaut *et al.* 2019; Soto *et al.* 2020; Barker *et al.* 2023). As above, reclassification rates for these taxon-level analyses are low, ranging between 57.46% and 63.74%.

The machine learning results for BEXHM 2005.29 are ambiguous, with it variously falling within Megalosauroidea, Baryonychinae, Spinosauridae, Tyrannosauroidea and Dromaeosauridae (Table 2). However, two of the six models support inclusion within Megalosauroidea.

Morphotype V

The results of the constrained search on the whole dentition matrix returned 2 trees (TL = 1311; CI = 0.198; RI = 0.456); 3 trees were found following TBR. NHMUK PV R37630 was placed at the base of a polytomous Tyrannosauroidea following a strict consensus of the recovered trees, which included several other early-diverging tyrannosauroid OTUs and a resolved branch containing Tyrannosauridae (Fig. 6I). This contrasts with the results of the constrained analysis of the same dataset using all the Wadhurst Clay formation morphotypes studied herein, which found NHMUK PV R37630 to nest within Dromaeosauridae (Fig. 4). Tyrannosauroidea is united by nine synapomorphies (mostly consisting of mesial dental characters) of which two are present in NHMUK PV R37630: 16–29 distal mid-crown denticles per 5 mm (Ch. 89:1) and short, poorly developed interdenticular sulci

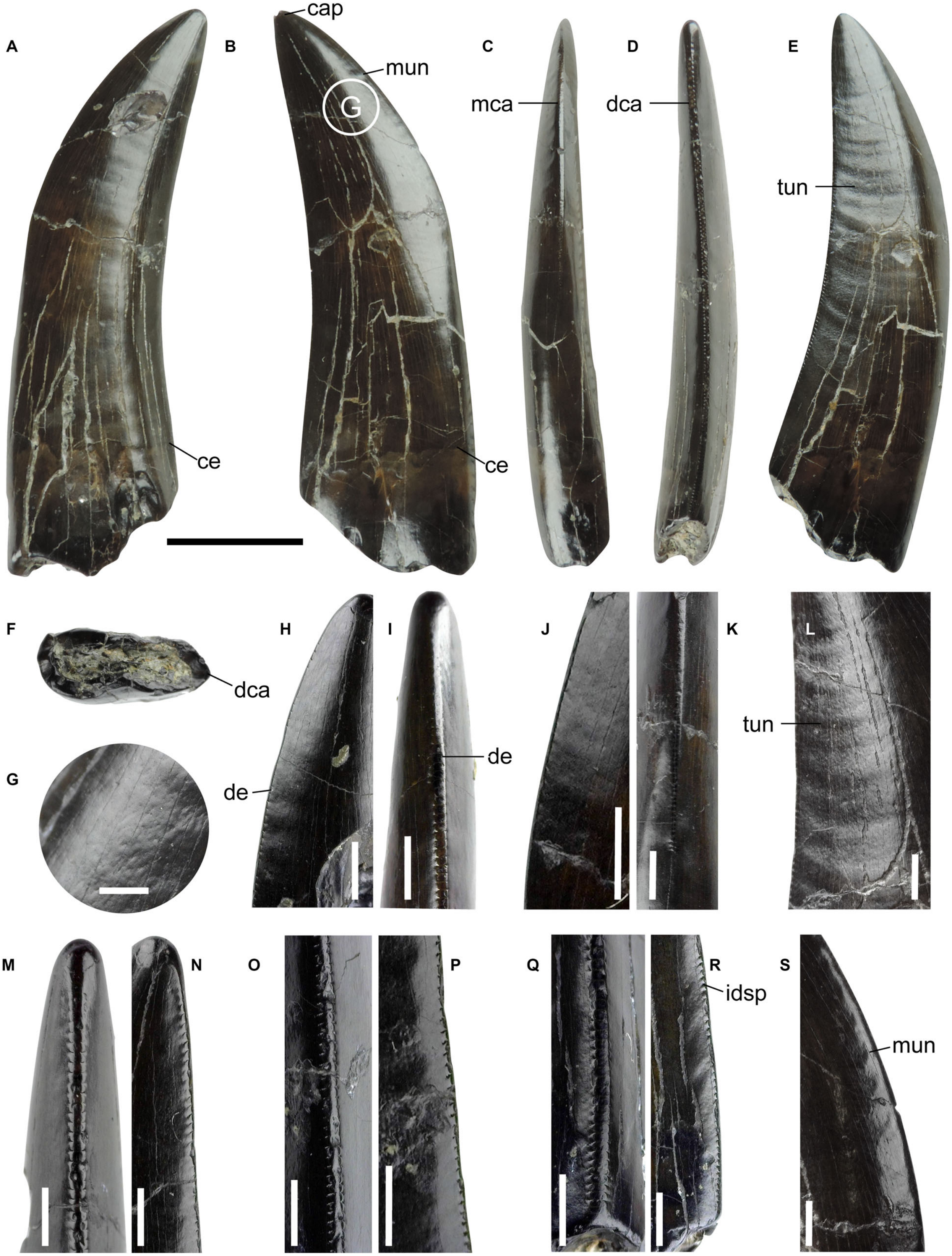
A
B
cap
mun
G
C
mca
D
dca
E
tun
ce
ce
F
dca
G
H
de
I
de
J
K
L
tun
M
N
O
P
Q
R
idsp
S
mun

FIG. 10. Morphotype IV (BEXHM 2005.29) in: A, lingual; B, labial; C, mesial; D, distal; E, labiodistal (emphasizing the transverse undulations); F, basal view. G, close-up of the enamel texture in the circled area in B. H–I, apical portion of the mesial carina in: H, lingual; I, mesial view. J–K, basalmost portion of the mesial carina (around the level of the mid-crown) in: J, lingual; K, mesial views. L, close-up of the transverse undulations in labial view (distal side). M–N, apical portion of the distal carina in: M, distal; N, lingual view. O–P, mid-crown portion of the distal carina in: O, distal; P, lingual view. Q–R, basalmost preserved portion of the distal carina in: Q, distal; R, lingual view. S, close-up of the marginal undulations in labial view (mesial side). *Abbreviations*: cap, crown apex; dca, distal carina; de, denticle; idsp, interdenticular space; mca, mesial carina; mun, marginal undulation; tun, transverse undulation. Scale bars represent: 10 mm (A–F); 1 mm (G); 2 mm (H–S).

present between distal mid-crown denticles (Ch. 109; Fig. 11).

The unconstrained search on the same dataset returned 232 trees (TL = 1064; CI = 0.244; RI = 0.584); 840 were recovered following the additional round of TBR. The strict consensus was relatively well resolved but contained few recognizable clades. NHMUK PV R37630 was positioned within a polytomous clade alongside various ceratosaurian, early-diverging coelurosaurian, tyrannosauroid, megaraptoran and dromaeosaurid OTUs, some of which formed small clades of their own. The *iterPCR* procedure found NHMUK PV R37630 to be one of four unstable OTUs, and as such a reduced consensus was not attempted.

Finally, the unconstrained analysis of the crown-only matrix produced 210 trees (TL = 643; CI = 0.247; RI = 0.627), with 64 941 trees recovered following the round of TBR. The strict consensus found all non-outgroup OTUs within a single large polytomy that contained several internal clades, although few are recognizable (e.g. abelisaurids, spinosaurids). NHMUK PV R37630 was one of many singleton OTUs located outside of any of the recovered clades. A total of 52 wildcard OTUs were identified by the *iterPCR* procedure, and the reduced consensus following their pruning found NHMUK PV R37630 in a polytomous and weakly supported (Bremer support value = 1) clade alongside *Megaraptor* and a lineage containing the dromaeosaurids *Deinonychus*, *Saurornitholestes* and *Atrociraptor*.

The results of the DFAs (Fig. 6J) recovered a largely dromaeosaurid signal for NHMUK PV R37630. While clade-level analyses using iterations of the whole dentition datasets including all tooth sizes classified the specimen as a noasaurid (RR = 61.02–61.99%), the tooth was consistently recovered as a dromaeosaurid when using the personal datasets (RR = 59.19–59.36%). Analyses of the whole dataset focusing on small teeth classified NHMUK PVR 37630 as a megalosaurid at the clade level (RR = 62.02–62.45%) and as *Deinonychus* at the genus level (RR = 64.72–68.14%). Dromaeosaurid affinities for this specimen were also consistently found at the genus level, which was either found to be similar to an unnamed dromaeosaurid taxon (whole dentition dataset, RR = 61.17%) or as *Deinonychus* (whole dentition dataset when the absence of denticles was considered inapplicable, RR = 59.37%; personal datasets, RR = 60.37–63.74%). Reclassification rates for the DFAs were nevertheless generally low.

The machine learning unambiguously classified NHMUK PV R37630 in Dromaeosauridae in all models irrespective of the training data used (Table 2). The posterior probabilities range from 0.55 (RF model on Hendrickx *et al.* (2020) data) to 1.0 (MDA model on Wills *et al.* (2023) data), with three out of the six models reporting posterior probabilities >0.9 and five out of the six reporting >0.75.

SYSTEMATIC PALAEONTOLOGY

Morphotype I

THEROPODA Marsh, 1881
TETANURAE Gauthier, 1986
SPINOSAURIDAE Stromer, 1915
Gen. et sp. indet.
Figures 3A, 7

Material. BEXHM 1995.485, an isolated crown (Fig. 7).

Locality & horizon. ‘Conglomerate Bed’, Wadhurst Clay Formation (Valanginian), Pevensey Pit, Ashdown Brickworks (TQ 720095) on Turkey Road (near Bexhill), East Sussex (UK).

Description. BEXHM 1995.485 is a well-preserved conidont crown, missing only the basal portions of the mesial and distal carina (Fig. 7A–D): the mesial carina is missing from the mid-crown, while the distal one is chipped in its basal quarter (their respective basal extremities are nevertheless preserved). The apex is incipiently worn, and some denticles appear slightly worn in this region. A small chip on the distal carina is present apically. A few minor cracks are observed across the enamel surface. The slight distal curvature allows mesiodistal orientation of the specimen, although it is less easy to determine between the labial and lingual surfaces. Ultimately, we used the slight inclination of the crown in distal view to differentiate the labial surface from the lingual one (Fig. 7C, D).

This specimen is weakly compressed labiolingually (CBR = 0.78; Fig. 7E) and moderately elongate (CHR = 2.29),

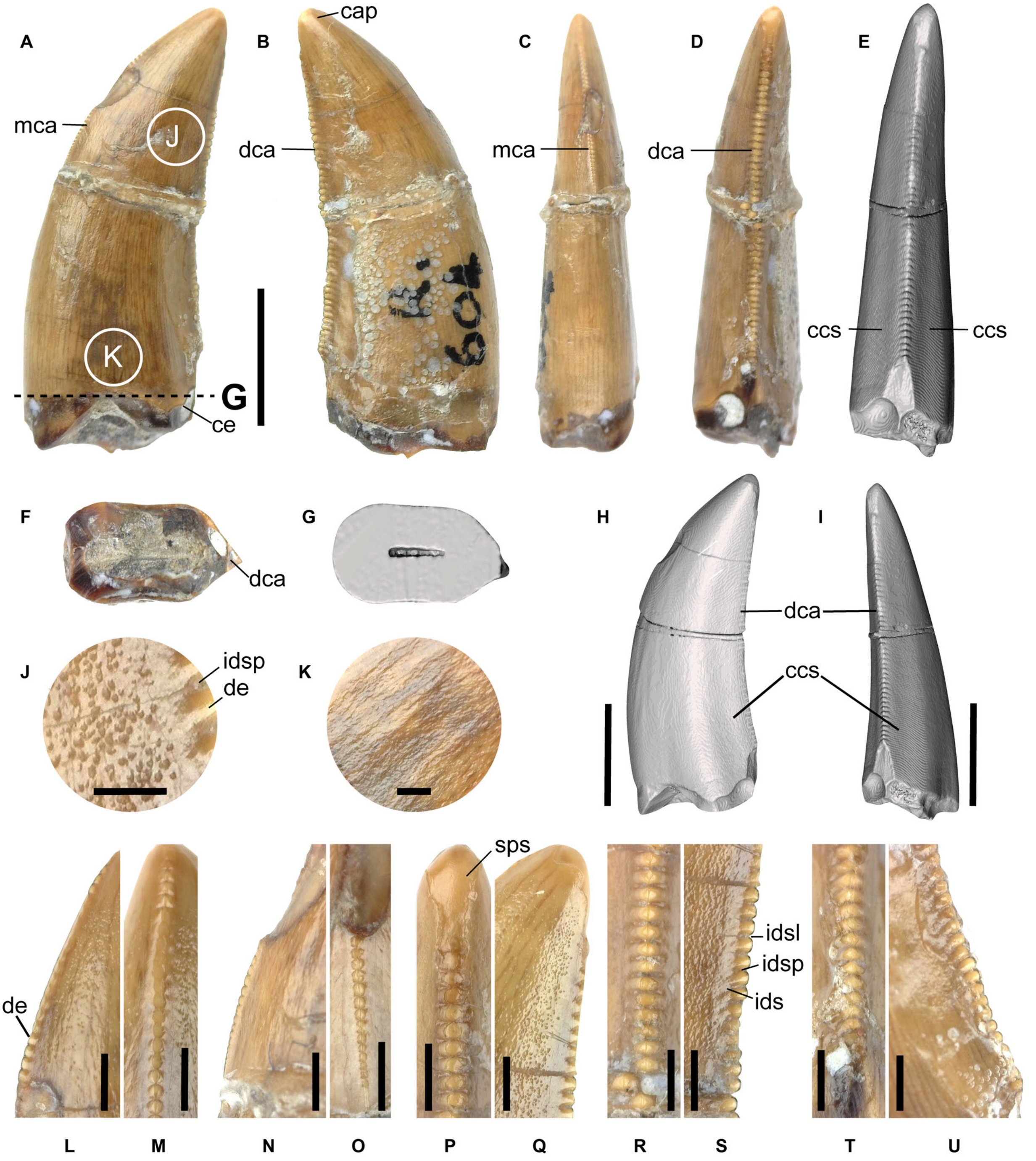

FIG. 11. Morphotype V (NHMUK PV R37630) in: A, lingual; B, labial (note the glue and old accession number on this surface); C, mesial; D–E, distal (E is a volume rendering); F–G, basal view. G is a volume rendering of the basal cross-section taken at the cervix; note the incipient constriction around the level of the midpoint. H–I, volume render emphasizing the concave surfaces adjacent to the distal carina, in: H, lingual; I, labiodistal view. J–K, close-up of the enamel texture in the circled areas in A at the: J, apex; K, base of the crown. L–M, apical portion of the mesial carina in: L, lingual; M, mesial views. N–O, basalmost portion of the mesial carina (around the level of the mid-crown) in: N, lingual; O, mesial view. P–Q, apical portion of the distal carina in: P, distal; Q, lingual view. R–S, mid-crown portion of the distal carina in: R, distal; S, lingual view. T–U, basalmost preserved portion of the distal carina in: T, distal; U, lingual view. *Abbreviations*: cap, crown apex; ccs, concave surface; ce, cervix; dca, distal carina; de, denticle; ent, enamel texture; ids, interdenticular sulcus; idsl, interdenticular slit; idsp, interdenticular space; mca, mesial carina; sps, spalled surface. Scale bars: (A–I) 5 mm, (J–K) 0.5 mm, (L–U) 1 mm.

with a subcircular basal and mid-crown (MCR = 0.73) cross-section. The mesial margin is convex and the distal one is slightly concave, imparting a weak distal curvature that roughly positions the crown's apex around the same level as the distal profile when viewed from the side. The labial and lingual surfaces are distinctly convex, and labial or lingual depressions are absent. The enamel extends basally slightly more centrally on the labial surface, imparting a more convex cervical margin relative to the straighter contralateral side.

The well-developed mesial and distal carinae are apicobasally extensive, running from the apex to just below the cervix (Fig. 7C, D). Both are denticulated, straight and centrally located when viewed mesially and distally, respectively (Fig. 7C, D). Concave surfaces adjacent to the carinae are absent.

A large number of minute denticles are present mesially and distally (Fig. 7G, H, J, M–P), oriented perpendicular to the crown surface, and show an irregular change in size along the carina. The number of denticles are easier to observe along the mid-crown regions compared with the apex, where it seems that the colouration and reflectiveness of the tooth, combined with the above-described wear, complicate the interpretation of apical denticles over a 5 mm distance (e.g. Fig. 7H vs Fig. 7P). Nevertheless, closest to the apex, around 9 denticles per millimetre are present on both mesial and distal carinae while 7 denticles per 5 mm are present at the level of the distal mid-crown. The number of basal denticles and the DSDI cannot be calculated due to damage to the mesial carina, while apicocentral denticles (at two-thirds CH) must have been present originally but are difficult to count due to wear. The denticles are mesiodistally subrectangular (MHR = 1.59; DHR = 1.13) and have largely planar external margins (e.g. Fig. 7P). The interdenticular spaces are typically wide (Fig. 7P), measuring over one-third of a denticle's apicobasal length, while the interdenticular slits are shallowly convex and lack an adjoining lamina when present; indeed, such slits appear negligible between many denticle pairs. Interdenticular sulci are absent.

BEXHM 1995.485 possesses fluted enamel surfaces: 7 flutes are present on the labial surface and 9 flutes on the lingual (Fig. 7A, B). The latter are better defined and more apicobasally extensive. Transverse undulations are present (Fig. 7A, F), most visible in the basal region, and some poorly visible ones extend beyond the cervix onto the root. While most are generally visible (albeit indistinct) and widely spaced (transverse undulation density = 2–3), one is pronounced and forms a protruding convex band (Fig. 7B). Marginal undulations are absent. The enamel possesses a distinctly veined texture across both labiolingual surfaces (Fig. 7F). This coarse enamel texture is apicobasally oriented centrally, although the marginal portions curve towards the carinae (e.g. Fig. 7P).

Identification. BEXHM 1995.485 was initially described as originating from the 'Ashdown Sands (Hauterivian)' of the Ashdown Brickworks and noted to possess carinae that 'do not extend the full distance to the base of the crown' by Charig & Milner (1997). This is erroneous: the Ashdown Formation is not exposed at the locality, the specimen is Valanginian in age, and the basalmost portions of both mesial and distal carinae do extend beyond the cervix (Fig. 7L, R) (Barker *et al.* 2023).

The spinosaurid affinities of BEXHM 1995.485 are unambiguous, despite the unusual results generated by select machine learning analyses. The referral of isolated Wealden Supergroup spinosaurid remains to *Baryonyx* was standard procedure until recently (Naish 2011), as evidenced by Charig & Milner's (1997) referral of the specimen to that genus. Our results do not support this classification, contra Charig & Milner (1997). In keeping with recent work (Barker *et al.* 2023), the automatic referral of isolated Wealden spinosaurid material to the genus is probably premature, and would appear to underestimate diversity of the clade within this temporally extensive succession. As noted elsewhere, the presence of a genus such as *Baryonyx* spanning such a range of geological time would be unusual (Naish 2011). Furthermore, BEXHM 1995.485 differs from *Baryonyx* in possessing labiolingually fluted crowns, and more resembles other Hastings and Wealden Group specimens in these features (Barker *et al.* 2021, 2023). Nevertheless, dental and morphological variation, including the number and position of flutes, may be under ontogenetic or positional control (Hendrickx *et al.* 2016, 2019). Our analyses also indicate that there is no reason to refer BEXHM 1995.485 to '*Suchosaurus*'. When also considering the wildcard status of the specimen in some of our phylogenetic analyses, and the ambiguity surrounding the validity of Baryonychinae more generally (Evers *et al.* 2015; Sales & Schultz 2017; Barker *et al.* 2021), we propose that this specimen is best interpreted as an indeterminate spinosaurid.

BEXHM 1995.485 differs from some other European spinosaurid teeth in its possession of a denticulated, basally extensive mesial carina that runs beneath the cervix; some Iberian specimens differ in that they may have an apically restricted mesial carina (Alonso *et al.* 2018; Isasmendi *et al.* 2020) or lack mesial denticles (Alonso & Canudo 2016). Spinosaurid crowns with apically restricted mesial carina are presently unknown from the Wealden Supergroup, although we note that further investigation of historical collections is required to better gain appreciation of morphological disparity. Wealden specimens lacking denticulated carinae are known ('*Suchosaurus cultridens*' specimens among them; Owen 1842), but this condition is probably a product of taphonomy (Buffetaut 2007) and serrations are present in the basal portion of the distal carina in the '*Suchosaurus cultridens*' holotype (CH pers. obs. 2015).

Morphotype II

COELUROSAURIA von Huene, 1914
TYRANNOSAUROIDEA Osborn, 1906
Gen. et sp. indet.
Figures 3B, 8

Material. BEXHM 2002.50.123, an isolated crown (Fig. 8).

Locality & horizon. '*Polacanthus* Bed', Wadhurst Clay Formation (Valanginian), Pevensey Pit, Ashdown Brickworks (TQ 720095) on Turkey Road (near Bexhill), East Sussex (UK).

Description. BEXHM 2002.50.123 can be oriented along its mesiodistal axis based on the distal curvature when viewed from the side (Fig. 8A, B). The slightly lingually trending mesial carina and labially offset distal carina provide labiolingual orientation (Fig. 8C–E) (Hendrickx *et al.* 2015a).

The specimen is a decently preserved crown, broken around the distobasal region, with a well-preserved mesiobasal region that appears to approximate the level of the cervix. Several large cracks are noticeable on the labiolingual and mesial surfaces. The mesial carina is extensively worn, although the basalmost denticles can be partially observed (Fig. 8C, H). The apical- and basal-most portions of the preserved distal carina are also worn, and the basalmost portion is incomplete as a result of the break. A small, centroapically positioned chip is present on the lingual surface.

BEXHM 2002.50.123 is a ziphodont crown bearing moderate apicobasal elongation (estimated CHR = 2.18) and labiolingual compression (estimated CBR = 0.63). The distal curvature generated by the convex mesial margin and slightly concave distal one means that the apex is largely in line with the distal profile when viewed laterally (Fig. 8A, B). Both lingual and labial surfaces are strongly convex, although the distobasal region of the latter is slightly flattened when viewed basally (Fig. 8E). Preservation precludes description of the enamel extension at the cervix, but enough of the basal region of the crown is preserved to suggest the absence of labial or lingual depressions.

Denticulated mesial and distal carinae are both present (Fig. 8G–N), the former terminating well above the cervix compared with the more apicobasally extensive distal one (Fig. 8C, D). The mesial carina is straight with a minor lingual trend in mesial view while the distal one is markedly deflected labially, rendering the crown highly asymmetrical when viewed distally (Fig. 8C–E). Based on our CH estimates and development of the basal distal carina, BEXHM 2002.50.123 is likely to have possessed a lanceolate mid-crown and basal cross-section.

Mesial denticles are preserved only in their basalmost portion and provide few morphological details (Fig. 8G, H). 20 denticles are present on the basalmost 5 mm of the mesial carina, which show regular size variation and basally reducing dimensions. 18 mesial denticles per 5 mm are present at the estimated two-thirds height of the crown.

The distal denticles are mostly well preserved and show regular size variation along the carina (Fig. 8I–N). 15 denticles per 5 millimetres are observed along the distal carina at mid-crown, although denticle numbers at the apex and base could not be calculated due to wear. A DSDI of 1.2 is estimated for this specimen. The distal denticles have subquadrangular morphologies (DHR *c.* 1) oriented perpendicular to the carina (e.g. Fig. 8J). Their external margins are symmetrically convex, and the distal series have shallowly parabolic outlines (e.g. Fig. 8J, L, N). The interdenticular space is broad, exceeding half the apicobasal height of the denticles, while the interdenticular slit is concave, relatively pronounced and lacks associated laminae (e.g. Fig. 8J, L, N). The interdenticular diaphysis cannot be observed due to mineral infill in this region. Interdenticular sulci are absent.

Weakly developed, widely spaced transverse undulations (3 per 5 mm) are present on both sides, extending for much of the apicobasal height (Fig. 8A). Flutes, marginal undulations and longitudinal grooves and ridges are absent. The enamel texture is weakly braided (Fig. 8F), with the ridges oriented apicobasally in the centre of the crown and more diagonally closer to the distal margins.

Identification. BEXHM 2002.50.123 is somewhat labiolingually broad (CBR = 0.63), as is typical of mesial dentition in ziphodont theropods. However, it lacks a lingually spiralling or lingually facing mesial carina, carina-adjacent concave surfaces, fluted enamel, or the longitudinal ridges or grooves typically seen in theropod mesial teeth (Hendrickx *et al.* 2015a). We thus consider BEXHM 2002.50.123 to represent a lateral tooth.

With the afore-described morphometric assumptions in mind, the cladistic analyses of the whole dentition matrix repeatedly recovered tyrannosauroid affinities for BEXHM 2002.50.123, with the constrained analyses placing it among non-tyrannosaurid tyrannosauroids (Figs 4, 6C). In contrast, the discriminant analyses generally classified the specimen among megalosauroids (e.g. piatnitzkysaurids) or dromaeosaurids. Interestingly, the recovered tyrannosauroid and dromaeosaurid signals (Table 3) echo previous works that have noted dental similarities between members of both clades (Rauhut *et al.* 2010; Williamson & Brusatte 2014). The machine learning analysis supports tyrannosauroid affinities for BEXHM 2002.50.123, with this result being recovered as the highest or second highest posterior probability in all classifiers. A summary of the morphological comparisons is given in Table 3.

We confidently reject a megalosauroid affinity for BEXHM 2002.50.123: ziphodont forms (i.e. piatnitzkysaurids, megalosaurids) are restricted to Jurassic strata (Rauhut 2003; Carrano *et al.* 2012), and there is no evidence of relict populations persisting in the Early Cretaceous of England. Furthermore, it lacks the centrally positioned distal carina described in megalosaurid lateral teeth, the variably developed interdenticular sulci seen in megalosaurids and piatnitzkysaurids, or the numerous transverse undulations that are synapomorphic for the latter clade (Hendrickx *et al.* 2015b, 2019).

A denticulated mesial carina that does not reach the cervix is present in some tyrannosauroids (e.g. *Eotyrannus*) but also in neovenatorids (e.g. *Neovenator*; in contrast, some allosauroids possess a more extensive mesial carina) and various dromaeosaurids (Hendrickx *et al.* 2019). Similarly, the strong labial displacement of the distal carina is synapomorphic for both mesial and lateral dentition in Tyrannosauroidea but is also present in some lateral teeth of *Neovenator* and certain dromaeosaurids (Table 3) (Brusatte *et al.* 2008; Hendrickx *et al.* 2019; Wills *et al.* 2023). Braided enamel texture is also present in a range of theropods including tyrannosauroids and dromaeosaurids (Hendrickx *et al.* 2019; Young *et al.* 2019). The relative estimated thickness of BEXHM 2002.50.123 (CBR = 0.63) is also closer to the condition seen in some tyrannosauroid lateral teeth (CBR > 0.64) (assuming our positional inference is correct) and is dissimilar to the narrower condition present in the dromaeosaurid lateral dentition (such CBR values are more typical of the mesial dentition in the latter clade) (Hendrickx *et al.* 2019).

A neovenatorid referral of BEXHM 2002.50.123 would be inconsistent with the results presented above. The specimen lacks the concave surfaces adjacent to the carina seen in lateral

TABLE 3. Morphological comparisons of lateral tooth characters between the ziphodont specimens from the Wadhurst Clay Formation and select theropod clades discussed in text.

	den	bco	CBR >0.64	CH (cm)	udca	umca	cos	8	mde	tmca	ddca	des	hd	md≠dd	codm	flu	tun	mun	ids	lri-lgr	ent
Piatnitzkysauridae	Z	0	M	3–6	0	0	0	0	1	la	la	~	1	<	0	0	1	1	1	0	B
Neovenator	Z	0	M	3–6	0	0	w	0	0	0	la	~	0	0	0	0	1	1	1	la-lri	B
Proceratosauridae	Z	m	M	1–6	0	0	M	1	0	w	w	~	0	<	0	0	1	0	1	m-bst	B
Pantyrannosauria	[ZP]	0	w	4–15	0	0	M	1	1	la	w	~	0	</la>**	0	la	1	1	1	m-lri	[BI]
Halzskaraptorinae	Z	M	?	<1	W	W	0	0	–	–	–	–	–	–	0	0	0	0	–	0	I
Unenlagiinae	[ZC]	0	M	<3	W	W	?	1	–	–	–	–	–	–	0	w	0	0	–	la-lri	I
Microraptorinae	Z	L	M	<3	w	W	M	1	0	M	M	>>	0	<	0	la	0	0	1	la-lri	[BI]
Velociraptorinae	Z	0	M	<4	0	w	M	1	1	w	M	~	1	<	0	m	1	0	1	la-lri	[BI]
Dromaeosaurinae	Z	0	M	1–5	0	0	M	1	1	w	w	~	1	la>	0	0	1	0	1	0	[BI]
Morphotype II (BEXHM 2002.50.123)	Z	0	0 (est.)	2.45 (est.)	0	0	0	0	0	0	1	~	0	<	0	0	1	0	0	0	B
Morphotype III (BEXHM 2002.50.124)	Z	0	0	0.916	0	0	1	1	0	0	0	~	0	–	0	0	1	0	1	0	B
Morphotype IV (BEXHM 2005.29)	Z	0	0	3.375	0	0	0	0	0	0	0	~	0	<	0	0	1	1	0	0	B
Morphotype V (NHMUK PV R 37630)	Z	0	0	1.58	0	0	1	1	0	0	0	~	0	<	0	0	0	0	1	0	[BI]

Theropod clades chosen based on the results of the cladistic and quantitative analyses. Modified from Hendrickx *et al.* (2019). Letters in brackets indicate polymorphic features.

Abbreviations: 0, absent; 1, present in at least some teeth or some taxa; 8, figure-eight-shaped cross-section at the cervix; ?, unknown; –, inapplicable; ~, medium-sized denticles (i.e. between 15 and 250 denticles on the carina); ≠, difference between mesial and distal denticles; <, distal denticles significantly larger than mesial ones (denticle size density index (DSDI) >1.2); >, mesial denticles significantly larger than distal ones (DSDI <0.9); >>, large denticles (i.e. fewer than 15 denticles on the carina); B, braided texture; bco, basal constriction at the cervix; bst, basal striations; C, conidonty (dentition with conical crowns); CBR, crown–base ratio; CH, crown height in the largest teeth; codm, convex distal margin; cos, concave surface adjacent to carinae; ddca, displaced distal carina; dd, distal denticles; den, dentition type; des, denticle size; est., estimated values/scores based on reconstructed metrics; ent, enamel texture; flu, fluted teeth; hd, hooked denticles; I, smooth or irregular non-oriented texture; ids, interdenticular sulci; L, present in all lateral teeth and, in the case of edentulism, edentulous posterior portion of the maxilla and/or dentary; la, present in some lateral teeth (e.g. la>, mesial denticles significantly larger than distal ones in some lateral teeth; la-lri, longitudinal ridge present in some lateral teeth); lgr, longitudinal groove; lri, longitudinal ridges; M, present in all mesial teeth and, in the case of edentulism, edentulous premaxilla and anterior portion of the dentary; m, present in some mesial teeth (e.g. m<, distal denticles significantly larger than mesial ones in some mesial teeth); md, mesial denticles; mde, mesial denticles reaching the cervix; mun, marginal undulations; P, pachydonty (dentition with particularly thick, blade-shaped crowns); tmca, twisted mesial carina; tun, transverse undulations; udca, unserrated distal carina; umca, unserrated mesial carina; W, present in the whole dentition and, in the case of edentulism, fully edentulous jaws; w, present in some mesial and lateral teeth; Z, ziphodonty (dentition with blade-shaped crowns).

**The dentition of basal tyrannosauroids has a DSDI >1.2 whereas some tyrannosaurid teeth have a DSDI <0.9.

teeth of the clade, or the interdenticular sulci present in *Neovenator* (Brusatte *et al.* 2008) or allosauroids more generally (Hendrickx *et al.* 2019). Interdenticular sulci are variably present in some tyrannosauroid teeth, and short sulci are present in various dromaeosaurids (Hendrickx *et al.* 2019). Nevertheless, such sulci are absent in many non-paravian neocoelurosaurs (Hendrickx *et al.* 2019; Young *et al.* 2019), thus supporting a coelurosaur referral of BEXHM 2002.50.123.

We reject dromaeosaurid affinities for this specimen. The large size tends to preclude dromaeosaurid crowns, and the probable lanceolate basal cross-section contrasts with the figure-eight-shaped morphology observed in many deinonychosaurs (including most dromaeosaurids) (Hendrickx *et al.* 2019; Wills *et al.* 2023).

Summarily, we thus consider the large estimated CH and CBR, lack of basal extension of the mesial carina, strong labial deflection of the distal carina, and braided enamel texture (Hendrickx *et al.* 2019) consistent with a tyrannosauroid identity for BEXHM 2002.50.123; this is also supported by our phylogenetic analyses. In addition, the teeth of tyrannosauroids tend to be less recurved than those of other theropods, a feature also seen in BEXHM 2002.50.123 (Williamson & Brusatte 2014). The dromaeosaurid signal imparted by several quantitative analyses may reflect the homoplasy exhibited by the maniraptorans and tyrannosauroids in question (Rauhut *et al.* 2010; Williamson & Brusatte 2014; Hendrickx *et al.* 2019).

Morphotype III

MANIRAPTORA Gauthier, 1986
DROMAEOSAURIDAE Matthew & Brown, 1922
Gen. et. sp. indet.
Figures 3B, 9

Material. BEXHM 2002.50.124, and isolated crown (Fig. 9).

Locality & horizon. '*Polacanthus* Bed', Wadhurst Clay Formation (Valanginian), Pevensey Pit, Ashdown Brickworks (TQ 720095) on Turkey Road (near Bexhill), East Sussex (UK).

Description. BEXHM 2002.50.124 is a complete and well-preserved crown, lacking a root, and showing minor cracking of its lateral surfaces as well as loss of the basalmost distal denticles (Fig. 9A, B). The mesiodistal orientation is easily recognizable thanks to its distal curvature in lateral view, and the labially offset distal carina helps prescribe the labiolingual surfaces (Fig. 9G) (Hendrickx *et al.* 2015a).

This is a small (CH = 9.16 mm) ziphodont crown. It is moderately apicobasally elongate (CHR = 1.8) and labiolingually compressed (CBR = 0.56), with distal curvature that positions the apex just behind the level of the distal margin due to its highly convex mesial margin and concave distal one (Fig. 9A–D). The crown is straight, lacking any labial or lingual curvature when viewed distally (Fig. 9D). The labial and lingual surfaces both appear planar in their basocentral region.

Mesial and distal carinae are present and both are well developed and denticulated (Fig. 9A, B, J, K), although denticles disappear along the former just above the level of two-thirds crown height, precluding various measurements (e.g. MDH, MDL, MDW, DSDI etc.; Fig. 9A). The same carina is centrally positioned and terminates above mid-crown level. The distal carina is more extensive and reaches the cervix, with slight labial deflection in its basal half when viewed distally. The basal cross-section is incipiently figure-eight-shaped, with a subtle midpoint constriction separating the labiolingually broader mesial portion from the narrower distal part (Fig. 9G). The mid-crown cross-section is lanceolate. Concave surfaces adjacent to both carinae are present on the labial side (Fig. 9H, I). The concavity adjacent to the distal carina is most pronounced basally, disappearing closer to the apex while the mesial concavity extends in parallel along most of the carina's apicobasal extent.

The mesial denticles are apicobasally subrectangular and oriented perpendicular to the carina (Fig. 9K, M). The external margins of the denticles are planar where well preserved, although two non-successive mesial denticles located in the apicocentral region are biconvex. There are 8 denticles per millimetre at the apex. The distal denticles are slightly apicobasally subrectangular to subquadrangular in the apicalmost region (Fig. 9O), becoming mesiodistally subrectangular from around mid-crown level (DHR = 1.17; Fig. 9Q, S), and all are oriented perpendicular to the carina. Five denticles per millimetre are present at the apex and mid-crown, while 6 per millimetre are present basally. The external margins of the denticles are parabolic near the apex (Fig. 9O), whereas the mid-crown and basal denticles have a more semicircular morphology (Fig. 9Q, S). The interdenticular spaces are large and well-developed between both mesial and distal denticles, with the former having shallow and slightly concave-to-triangular interdenticular slits (e.g. Fig. 9K) compared with the more deeply triangular morphology present between distal denticles (e.g. Fig. 9Q); all interdenticular slits lack adjoining laminae. Interdenticular sulci can be observed between a few mid-crown distal denticles, and these are short and poorly developed when present (Fig. 9Q). Both mesial and distal denticles show regular size variation across their respective carinae.

Numerous (*c.* 10 per 5 mm) weakly developed and tenuously visible transverse undulations can be observed (Fig. 9A, B, F). Flutes, marginal undulations, as well as longitudinal grooves and ridges, are absent. The enamel texture is weakly braided (Fig. 9E). A small apical wear facet is preserved on the labial side.

Identification. The labiolingually compressed shape (CBR > 0.64), centrally positioned and denticulated mesial carina, and lack of fluted surfaces or longitudinal ridges or grooves suggest that BEXHM 2002.50.124 is a lateral tooth (Hendrickx *et al.* 2015a). Its small size is potentially problematic given the impact of ontogeny: it may represent a juvenile of a larger ziphodont taxon. Dromaeosaurid affinities are supported by the constrained and unconstrained phylogenetic analyses of the whole dentition dataset, although the discriminant analyses are less consistent, with only one-third recovering a dromaeosaurid signal. The machine learning unambiguously supports the dromaeosaurid affinities of BEXHM 2002.50.124, with four of six models recovering this classification, in each case with posterior probabilities of >0.99. A summary of the morphological comparisons is given in Table 3.

A mesial carina terminating above the root in lateral dentition is synapomorphic for Maniraptora in some analyses (Hendrickx *et al.* 2019), but this is also observed in disparate theropod groups, including neovenatorids and tyrannosauroids (Hendrickx *et al.* 2019), both of which are present in the Wealden Supergroup. Similarly, the lack of a basal constriction is typical of dromaeosaurids (Turner *et al.* 2012), as is small crown size (even in large taxa) and figure-eight-shaped basal cross-section (Hendrickx *et al.* 2019; Wills *et al.* 2023). However, these characters are also seen in a range of non-maniraptoriform theropods including coelurosaurs such as tyrannosauroids (Williamson & Brusatte 2014; Hendrickx *et al.* 2019). Transverse undulations and braided enamel texture are present in many eudromaeosaurians but are also observed in a range of averostran theropods, the former in particular conveying limited grouping information (Hendrickx *et al.* 2019).

Its sister group relationship with *Deinonychus* evidenced by the constrained phylogenetic analysis (Barker *et al.* 2024) confuses the initial referral of the specimen to Velociraptorinae (Austen *et al.* 2010): while sometimes considered a member of the clade (Currie 1995; Turner *et al.* 2012; Averianov & Lopatin 2021), *Deinonychus* has undergone little revision since its initial description, and phylogenetic studies have found it occupying disparate positions within Dromaeosauridae given its mosaic of velociraptorine, saurornitholestine and unique character combinations (Longrich & Currie 2009; Evans *et al.* 2013; Jasinski *et al.* 2020; Powers *et al.* 2022). Indeed, our reduced consensus placed BEXHM 2002.50.124 and *Deinonychus* within a poorly differentiated eudromaeosaurian clade that includes saurornitholestines and dromaeosaurines. The results of the constrained analysis may thus be impacted by the choice of eudromaeosaurian topology.

Hendrickx *et al.* (2019) found only two characters of the premaxillary dentition to unite Velociraptorinae. Similarly, Turner *et al.* (2012) found a single premaxillary tooth character uniting a subset of velociraptorines; both results prevent comparison with BEXHM 2002.50.124. Several of the features listed as typical of velociraptorine lateral teeth by Hendrickx *et al.* (2019) are not unique to the clade (e.g. ziphodonty, serrated mesial and distal carina). BEXHM 2002.50.124 possesses these features and, while having the apically restricted mesial carina and figure-eight-shaped basal cross-section typical of velociraptorines, it differs from many in lacking ridged lateral crowns while presenting transverse undulations more typical of dromaeosaurines (Hendrickx *et al.* 2019). Larger distal denticles relative to mesial denticles has also been used as a synapomorphy for Velociraptorinae (Rauhut & Werner 1995; Sweetman 2004) but this is present in a range of dromaeosaurids (Turner *et al.* 2012; Hendrickx *et al.* 2019) as well as various non-maniraptoriform taxa, including tyrannosauroids (Hendrickx & Mateus 2014; Williamson & Brusatte 2014; Hendrickx *et al.* 2019). The velociraptorine affinities of BEXHM 2002.50.124 are thus ambiguous.

Finally, we draw attention to an unusual feature of BEXHM 2002.50.124 that is atypical of dromaeosaurid lateral dentition (assuming our positional inference is correct): the presence of concave surfaces adjacent to the carinae. These are uncommon in lateral teeth and are instead typical of the mesial dentition (Hendrickx *et al.* 2019). Such concave surfaces are present in the lateral dentition of neovenatorids such as *Neovenator* but are generally lacking in tyrannosauroids (although see our discussion of morphotype V below) (Hendrickx *et al.* 2019).

Overall, we propose that our analyses, combined with our morphological observations, recover sufficient support to classify BEXHM 2002.50.124 within Dromaeosauridae. Moreover, with similarities between dromaeosaurid and tyrannosauroid dentition in mind (Rauhut *et al.* 2010; Williamson & Brusatte 2014), our results were not substantially diluted by a potential tyrannosauroid signal, providing further support for our identification. In view of current uncertainty surrounding eudromaeosaurian interrelationships, the lack of unambiguous velociraptorine lateral tooth synapomorphies, and the varied dromaeosaurid signal recovered in our phylogenetic analyses, we conservatively classify BEXHM 2002.50.124 as an indeterminate dromaeosaurid.

Morphotype IV

?COELUROSAURIA von Huene, 1914
?TYRANNOSAUROIDEA Osborn, 1906
Gen. et sp. indet.
Figures 3D, 10

Material. BEXHM 2005.29, an isolated crown (Fig. 10).

Locality & horizon. ‘Conglomerate Bed’, Wadhurst Clay (Valanginian), Pevensey Pit, Ashdown Brickworks (TQ 720095) on Turkey Road (near Bexhill), East Sussex (UK).

Description. BEXHM 2005.29 is a complete crown and basal part of the root (Fig. 10A–D). Distal curvature provides mesiodistal orientation, while the labially deflected distal carina and lingually deflected mesial carina, combined with the overall curvature of the crown in distal view, provide labiolingual orientation (Hendrickx *et al.* 2015a). The crown is largely complete but polished; wear has eroded all denticles to their basalmost parts. The enamel surfaces are cracked and minor basal crushing is present labially. Chipped regions are present on the mesial carina and apical lingual surface.

This large ziphodont tooth possesses an elongate (CHR = 2.61; Fig. 10A–D), labiolingually compressed (CBR = 0.47; Fig. 10F) crown. It is strongly recurved distally when viewed labiolingually, with convex mesial and concave distal margins, and the apex is positioned behind the distal profile of the crown (e.g. Fig. 10A). The crown curves slightly lingually in distal view (Fig. 10C, D). Its basal cross-section is lanceolate, while the mid-crown cross-section is narrowly lenticular. The enamel appears to extend symmetrically across the tooth. A labial depression is present on the preserved portion of root and does not seem to extend beyond the cervix.

BEXHM 2005.29 possesses denticulated mesial and distal carinae (Fig. 10C, D, H–K, M–R). The slightly lingually deflected mesial carina does not extend as far as the distal one, terminating at around mid-crown level. The distal carina is more extensive, descending beyond the cervix (the full basal extent is not preserved); this basal portion of the carina is denticulated. In addition, the distal carina appears slightly bowed when viewed distally, shifting from a central position apically to a labial position basally. No concave surfaces adjacent to the carinae are observed.

The denticles are poorly preserved and provide little anatomical information. Size variation, at least in terms of denticle length (i.e. MDL, DDL), is regular. Along 5 mm sections of the mesial carina, *c.* 17 denticles are present apically and 22 are observed at mid-crown. Over the same distance on the distal carina, 15 denticles are present apically, 17 are present at mid-crown and 20 are present on the basalmost preserved section (DAVG = 17.3 denticles per 5 mm). Distal denticles are larger relative to mesial denticles (DSDI = 1.29). Interdenticular sulci appear to be absent.

The apex lacks any wear facets or spalled surfaces. Readily visible, numerous and closely spaced (4–5 per 5 mm) transverse undulations are present on both surfaces, covering the majority of apicobasal height (Fig. 10E, L), and marginal undulations are also present. Flutes, striations and longitudinal ridges are absent. The enamel texture is difficult to discern due to the specimen's taphonomically derived polish, but it appears to have been braided (Fig. 10G).

Identification. BEXHM 2005.29 is probably a lateral tooth given its high degree of labiolingual compression (Hendrickx *et al.* 2015a). Its affinities are difficult to resolve based on our analyses, in part due to the limited preserved denticle data (although denticle shape appears to bear little grouping information; Hendrickx *et al.* 2019). The piatnitzkysaurid affinities recovered by the constrained phylogenetic analysis are supported by characters that are widely distributed within Theropoda (e.g. Table 3). Indeed, as mentioned above, transverse undulations and denticle size difference provide little grouping information: numerous transverse undulations are present in many non-neocoelurosaurian avetheropods and some dromaeosaurids, and a DSDI above 1.2 was independently acquired in dilophosaurids, ceratosaurs such as abelisaurids and noasaurids, and tyrannosauroid and dromaeosaurid coelurosaurs (Hendrickx *et al.* 2019). Additional characters that typify piatnitzkysaurid dentition and are present in BEXHM 2005.29 can also be observed in various other theropods: a mesial carina that does not reach the cervix and braided enamel texture, for instance, are present in *Neovenator*, tyrannosauroids and eudromaeosaurians (Hendrickx *et al.* 2019). Furthermore, and as expressed previously, piatnitzkysaurid (or non-spinosaurid megalosauroid; see also our DFA results) affinities are incongruous with the spatiotemporal range of the clade. Combined with the uninformative results obtained from the unconstrained phylogenetic searches and lack of support from most of the quantitative analyses, there is insufficient evidence to refer BEXHM 2005.29 to Piatnitzkysauridae, and its affinities are further examined below.

The dromaeosaurid signal recovered by the discriminant analyses is unexpected, especially given the specimen's crown height. These results tend to associate BEXHM 2005.29 with an unpublished dromaeosaurid specimen known from mesial dentition (see Results section), further complicating comparisons. The machine learning results for BEXHM 2005.29 are equally ambiguous and place the specimen within Megalosauroidea, Baryonychinae, Spinosauridae, Tyrannosauroidea and Dromaeosauridae. Mid-sized (i.e. 2–3 m) Wealden Supergroup dromaeosaurids are known from postcranial material (Longrich *et al.* 2022), but BEXHM 2005.29 exceeds the crown height of Wealden teeth previously referred to this clade (some of which may in fact pertain to tyrannosauroids) (Sweetman 2004; Rauhut *et al.* 2010). The lack of a basal constriction and presence of a highly concave distal margin in the specimen are synapomorphic for Dromaeosauridae, although these characters are not unique to the clade (Hendrickx *et al.* 2019).

Furthermore, the presence of marginal undulations is atypical of dromaeosaurids and more characteristic of large, non-neocoelurosaurian taxa including (among ziphodont forms) non-carcharodontosaurine and neovenatorid allosauroids and various tyrannosauroids (Hendrickx *et al.* 2019). Similarly, the absence of interdenticular sulci is a notable difference from eudromaeosaurians (Hendrickx *et al.* 2019), while extension of the distal carinae well beneath the cervix is unusual for dromaeosaurids generally (it appears present only in *Saurornitholestes*). The latter character instead typifies the lateral dentition of non-neocoelurosaurs, including allosauroids and tyrannosauroids. We thus consider a dromaeosaurid affinity unlikely.

Superficially, BEXHM 2005.29 resembles *Neovenator* in size, labiolingual compression, its flattened basocentral labial surface (synapomorphic of neovenatorids), similar DC values (14.5–18 in *Neovenator*; 17 in BEXHM 2005.29) and presence of numerous transverse undulations (synapomorphic for allosauroid lateral dentition) (Brusatte *et al.* 2008; Hendrickx *et al.* 2019, 2020). However, it differs in aspects that hinder referral to a *Neovenator*-like taxon. The mesial carina and associated serrations terminate around the mid-crown in BEXHM 2009.50, whereas these are restricted to the apical third in *Neovenator* (Brusatte *et al.* 2008; Hendrickx *et al.* 2020). Given our positional inference, the lack of concave surfaces adjacent to the carinae is also dissimilar to at least some *Neovenator* lateral teeth, being closer to the condition present in tyrannosauroids (however, see below) (Hendrickx *et al.* 2019, 2020).

Support for tyrannosauroid affinities also comes from the elevated DSDI: the presence of distal denticles that are large relative to mesial ones is typical of basal tyrannosauroids but observed only in some *Allosaurus* lateral crowns among allosauroids (*Neovenator* has subequal mesial and distal denticles, while carcharodontosaurids have smaller distal denticles compared with mesial ones; see also Table 3) (Hendrickx *et al.* 2019, 2020). In addition, the presence of fewer than 20 distal mid-crown denticles (DC = 17 in BEXHM 2005.29) and between 16 and 29 mesial denticles at two-thirds crown height (*c.* 20 estimated in BEXHM 2005.29) have been recovered as synapomorphies of tyrannosauroid lateral dentition (Hendrickx *et al.* 2019). Interdenticular sulci, which are absent in BEXHM 2005.29, are typical of *Neovenator* teeth (Brusatte *et al.* 2008) and synapomorphic for Allosauroidea more generally (when present along the distal mid-crown) (Hendrickx *et al.* 2019); they are only variably present in tyrannosauroid lateral crowns (Hendrickx *et al.* 2019). If our tyrannosauroid referral is correct, the specimen is notable for its crown height (33.75 mm), which exceeds the largest tooth known for the *Eotyrannus* holotype (26 mm) (Naish & Cau 2022). *Eotyrannus* is currently the largest (*c.* 4.5 m, albeit immature) tyrannosauroid from the UK, and a tyrannosauroid affinity for BEXHM 2005.29 might support the presence of larger specimens within Wealden Supergroup predatory guilds.

In summary, we propose there to be sufficient morphological evidence to tentatively refer BEXHM 2005.29 to Tyrannosauroidea; the lack of consensus in our analytical results is likely to be the product of the previously mentioned high degree of dental homoplasy exhibited by piatnitzkysaurids, allosauroids, tyrannosauroids and dromaeosaurids (Hendrickx *et al.* 2019).

Morphotype V

COELUROSAURIA von Huene, 1914
TYRANNORAPTORA Sereno, 1999
Gen. et sp. indet.
Figures 3E, 11

Material. NHMUK PV R37630, an isolated crown (Fig. 11).

Locality & horizon. Specific locality uncertain, Wadhurst Clay Formation (Valanginian), Hastings, East Sussex (UK).

Description. The mesiodistal orientation of NHMUK PV R37630 is demonstrated by its distally recurved morphology (Fig. 11A, B). The relative labiolingual orientation is more difficult to appreciate but we use the slightly labially offset distal carina (Fig. 11F) to designate the labiolingual surfaces (Hendrickx *et al.* 2015a).

NHMUK PV R37630 is a well-preserved, apicobasally elongate (CH = 2.25) ziphodont crown with strong distal curvature, a convex mesial margin and a concave distal margin (Fig. 11A, B). This distal concavity is sufficiently marked that the apex is behind the crown's apex in lateral view. Viewed distally, the crown is straight for much of its length (Fig. 11D, E). The enamel is slightly more basally extensive on the labial surfaces. In basal cross-section, the crown is incipiently figure-eight-shaped (Fig. 11G) and lenticular in cross-section at mid-crown. Damage includes a mesiodistally oriented crack located around the midpoint and the loss of a section of the mesial carina and adjacent lingual surface, near the apex. The distal carina appears chipped at its base and a centrally positioned chip is located immediately below the cervix on the lingual side. The denticles are worn in places (e.g. apically, below the mid-crown distally), and glue covers some portion of the labial surface.

Both mesial and distal carinae are denticulated (Fig. 11C, D). The mesial carina terminates well above the cervix, around the midpoint of the crown, and denticles are present along most of its length; these extend close to the apex. The distal carina is comparatively more extensive, forming much of the distal margin of the tooth, but its apical and basal extent is not clear due to damage in those regions. Denticles are also present along the entirety of its preserved length and, given the development of the basalmost preserved denticles, the carinae probably extended to the cervix at the least. The mesial carina is centrally positioned while the distal carina is slightly offset labially (especially when the crown is viewed from below). Shallow concave surfaces are adjacent to the distal carina on both labial and lingual sides (Fig. 11E, H, I).

The apical mesial denticles are smaller than the distal ones, with an estimated 25 denticles per 5 mm present compared with the 18 on the distal carina (the apical pair are highly worn in the latter, and the extent of the distal denticles relative to the apex is uncertain). Approximately 5 mesial denticles per millimetre are present at two-thirds crown height (more extensive measurements could not be taken due to damage), and 18 denticles per 5 mm are present along the distal mid-crown, giving an estimated DSDI of 1.39. The mesial denticles reduce in size basally around the apicocentral (two-thirds CH) region, and the carina is absent at mid-crown level. Damage precludes accurate measurement over 5 mm of the distobasal carina, although four denticles are present along the basalmost preserved millimetre.

All denticles are perpendicular to their respective carina. Mesial denticles are vertically subrectangular (MHR = 0.58) and have shallowly parabolic to almost planar external margins (Fig. 11L, N). Distal denticles have a subquadrangular morphology (DHR = 0.96; e.g. Fig. 11S); where unworn, their external margins are symmetrically convex. The denticles show regular size variation across both carinae. The interdenticular spaces are shallow, being narrow in mesial denticles (less than one-third of a denticle's height; Fig. 11L) and broad in distal ones (Fig. 11S). Interdenticular diaphyses, if present, are difficult to distinguish. The interdenticular slit is subtriangular between mesial denticles (Fig. 11L, N), and concave between distal denticles (e.g. Fig. 11S), and both lack laminae. Interdenticular sulci are present between various distal mid-crown denticles on the lingual side, but are short and poorly developed (Fig. 11S). The mesial denticles, however, appear to lack these sulci.

The enamel possesses an incipiently braided texture basally that becomes irregular more apically (Fig. 11J, K). Flutes, longitudinal ridges, and transverse and marginal undulations are absent. A small, shallow spalled surface is present at the crown apex, descending basally a short distance along the distal carina.

Identification. NHMUK PV R37630 is probably a lateral tooth given its labiolingually compressed morphology (CBR = 0.61) (Hendrickx *et al.* 2015a). The analyses recovered tyrannosauroid and dromaeosaurid affinities for NHMUK PV R37630: the constrained analyses of the whole dentition matrices recovered the specimen among tyrannosauroids or dromaeosaurids (Figs 4, 6I), while most of the quantitative results classified the specimen in Dromaeosauridae, a position tenuously supported by the reduced consensus of the crown-only phylogenetic dataset. This may reflect the previously documented dental similarities shown by these theropods (Table 3) (Rauhut *et al.* 2010; Williamson & Brusatte 2014). Megalosauroid and noasaurid affinities suggested by some of the DFA results are rejected on morphological (e.g. the apically restricted mesial carina in NHMUK PV R37630 differs from the more extensive carina observed in noasaurids and non-megalosaurid megalosauroids) (Hendrickx *et al.* 2019) and temporal grounds in the case of megalosauroids (only spinosaurid megalosauroids appear to have survived into the Cretaceous). Furthermore, noasaurid and dromaeosaurid dentitions share important morphological similarities (Fanti & Therrien 2007; Hendrickx & Mateus 2014; Evans *et al.* 2015; Hendrickx *et al.* 2016); this may partly explain the noasaurid signal and lend additional support to a dromaeosaurid affinity. Incidentally, any mention of a possible noasaurid presence in the Wealden is of interest given suggestions that skeletal remains from the Hastings Group and Wessex Formation might be representative of this group (Naish 2011). We emphasize that this is emphatically not supported by our results here.

Previously recovered tyrannosauroid dental synapomorphies mainly focus on mesial characters (Hendrickx *et al.* 2019). The one lateral tooth character recovered by Hendrickx *et al.* (2019) pertains to the possession of less than 30 mesial denticles per 5 mm at two-thirds crown height, a character seen in the extrapolated data collected for NHMUK PV R37630 (denticles were measured over a 1 mm section due to preservation). The synapomorphies uniting NHMUK PV R37630 with Tyrannosauroidea based on our constrained analysis include short, poorly developed interdenticular sulci present at mid-crown in lateral teeth, and 16–29 distal mid-crown denticles per 5 mm; such distal mid-crown denticle density is also present in allosauroids and dromaeosaurids (Hendrickx *et al.* 2019).

The presence of concave surfaces adjacent to the distal carina is unusual for tyrannosauroid lateral teeth (and coelurosaurs more generally), being more typical for neovenatorid allosauroids (and the phylogenetically labile megaraptorans) (Hendrickx *et al.* 2019). However, the typical absence of such concavities in tyrannosauroid lateral dentition is based on the assumption that Megaraptora is best interpreted as an allosauroid clade (Benson *et al.* 2010; Carrano *et al.* 2012). Recent consensus supports coelurosaurian affinities for Megaraptora, and they may be within or close to Tyrannosauroidea (Novas *et al.* 2013; Porfiri *et al.* 2014; Apesteguía *et al.* 2016; Aranciaga Rolando *et al.* 2019, 2022; Naish & Cau 2022). This latter position indicates a more widespread distribution of concave surfaces within coelurosaurian lateral dentition, and reinforces the idea that choice of constrained topology may affect the output of phylogenetic analyses of isolated theropod teeth (Hendrickx *et al.* 2024). Concave surfaces are present in the mesial, rather than lateral, dentition of several dromaeosaurid clades (Hendrickx *et al.* 2019).

Regarding the dromaeosaurid signal recovered by some of our results, a lack of basal constriction present in NHMUK PV R 37630 is apomorphic for Dromaeosauridae but is also present elsewhere, including tyrannosauroids and neovenatorids (Hendrickx *et al.* 2019). Similarly, a figure-eight-shaped basal cross-section is present in allosaurid, megaraptoran, dromaeosaurid and tyrannosauroid dentition (Hendrickx *et al.* 2019; Wills *et al.* 2023). The presence of larger distal denticles relative to mesial ones is synapomorphic for Coelurosauria and present in dromaeosaurids and tyrannosauroids (Rauhut *et al.* 2010; Williamson & Brusatte 2014; Hendrickx *et al.* 2019; Wills *et al.* 2023). It is the case that some dromaeosaurids possess hooked denticles (Currie & Varricchio 2004; Currie & Evans 2020), but most possess symmetrically to asymmetrically convex serrations, as also seen in allosauroids and tyrannosauroids (Hendrickx *et al.* 2019). It is thus difficult to unambiguously support dromaeosaurid affinities for NHMUK PV R37630.

In summary, the tyrannosauroid affinities of NHMUK PV R37630 are not as clear-cut as suggested by the constrained phylogenetic analysis. The machine learning models strongly suggest dromaeosaurid affinities. Although the specimen lacks typical allosauroid characters, such as the subquadrangular mesial denticles at two-thirds crown height and absence of transverse undulations (Hendrickx *et al.* 2019), the concave surfaces adjacent to the distal carina (typical of neovenatorid allosauroids) impart a confusing signal depending on the phylogenetic position of Megaraptora. The homoplasy exhibited by many of the relevant characters also prevents unambiguous distinction between tyrannosauroid and dromaeosaurid affinities. Given this lack of consensus, and in tandem with our analytical results, we conservatively identify NHMUK PV R37630 as an indeterminate tyrannoraptoran within Coelurosauria. This suggests that at least some specimens previously referred to '*Megalosaurus dunkeri*' have coelurosaurian affinities, a contrast to the tentative non-coelurosaurian tetanuran identification previously ascribed to this taxon (Naish 2011).

DISCUSSION

Theropod diversity in the Wadhurst Clay Formation

Identification of the ziphodont specimens from the Wadhurst Clay Formation to higher taxonomic ranks proved difficult due to various interconnecting factors. Notably, the lateral dentitions of allosauroids, basal tyrannosauroids and dromaeosaurids (all of which are known from the Wealden Supergroup) share many dental features, subtle differences alone enabling the differentiation of these clades (Hendrickx *et al.* 2019). Maniraptoriforms also show high amounts of dental homoplasy with various other coelurosaurs, and dental characters provide the least important grouping information with respect to dromaeosaurid phylogeny (Hendrickx *et al.* 2019). Methodologically, although the virtues of phylogenetic analysis in the identification of isolated theropod teeth have been explored previously (Hendrickx *et al.* 2020), the prevalence of polymorphic characters and use of constrained analyses (which may require tedious revision due to updated knowledge of theropod systematics) complicate its use (Hendrickx *et al.* 2024). We note also that discriminant analyses may perform suboptimally when certain values are missing and in identifying large ziphodont teeth, and they should be applied with caution (Hendrickx *et al.* 2015b, 2024; Delcourt *et al.* 2020; Wills *et al.* 2021). Nevertheless, the use of combined analytical methods has enabled an updated, novel interpretation of the British Valanginian theropod fauna, and our results provide a basis for comparisons between Wealden theropod faunas more generally.

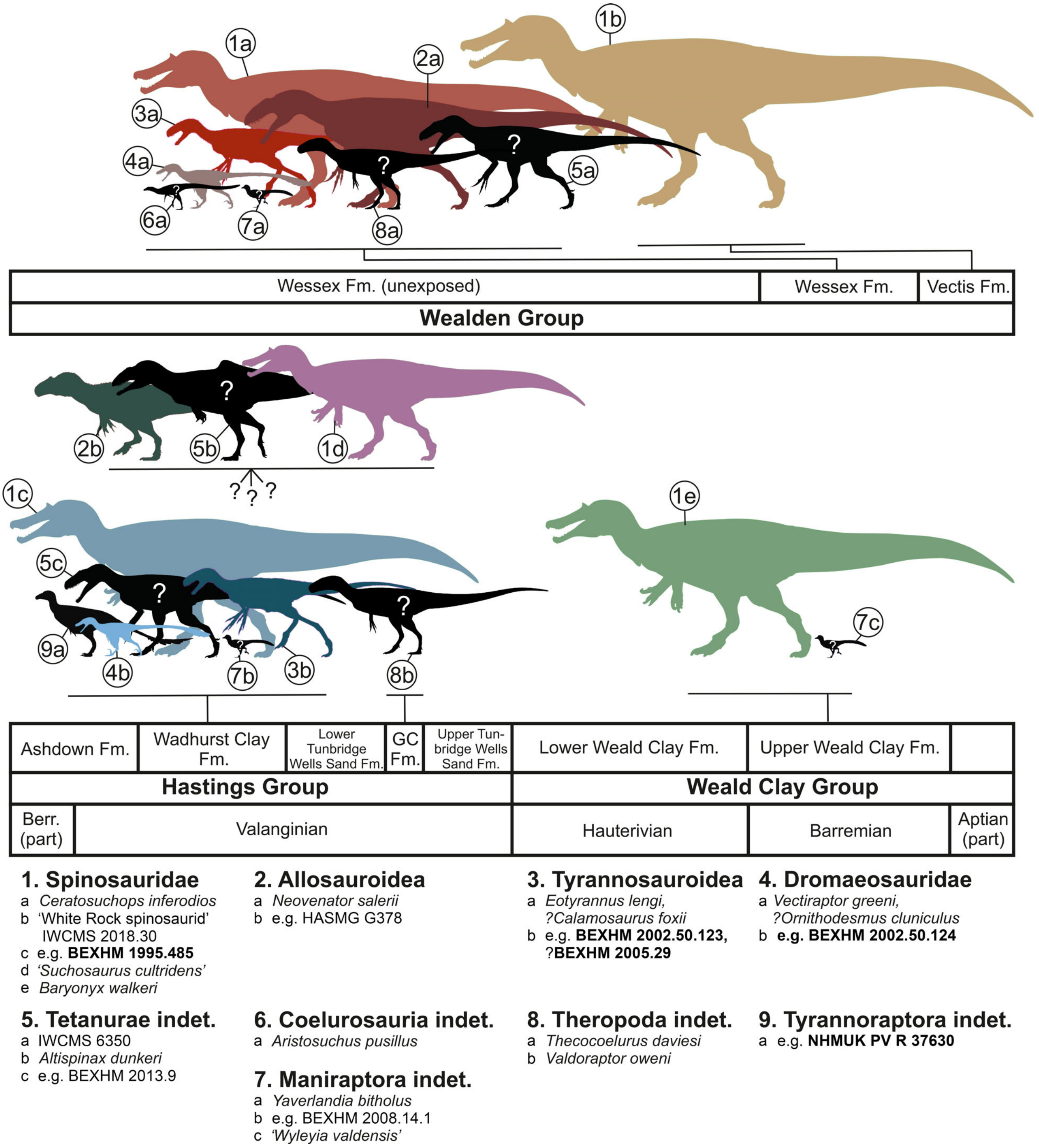

FIG. 12. Schematic representation of the theropod diversity throughout the Wealden Supergroup, with specimens from the Wealden Group (Wessex sub-basin) and the Hastings and Weald Clay groups (Weald sub-basin). Specimens studied herein are highlighted (see text for additional details). Silhouette images from PhyloPic (https://www.phylopic.org/): Alessio Ciaffi (Spinosauridae CC BY 4.0); Tasman Dixon (Allosauridae (2b), Maniraptora both CC0 1.0); Scott Hartman (Allosauroidea (2a), Dromaeosauridae, Tetanurae (5a, c), Tyrannosauroidea, all CC BY-NC-SA 3.0); Ivan Iofrida (Tetanurae (5b) CC BY 4.0), Jagged Fang Designs (Coelurosauria CC0 1.0); Matt Martyniuk (Tyrannoraptora CC BY-NC-SA 3.0) and SlvrHwk (Theropoda CC BY 4.0). For full details, see Table S1.

Our results suggest that the general composition of the Wealden theropod fauna remained relatively uniform throughout the deposition of this extensive succession (Fig. 12). This fauna, best typified by the Barremian outcrops of the Wessex Formation and composed of large allosauroids and spinosaurids, and small to mid-sized coelurosaurs that included tyrannosauroids and dromaeosaurids (Naish *et al.* 2001; Weishampel *et al.* 2004; Naish 2011; Lomax & Tamura 2014), was similarly rich in the older Wadhurst Clay Formation. The unambiguous presence of spinosaurids in the Valanginian of England marks the oldest definitive occurrence of the clade in Europe (Barker *et al.* 2023). The novel identification of tyrannosauroids in Hastings Group strata also bridges the temporal gap in the British record, and which previously extended between the Tithonian (Benson 2008; Brusatte & Benson 2013) and Barremian (Hutt *et al.* 2001; Naish & Cau 2022). The interpretation of BEXHM 2002.50.124 as a small dromaeosaurid provides new information given how rare small theropods are in the Weald sub-basin (Naish 2011; Naish & Sweetman 2011). Dromaeosaurids are relatively poorly documented from the Wealden Supergroup: Longrich *et al.* (2022) established the Wessex Formation taxon *Vectiraptor greeni* on the basis of several dorsal vertebrae but Wealden dromaeosaurids identified on the basis of teeth alone require restudy in order that their affinities are better established (Sweetman 2004; Rauhut *et al.* 2010). We cannot support the previously proposed velociraptorine affinity for BEXHM 2002.50.124 and suggest that a conservative approach be taken for the identification of Wealden dromaeosaurid teeth, as previously intimated by Naish & Martill (2007).

We were unable to identify allosauroids despite the presence of large ziphodont crowns in our sample, contradicting the accession histories of several of the specimens (see above). A putative, poorly preserved allosauroid tooth (BEXHM 2019.49.252) has been described from the Ashdown Brickworks (Turmine-Juhel *et al.* 2019), although the characters used for this referral are widely distributed among theropods and the specimen is best considered an indeterminate theropod. Nonetheless, allosauroids do appear present in the Hastings Group more generally (Naish 2003), and we consider it likely that renewed study of Wadhurst Clay Formation ziphodont crowns, such as those referred to '*Megalosaurus dunkeri*', will support the presence of the clade in this unit.

Similarities between BEXHM 2002.50.124 and NHMUK PV R37630 (e.g. distal denticles larger than mesial ones, presence of concave surfaces adjacent to carinae, apically restricted mesial carina, similar curvature) suggest that they might belong to semaphoronts of the same taxon, a hypothesis tentatively supported by at least one of our analyses (e.g. Fig. 4). Counting against this possibility, however, is that transverse undulations are absent in NHMUK PV R37630, that differences are present in basal denticle morphology (parabolic vs semicircular, respectively), and that conflicting signals were recovered from our analyses. Similarly, BEXHM 2002.50.123 and 2005.29 might represent teeth belonging to a singular tyrannosauroid taxon (assuming our referral latter specimen is correct), with the observed differences reflecting differing positions within the dental arcade. However, the absence of additional material renders such discussions speculative at this time.

European Valanginian theropod record

The Valanginian is a poorly understood time interval with respect to the study of dinosaur diversity and evolution (Weishampel *et al.* 2004; Csiki-Sava *et al.* 2016), rendering the specimens described here, as well as other Valanginian specimens from southern England (e.g. *Valdoraptor*), important in the study of theropod diversity at this time. Here, we compare our interpretation of the Valanginian theropod fauna of England to that of other European localities.

The Iberian Lower Cretaceous fossil record is largely contemporaneous with that of the British Wealden Supergroup and has yielded numerous theropod specimens, although the 'Lower Wealden' (i.e. Valanginian – lower Hauterivian) possesses a poor fossil record (Pereda-Suberbiola *et al.* 2012). In their review of Iberian dinosaur faunas, Pereda-Suberbiola *et al.* (2012) noted that allosauroids alone are known from the 'Lower Wealden'; however, both putative allosauroid and dromaeosaurid teeth have been recovered from the Valanginian–Hauterivian Villanueva de Huerva Formation (Gasca *et al.* 2012). Most other Iberian dromaeosaurid specimens appear limited to younger Hauterivian–Aptian deposits (Pereda-Suberbiola *et al.* 2012; Berrocal-Casero *et al.* 2023).

Similarly, while spinosaurids are present in the Iberian Lower Cretaceous, their oldest records are from the upper Hauterivian (Malafaia *et al.* 2020). Montealegre *et al.* (2024) interpreted the Iberian Peninsula as pivotal in our understanding of spinosaurid origins given the presence there of the oldest representatives of both spinosaurid clades. However, baryonychine- and spinosaurine-type teeth are known from the Berriasian–Valanginian of Brazil (Sales *et al.* 2017; Lacerda *et al.* 2023) and (as reported here) the British Wadhurst Clay Formation. Clearly, the Iberian Peninsula cannot claim a monopoly of early spinosaurid records and the spatial origins of Spinosauridae remain unclear (Barker *et al.* 2023; Lacerda *et al.* 2023).

Until recently, tyrannosauroids appeared absent from the Iberian Lower Cretaceous (Antunes & Mateus 2003; Pereda-Suberbiola *et al.* 2012), leading Montealegre *et al.* (2024) to propose competition from spinosaurids and allosauroids as a possible reason for their absence in Spanish deposits specifically. However, potential tyrannosauroid remains have since been identified from Barremian deposits in Spain (Berrocal-Casero *et al.* 2023), and other Lower Cretaceous units such as the Wessex Formation preserve faunas containing contemporaneous allosauroids, spinosaurids and tyrannosauroids (Naish *et al.* 2001; Naish 2011). These data suggest that a competitive exclusion hypothesis may be poorly founded. Nevertheless, to the best of our knowledge, tyrannosauroids have yet to be reported from Valanginian-aged Iberian strata.

To date, the Lower Cretaceous outcrops of France have yielded few theropod remains compared with those of England and Spain (Allain & Suberbiola 2003): only the indeterminate '*Megalosaurus insignis*' (Parent 1893) and an indeterminate tetanuran previously referred to Allosauroidea (Pérez-Moreno *et al.* 1993; Carrano *et al.* 2012) have been reported. A carcharodontosaurid tooth has been reported from Romania, and probably originated from the late Valanginian Alimanu Member of the Cernavodă Formation (Csiki-Sava *et al.* 2016).

CONCLUSION

The Wadhurst Clay Formation is a fossiliferous Valanginian unit of the Hastings Group, and part of the Wealden Supergroup. Like most sections of the Wealden Supergroup, it yields dinosaurs, but its assemblage, to date, is low in diversity, the only substantial remains pertaining to iguanodontians (Naish & Martill 2008; Norman 2011). The remainder (mostly isolated teeth) represent indeterminate titanosauriform sauropods and theropods in addition to ankylosaurian remains (Benton & Spencer 1995; Charig & Milner 1997; Austen *et al.* 2010; Naish & Sweetman 2011; Upchurch *et al.* 2011; Turmine-Juhel *et al.* 2019). Prior to the present study, theropod teeth from the Wadhurst Clay Formation have not been subjected to rigorous analysis. Our use of statistical, comparative, phylogenetic and machine learning methods indicates a phylogenetically diverse tetanuran fauna that has much in common with that of the better-known Barremian units of the Wealden Supergroup, the Wessex Formation in particular.

Of the five specimens analysed here, BEXHM 1995.485 represents a non-*Baryonyx* spinosaurid, and as such further supports the hypothesis that multiple spinosaurid lineages were present during the time that Wealden Supergroup sediments were deposited (Barker *et al.* 2023). BEXHM 2002.50.123 and BEXHM 2005.29 possess tyrannosauroid affinities, indicating for the first time the presence of this clade in the lower units of the Wealden Supergroup. BEXHM 2002.50.124 appears to represent a small dromaeosaurid, and we were unable to confirm previous reports of velociraptorines in the Wadhurst Clay Formation (Austen *et al.* 2010; Naish & Sweetman 2011). Finally, NHMUK PV R37630 probably represents a tyrannoraptoran (and possibly dromaeosaurid) coelurosaur, but more specific identification is not possible given the presence of homoplastic characters and conflicting analytical results.

Previous efforts to determine the theropod fauna of the Wadhurst Clay Formation have relied on gross anatomical similarity in identifying respective groups, and as such the suggested identifications were either vague and unable to reliably differentiate groups in which the dentitions can exhibit high degrees of similarity, such as dromaeosaurids and tyrannosauroids (Rauhut *et al.* 2010; Williamson & Brusatte 2014; Hendrickx *et al.* 2019), or (as in the case of spinosaurid teeth referred to *Baryonyx* and *B. walkeri*; Charig & Milner 1997; Naish & Sweetman 2011) were influenced by a taxonomy since made obsolete by additional discoveries (Barker *et al.* 2021, 2023). Our identifications thus substantially update interpretations of the theropod fauna from a poorly understood time interval (the Valanginian) in both the British and European fossil records and highlight substantial potential for the discovery of additional remains in this unit. Skeletal remains from the Wadhurst Clay Formation, and Hastings Group more broadly, should be evaluated with potential tyrannoraptoran, tyrannosauroid and dromaeosaurid identifications in mind, in addition to the spinosaurid and oviraptorosaurian possibilities evident from previous works (Charig & Milner 1997; Naish & Sweetman 2011).

Acknowledgements. We thank Julian Porter, Susie Maidment and Mike Day for help in facilitating the study of the specimens under their care. Luis Coy is thanked for his assistance with the photography of the specimens. We thank Ibstock Bricks Ashdown for allowing DB to access the site. We also thank David Button and Sally Thomas for their editorial work on this paper, as well as Raphael Delcourt and another anonymous reviewer for their constructive comments. We acknowledge the use of the Willi Hennig Society edition of TNT for the phylogenetic analyses.

Author contributions. **Conceptualization** Chris T Barker (CTB), Darren Naish (DN), Neil J Gostling (NJG); **Formal analysis** CTB, L Handford (LH), S Wills (SW), C Hendrikx (CH); **Investigation** CTB, LH, SW; **Resources** D Brockhurst (DB); **Visualization** CTB, P Hadland (PH); **Writing – Original Draft Preparation**: CTB, SW (machine learning sections); **Writing – Review & Editing** CTB, LH, DN, SW, CH, PH, DB, NJG.

DATA ARCHIVING STATEMENT

Data for this study (including the phylogenetic character matrices, .dat files for the DFAs, and machine learning protocol) are available in the Dryad digital repository: https://doi.org/10.5061/dryad.kwh70rzdw A 3D mesh of NHMUK PV R37630 (https://doi.org/10.17602/M2/

M660249) is available on MorphoSource: https://www.morphosource.org/concern/media/000660249.

Editor. David Button

SUPPORTING INFORMATION

Additional Supporting Information can be found online (https://doi.org/10.1002/spp2.1604):

Table S1. Licence information for PhyloPic images used in Figures 4, 5, 11 and 12.

REFERENCES

Akinlotan, O. O. 2015. The sedimentology of the Ashdown Formation and the Wadhurst Clay Formation, southeast England. Doctoral dissertation, University of Brighton, UK.

Allain, R. and Suberbiola, X. P. 2003. Dinosaurs of France. *Comptes Rendus Palevol*, **2**, 27–44.

Allain, R., Vullo, R., Le Loeuff, J. and Tournepiche, J.-F. 2014. European ornithomimosaurs (Dinosauria, Theropoda): an undetected record. *Geologica Acta*, **12**, 127–135.

Allen, P. 1949. Notes on Wealden bone-beds. *Proceedings of the Geologists' Association*, **60**, 275–283.

Allen, P. 1975. Wealden of the Weald: a new model. *Proceedings of the Geologists' Association*, **86**, 389–437.

Alonso, A. and Canudo, J. I. 2016. On the spinosaurid theropod teeth from the early Barremian (Early Cretaceous) Blesa Formation (Spain). *Historical Biology*, **28**, 823–834.

Alonso, A., Gasca, J., Navarro-Lorbés, P., Rubio, C. and Canudo, J. 2018. A new contribution to our knowledge of the large-bodied theropods from the Barremian of the Iberian Peninsula: the "Barranco del Hocino" site (Spain). *Journal of Iberian Geology*, **44**, 7–23.

Antunes, M. T. and Mateus, O. 2003. Dinosaurs of Portugal. *Comptes Rendus Palevol*, **2**, 77–95.

Apesteguía, S., Smith, N. D., Valieri, R. J. and Makovicky, P. J. 2016. An unusual new theropod with a didactyl manus from the Upper Cretaceous of Patagonia, Argentina. *PLoS One*, **11**, e0157793.

Aranciaga Rolando, A. M., Novas, F. E. and Agnolín, F. L. 2019. A reanalysis of *Murusraptor barrosaensis* Coria & Currie (2016) affords new evidence about the phylogenetical relationships of Megaraptora. *Cretaceous Research*, **99**, 104–127.

Aranciaga Rolando, A. M., Motta, M. J., Agnolín, F. L., Manabe, M., Tsuihiji, T. and Novas, F. E. 2022. A large Megaraptoridae (Theropoda: Coelurosauria) from Upper Cretaceous (Maastrichtian) of Patagonia, Argentina. *Scientific Reports*, **12**, 6318.

Austen, P. A. and Austen, J. 2016. Bexhill dinosaurs. *Hastings & District Geological Society Journal*, **22**, 38–39.

Austen, P. A. and Batten, D. J. 2018. English Wealden fossils: an update. *Proceedings of the Geologists' Association*, **129**, 171–201.

Austen, P., Brockhurst, D. and Honeysett, K. 2010. Vertebrate fauna from Ashdown brickworks, Bexhill, east Sussex. *Wealden News*, **8**, 13–23.

Averianov, A. and Lopatin, A. 2021. A new theropod dinosaur (Theropoda, Dromaeosauridae) from the Late Cretaceous of Tajikistan. *Doklady Earth Sciences*, **499**, 570–574.

Barker, C. T., Hone, D. W., Naish, D., Cau, A., Lockwood, J. A., Foster, B., Clarkin, C. E., Schneider, P. and Gostling, N. J. 2021. New spinosaurids from the Wessex Formation (Early Cretaceous, UK) and the European origins of Spinosauridae. *Scientific Reports*, **11**, 19340.

Barker, C. T., Lockwood, J. A., Naish, D., Brown, S., Hart, A., Tulloch, E. and Gostling, N. J. 2022. A European giant: a large spinosaurid (Dinosauria: Theropoda) from the Vectis Formation (Wealden Group, Early Cretaceous), UK. *PeerJ*, **10**, e13543.

Barker, C. T., Naish, D. and Gostling, N. J. 2023. Isolated tooth reveals hidden spinosaurid dinosaur diversity in the British Wealden Supergroup (Lower Cretaceous). *PeerJ*, **11**, e15453.

Barker, C. T., Handford, L., Naish, D., Wills, S., Hendrickx, C., Hadland, P., Brockhurst, D. and Gostling, N. J. 2024. Data from: Theropod dinosaur diversity of the lower English Wealden: analysis of a tooth-based fauna from the Wadhurst Clay Formation (Lower Cretaceous: Valanginian) via phylogenetic, discriminant and machine learning methods [Dataset]. Dryad. https://doi.org/10.5061/dryad.kwh70rzdw

Batten, D. J. 2011a. *English Wealden fossils*. The Palaeontological Association, Field Guides to Fossils, 14, 769 pp.

Batten, D. J. 2011b. Wealden geology. 7–14. *In* Batten, D. J. (ed.) *English Wealden fossils*. The Palaeontological Association, Field Guides to Fossils, 14, 769 pp.

Batten, D. J. and Austen, P. A. 2011. The Wealden of South-East England. 15–51. *In* Batten, D. J. (ed.) *English Wealden fossils*. The Palaeontological Association, Field Guides to Fossils, 14, 769 pp.

Benson, R. B. 2008. New information on *Stokesosaurus*, a tyrannosauroid (Dinosauria: Theropoda) from North America and the United Kingdom. *Journal of Vertebrate Paleontology*, **28**, 732–750.

Benson, R. B., Brusatte, S. L., Hutt, S. and Naish, D. 2009. A new large basal tetanuran (Dinosauria: Theropoda) from the Wessex Formation (Barremian) of the Isle of Wight, England. *Journal of Vertebrate Paleontology*, **29**, 612–615.

Benson, R. B., Carrano, M. T. and Brusatte, S. L. 2010. A new clade of archaic large-bodied predatory dinosaurs (Theropoda: Allosauroidea) that survived to the latest Mesozoic. *Naturwissenschaften*, **97**, 71–78.

Benton, M. J. and Spencer, P. S. 1995. British Cretaceous fossil reptile sites. 215–270. *In* Benton, M. J. and Spencer, P. S. (eds) *Fossil reptiles of Great Britain*. Springer.

Berrocal-Casero, M., Alcalde-Fuentes, M. R., Audije-Gil, J. and Sevilla, P. 2023. Theropod teeth from the upper Barremian (Lower Cretaceous) of Vadillos-1, Spain. *Cretaceous Research*, **142**, 105392.

Blows, W. T. 1998. A review of Lower and Middle Cretaceous dinosaurs of England. *New Mexico Museum of Natural History & Science Bulletin*, **14**, 29–38.

Blows, W. T. and Honeysett, K. 2014. First Valanginian Polacanthus foxii (Dinosauria, Ankylosauria) from England, from the Lower Cretaceous of Bexhill, Sussex. *Proceedings of the Geologists' Association*, **125**, 233–251.

Brusatte, S. L. and Benson, R. B. 2013. The systematics of Late Jurassic tyrannosauroid theropods from Europe and North America. *Acta Palaeontologica Polonica*, **58**, 47–54.

Brusatte, S. L., Benson, R. B., Carr, T. D., Williamson, T. E. and Sereno, P. C. 2007. The systematic utility of theropod enamel wrinkles. *Journal of Vertebrate Paleontology*, **27**, 1052–1056.

Brusatte, S. L., Benson, R. B. J. and Hutt, S. 2008. The osteology of *Neovenator salerii* (Dinosauria: Theropoda) from the Wealden Group (Barremian) of the Isle of Wight. *Monograph of the Palaeontographical Society*, **162**, 1–75.

Buffetaut, E. 2007. The spinosaurid dinosaur *Baryonyx* (Saurischia, Theropoda) in the Early Cretaceous of Portugal. *Geological Magazine*, **144**, 1021–1025.

Buffetaut, E. 2010. Spinosaurs before Stromer: early finds of spinosaurid dinosaurs and their interpretations. 175–188. *In* Moody, R. T. J., Buffetaut, E., Naish, D. and Martill, D. M. (eds) *Dinosaurs and other extinct saurians: A historical perspective*. Geological Society, London Special Publications, 343.

Buffetaut, E., Suteethorn, S., Suteethorn, V., Tong, H. and Wongko, K. 2019. Spinosaurid teeth from the Lower Cretaceous of Ko Kut, eastern Thailand. *Annales de Paléontologie*, **105**, 239–243.

Carrano, M. T., Benson, R. B. and Sampson, S. D. 2012. The phylogeny of Tetanurae (Dinosauria: Theropoda). *Journal of Systematic Palaeontology*, **10**, 211–300.

Charig, A. J. and Milner, A. C. 1986. *Baryonyx*, a remarkable new theropod dinosaur. *Nature*, **324**, 359–361.

Charig, A. J. and Milner, A. C. 1997. *Baryonyx walkeri*, a fish-eating dinosaur from the Wealden of Surrey. *Bulletin-Natural History Museum Geology Series*, **53**, 11–70.

Chowchuvech, W., Manitkoon, S., Chanthasit, P. and Ketwetsuriya, C. 2024. The first occurrence of a basal tyrannosauroid in Southeast Asia: dental evidence from the Upper Jurassic of Northeastern Thailand. *Tropical Natural History*, **24**, 84–95.

Csiki-Sava, Z., Brusatte, S. L. and Vasile, Ş. 2016. "*Megalosaurus* cf. *superbus*" from southeastern Romania: the oldest known Cretaceous carcharodontosaurid (Dinosauria: Theropoda) and its implications for earliest Cretaceous Europe–Gondwana connections. *Cretaceous Research*, **60**, 221–238.

Currie, P. J. 1995. New information on the anatomy and relationships of *Dromaeosaurus albertensis* (Dinosauria: Theropoda). *Journal of Vertebrate Paleontology*, **15**, 576–591.

Currie, P. J. and Evans, D. C. 2020. Cranial anatomy of new specimens of *Saurornitholestes langstoni* (Dinosauria, Theropoda, Dromaeosauridae) from the Dinosaur Park formation (Campanian) of Alberta. *The Anatomical Record*, **303**, 691–715.

Currie, P. J. and Varricchio, D. J. 2004. A new dromaeosaurid from the Horseshoe Canyon Formation (upper Cretaceous) of Alberta, Canada. 112–132. *In* Currie, P. J., Koppelhus, E. B., Shugar, M. A. and Wright, J. L. (eds) *Feathered dragons: Studies on the transition from dinosaurs to birds*. Indiana University Press.

Currie, P. J., Rigby, J. K. and Sloan, R. E. 1990. Theropod teeth from the Judith river formation of southern Alberta, Canada. 107–125. *In* Carpenter, K. and Currie, P. J. (eds) *Dinosaur systematics: Approaches and perspectives*. Cambridge University Press.

Delcourt, R., Brilhante, N. S., Grillo, O. N., Ghilardi, A. M., Augusta, B. G. and Ricardi-Branco, F. 2020. Carcharodontosauridae theropod tooth crowns from the Upper Cretaceous (Bauru Basin) of Brazil: a reassessment of isolated elements and its implications to palaeobiogeography of the group. *Palaeogeography, Palaeoclimatology, Palaeoecology*, **556**, 109870.

Delcourt, R., Brilhante, N. S., Pires-Domingues, R. A., Hendrickx, C., Grillo, O. N., Augusta, B. G., Maciel, B. S., Ghilardi, A. M. and Ricardi-Branco, F. 2024. Biogeography of theropod dinosaurs during the Late Cretaceous: evidence from central South America. *Zoological Journal of the Linnean Society*, **202**, zlad184.

Evans, D. C., Larson, D. W. and Currie, P. J. 2013. A new dromaeosaurid (Dinosauria: Theropoda) with Asian affinities from the latest Cretaceous of North America. *Naturwissenschaften*, **100**, 1041–1049.

Evans, D. C., Barrett, P. M., Brink, K. S. and Carrano, M. T. 2015. Osteology and bone microstructure of new, small theropod dinosaur material from the early Late Cretaceous of Morocco. *Gondwana Research*, **27**, 1034–1041.

Evers, S. W., Rauhut, O. W., Milner, A. C., McFeeters, B. and Allain, R. 2015. A reappraisal of the morphology and systematic position of the theropod dinosaur *Sigilmassasaurus* from the "middle" Cretaceous of Morocco. *PeerJ*, **3**, e1323.

Fanti, F. and Therrien, F. 2007. Theropod tooth assemblages from the Late Cretaceous Maevarano Formation and the possible presence of dromaeosaurids in Madagascar. *Acta Palaeontologica Polonica*, **52**, 155–166.

Gallois, R. and Edmunds, F. 1965. *The Wealden District: British Regional Geology*. HM Stationery Office.

Gasca, J. M., Badiola, A., Canudo, J., Moreno-Azanza, M., Puértolas, E., Huerta, P. and Torcida, F. 2012. La asociación de vertebrados fósiles del yacimiento Pochancalo 1 (Valanginiense-Hauteriviense, Villanueva de Huerva, Zaragoza, España). 159–172. *In* Huerta, P., Torcida Fernández-Baldor, F. and Canudo, J. I. (eds) *Actas de las V Jornadas Internacionales sobre Paleontología de Dinosaurios y su Entorno*. Colectivo Arqueológico y Paleontológico de Salas.

Gauthier, J. 1986. Saurischian monophyly and the origin of birds. *Memoirs of the California Academy of Sciences*, **8**, 1–55.

Goloboff, P. A. and Morales, M. E. 2023. TNT version 1.6, with a graphical interface for MacOS and Linux, including new routines in parallel. *Cladistics*, **39**, 144–153.

Goloboff, P. A. and Szumik, C. A. 2015. Identifying unstable taxa: efficient implementation of triplet-based measures of stability, and comparison with Phyutility and RogueNaRok. *Molecular Phylogenetics and Evolution*, **88**, 93–104.

Hammer, Ø., Harper, D. A. and Ryan, P. D. 2001. PAST: Paleontological statistics software package for education and data analysis. *Palaeontologia Electronica*, **4** (1), 4.

Harrison, C. J. O. and Walker, C. A. 1973. *Wyleyia*: a new bird humerus from the Lower Cretaceous of England. *Palaeontology*, **16**, 721–728.

Hastie, M. T., Tibshirani, R., Leisch, F., Hornik, K., Ripley, B. D. and Narasimhan, B. 2020. mda: Mixture and Flexible Discriminant Analysis. R package version 0.5-2. https://cran.r-project.org/web/packages/mda/index.html

Hayward, R. 1996. The geology of part of the Wadhurst Clay Formation and part of the Tunbridge Wells Formation at the

Ashdown Brick Works, Bexhill, Sussex. Unpublished BSc Dissertation, University of Greenwich, School of Earth Sciences, 179 pp.

Hendrickx, C. and Mateus, O. 2014. Abelisauridae (Dinosauria: Theropoda) from the Late Jurassic of Portugal and dentition-based phylogeny as a contribution for the identification of isolated theropod teeth. *Zootaxa*, **3759**, 1–74.

Hendrickx, C., Mateus, O. and Araújo, R. 2015a. A proposed terminology of theropod teeth (Dinosauria, Saurischia). *Journal of Vertebrate Paleontology*, **35**, e982797.

Hendrickx, C., Mateus, O. and Araújo, R. 2015b. The dentition of megalosaurid theropods. *Acta Palaeontologica Polonica*, **60**, 627–642.

Hendrickx, C., Mateus, O. and Buffetaut, E. 2016. Morphofunctional analysis of the quadrate of Spinosauridae (Dinosauria: Theropoda) and the presence of *Spinosaurus* and a second spinosaurine taxon in the Cenomanian of North Africa. *PLoS One*, **11**, e0144695.

Hendrickx, C., Mateus, O., Araújo, R. and Choiniere, J. 2019. The distribution of dental features in non-avian theropod dinosaurs: taxonomic potential, degree of homoplasy, and major evolutionary trends. *Palaeontologia Electronica*, **22** (3), 74.

Hendrickx, C., Tschopp, E. and D. Ezcurra, M. 2020. Taxonomic identification of isolated theropod teeth: the case of the shed tooth crown associated with *Aerosteon* (Theropoda: Megaraptora) and the dentition of Abelisauridae. *Cretaceous Research*, **108**, 104312.

Hendrickx, C., Trapman, T. H., Wills, S., Holwerda, F. M., Stein, K. H., Rauhut, O. W., Melzer, R. R., Woensel, J. V. and Reumer, J. W. 2024. A combined approach to identify isolated theropod teeth from the Cenomanian Kem Kem Group of Morocco: cladistic, discriminant, and machine learning analyses. *Journal of Vertebrate Paleontology*, **43**, e2311791.

Hone, D., Xu, X. and Wang, D. 2010. A probable baryonychine (Theropoda: Spinosauridae) tooth from the Upper Cretaceous of Henan Province, China. *Vertebrata PalAsiatica*, **48**, 19–26.

Hopson, P., Wilkinson, I. and Woods, M. 2008. A stratigraphical framework for the Lower Cretaceous of England. British Geological Survey. Research Report RR/08/03. https://nora.nerc.ac.uk/id/eprint/3236

Hutt, S., Martill, D. M. and Barker, M. J. 1996. The first European allosaurid dinosaur (Lower Cretaceous, Wealden Group, England). *Neues Jahrbuch für Geologie und Palä ontologie-Monatshefte*, **10**, 635–644.

Hutt, S., Naish, D., Martill, D. M., Barker, M. J. and Newbery, P. 2001. A preliminary account of a new tyrannosauroid theropod from the Wessex Formation (Early Cretaceous) of southern England. *Cretaceous Research*, **22**, 227–242.

Insole, A. N. and Hutt, S. 1994. The palaeoecology of the dinosaurs of the Wessex Formation (Wealden Group, Early Cretaceous), Isle of Wight, Southern England. *Zoological Journal of the Linnean Society*, **112**, 197–215.

Isasmendi, E., Sáez-Benito, P., Torices, A., Navarro-Lorbés, P. and Pereda-Suberbiola, X. 2020. New insights about theropod palaeobiodiversity in the Iberian Peninsula and Europe: spinosaurid teeth (Theropoda, Megalosauroidea) from the Lower Cretaceous of La Rioja (Spain). *Cretaceous Research*, **116**, 104600.

Isasmendi, E., Pérez-Pueyo, M., Moreno-Azanza, M., Alonso, A., Puértolas-Pascual, E., Bádenas, B. and Canudo, J. I. 2024. Theropod teeth palaeodiversity from the uppermost Cretaceous of the South Pyrenean Basin (NE Iberia) and the intra-Maastrichtian faunal turnover. *Cretaceous Research*, **162**, 105952.

Jasinski, S. E., Sullivan, R. M. and Dodson, P. 2020. New dromaeosaurid dinosaur (Theropoda, Dromaeosauridae) from New Mexico and biodiversity of dromaeosaurids at the end of the Cretaceous. *Scientific Reports*, **10**, 5105.

Juarez, M., Hechenleitner, E. M., Martinelli, A. G., Rocher, S. and Fiorelli, L. E. 2023. First record of abelisaurid theropods and a peirosaurid crocodyliform from the Upper Cretaceous of Precordillera of La Rioja, NW Argentina. *Cretaceous Research*, **152**, 105679.

Katsuhiro, K. and Yoshikazu, T. Y. A. H. 2017. Second discovery of a spinosaurid tooth from the Sebayashi Formation (Lower Cretaceous), Kanna Town, Gunma Prefecture, Japan. *Bulletin of Gunma Museum of Natural History*, **21**, 1–6.

Kuhn, M. 2008. Building predictive models in R using the caret package. *Journal of Statistical Software*, **28**, 1–26.

Kuhn, M., Weston, S., Culp, M., Coulter, N. and Quinlan, R. 2018. C5.0 decision trees and rule-based model. R package version 0.1.8. RuleQuest Research Pty Ltd. https://cran.r-project.org/web/packages/C50/index.html

Lacerda, M. B. S., Aragão, P. R. L., Vieira, F. S., Sales, M. A. F. and Liparini, A. 2023. On the first Baryonychinae (Theropoda, Spinosauridae) teeth from South America. *Zootaxa*, **5264**, 526–544.

Lake, R. D. and Shepard-Thorn, E. R. 1987. *Geology of the country around Hastings and Dungeness: Memoir for 1:50 000 geological sheets 320 and 321 (England and Wales)*. British Geological Survey, London, 81 pp.

Liaw, A. and Wiener, M. 2002. Classification and regression by randomForest. *R News*, **2**, 18–22.

Lomax, D. R. and Tamura, N. 2014. *Dinosaurs of the British Isles*. Siri Scientific Press, 414 pp.

Longrich, N. R. and Currie, P. J. 2009. A microraptorine (Dinosauria–Dromaeosauridae) from the late Cretaceous of North America. *Proceedings of the National Academy of Sciences*, **106**, 5002–5007.

Longrich, N. R., Martill, D. M. and Jacobs, M. L. 2022. A new dromaeosaurid dinosaur from the Wessex Formation (Lower Cretaceous, Barremian) of the Isle of Wight, and implications for European palaeobiogeography. *Cretaceous Research*, **134**, 105123.

Lydekker, R. 1888. *Catalogue of the Fossil Reptilia and Amphibia in the British Museum (Natural History). Part I.* British Museum, Department of Geology, 309 pp.

Lydekker, R. 1889. Note on some points in the nomenclature of fossil reptiles and amphibians, with preliminary notices of two new species. *Geological Magazine*, **6**, 325–326.

Lydekker, R. 1890. *Catalogue of the Fossil Reptilia and Amphibia in the British Museum (Natural History). Part IV. Containing the orders Anomodontia, Ecaudata, Caudata and Labyrinthodontia; and Supplement*. British Museum (Natural History).

Maisch, M. W. 2016. The nomenclatural status of the carnivorous dinosaur genus Altispinax v. Huene, 1923 (Saurischia, Theropoda) from the Lower Cretaceous of England. *Neues*

Jahrbuch für Geologie und Paläontologie-Abhandlungen, **280**, 215–219.

Malafaia, E., Gasulla, J., Escaso, F., Narvaéz, I. and Ortega, F. 2020. An update of the spinosaurid (Dinosauria: Theropoda) fossil record from the Lower Cretaceous of the Iberian Peninsula: distribution, diversity, and evolutionary history. *Journal of Iberian Geology*, **46**, 431–444.

Marsh, O. C. 1881. Principal characters of American Jurassic dinosaurs, part V. *American Journal of Science*, **s3-21**, 417–423.

Martill, D. M. and Hutt, S. 1996. Possible baryonychid dinosaur teeth from the Wessex Formation (Lower Cretaceous, Barremian) of the Isle of Wight, England. *Proceedings of the Geologists' Association*, **107**, 81–84.

Martill, D. M. and Naish, D. (eds). 2001. *Dinosaurs of the Isle of Wight*. The Palaeontological Association, Field Guides to Fossils, 10, 433 pp.

Mateus, O., Araujo, R., Natário, C. and Castanhinha, R. 2011. A new specimen of the theropod dinosaur *Baryonyx* from the early Cretaceous of Portugal and taxonomic validity of *Suchosaurus*. *Zootaxa*, **2827**, 54–68.

Matthew, W. D. and Brown, B. 1922. The family Deinodontidae, with notice of a new genus from the Cretaceous of Alberta. *Bulletin of the American Museum of Natural History*, **46**, 367–385.

Meso, J. G., Hendrickx, C., Baiano, M. A., Canale, J. I., Salgado, L. and Díaz Martínez, I. 2021a. Isolated theropod teeth associated with a sauropod skeleton from the Late Cretaceous Allen Formation of Río Negro, Patagonia, Argentina. *Acta Palaeontologica Polonica*, **66**, 409–423.

Meso, J. G., Valieri, R. J., Porfiri, J. D., Correa, S., Martinelli, A. G., Casal, G., Canudo, J., Poblete, F. and Dos Santos, D. 2021b. Testing the persistence of Carcharodontosauridae (Theropoda) in the Upper Cretaceous of Patagonia based on dental evidence. *Cretaceous Research*, **125**, 104875.

Meso, J. G., Gianechini, F., Gomez, K. L., Muci, L., Baiano, M. A., Pol, D., Kaluza, J., Garrido, A. and Pittman, M. 2024. Shed teeth from Portezuelo formation at Sierra del Portezuelo reveal a higher diversity of predator theropods during Turonian–Coniacian times in northern Patagonia. *BMC Ecology and Evolution*, **24**, 59.

Milner, A. C. 2003. Fish-eating theropods: a short review of the systematics, biology and palaeobiogeography. 129–138. *In Actas de las II Jornadas Internacionales sobre Paleontología de Dinosaurios y su Entorno*. Colectivo Arqueológico y Paleontológico de Salas.

Montealegre, A., Castillo-Visa, O. and Sellés, A. 2024. New theropod remains from the late Barremian (Early Cretaceous) of Eastern Iberian Peninsula. *Historical Biology*, 1–11. https://doi.org/10.1080/08912963.2024.2308220

Naish, D. 1999. Theropod dinosaur diversity and palaeobiology in the Wealden Group (Early Cretaceous) of England: evidence from a previously undescribed tibia. *Geologie en Mijnbouw*, **78**, 367–373.

Naish, D. 2003. A definitive allosauroid (Dinosauria; Theropoda) from the Lower Cretaceous of east Sussex. *Proceedings of the Geologists' Association*, **114**, 319–326.

Naish, D. 2011. Theropod dinosaurs. 526–559. *In* Batten, D. J. (ed.) *English Wealden fossils*. The Palaeontological Association, Field Guides to Fossils, 14, 769 pp.

Naish, D. and Cau, A. 2022. The osteology and affinities of *Eotyrannus lengi*, a tyrannosauroid theropod from the Wealden Supergroup of southern England. *PeerJ*, **10**, e12727.

Naish, D. and Martill, D. M. 2007. Dinosaurs of Great Britain and the role of the Geological Society of London in their discovery: basal Dinosauria and Saurischia. *Journal of the Geological Society*, **164**, 493–510.

Naish, D. and Martill, D. M. 2008. Dinosaurs of Great Britain and the role of the Geological Society of London in their discovery: Ornithischia. *Journal of the Geological Society*, **165**, 613–623.

Naish, D. and Sweetman, S. C. 2011. A tiny maniraptoran dinosaur in the Lower Cretaceous Hastings Group: evidence from a new vertebrate-bearing locality in south-east England. *Cretaceous Research*, **32**, 464–471.

Naish, D., Hutt, S. and Martill, D. M. 2001. Saurischian dinosaurs 2: Theropods. 242–309. *In* Martill, D. M. and Naish, D. (eds) *Dinosaurs of the Isle of Wight*. The Palaeontological Association, Field Guides to Fossils, 10, 440 pp.

Norman, D. B. 2011. Ornithopod dinosaurs. 407–475. *In* Batten, D. J. (ed.) *English Wealden fossils*. The Palaeontological Association, Field Guides to Fossils, 14, 769 pp.

Novas, F. E., Agnolín, F. L., Ezcurra, M. D., Porfiri, J. and Canale, J. I. 2013. Evolution of the carnivorous dinosaurs during the Cretaceous: the evidence from Patagonia. *Cretaceous Research*, **45**, 174–215.

Olshevsky, G. 1991. *A revision of the parainfraclass Archosauria Cope, 1869, excluding the advanced Crocodylia*. Published by the author. Mesozoic Meanderings, 2, 196 pp.

Osborn, H. F. 1906. Article 16. Tyrannosaurus, Upper Cretaceous carnivorous dinosaur. (Second communication.). *Bulletin of the American Museum of Natural History*, **22**, 281–297.

Ősi, A., Apesteguía, S. and Kowalewski, M. 2010. Non-avian theropod dinosaurs from the early Late Cretaceous of Central Europe. *Cretaceous Research*, **31**, 304–320.

Owen, R. 1840–1845. *Odontography; or, A treatise on the comparative anatomy of the teeth; their physiological relations, mode of development, and microscopic structure, in the vertebrate animals*. Hippolyte Baillière, London.

Owen, R. 1842. Report on British Fossil Reptiles Part II. *Reports of the Meetings of the British Association for the Advancement of Science*, **11**, 61–204.

Parent, H. 1893. Le Wealdien du Bas-Boulonnais. *Annales de la Société Géologique du Nord*, **21**, 50–91.

Patterson, C. 1966. British Wealden sharks. *Bulletin of the British Museum of Natural History (Geology)*, **11**, 283–350.

Pereda-Suberbiola, X., Ruiz-Omeñaca, J. I., Canudo, J. I., Torcida, F. and Sanz, J. L. 2012. Dinosaur faunas from the Early Cretaceous (Valanginian–Albian) of Spain. 379–407. *In* Godefroit, P. (ed.) *Bernissart dinosaurs and early Cretaceous terrestrial ecosystem*. Indiana University Press.

Pérez-Moreno, B. P., Sanz, J. L., Sudre, J. and Sigé, B. 1993. A theropod dinosaur from the Lower Cretaceous of southern France. *Revue de Paléobiologie*, **7**, 173–188.

Pol, D. and Escapa, I. H. 2009. Unstable taxa in cladistic analysis: identification and the assessment of relevant characters. *Cladistics*, **25**, 515–527.

Porfiri, J. D., Novas, F. E., Calvo, J. O., Agnolín, F. L., Ezcurra, M. D. and Cerda, I. A. 2014. Juvenile specimen of *Megaraptor*

(Dinosauria, Theropoda) sheds light about tyrannosauroid radiation. *Cretaceous Research*, **51**, 35–55.

Powers, M. J., Fabbri, M., Doschak, M. R., Bhullar, B.-A. S., Evans, D. C., Norell, M. A. and Currie, P. J. 2022. A new hypothesis of eudromaeosaurian evolution: CT scans assist in testing and constructing morphological characters. *Journal of Vertebrate Paleontology*, **41**, e2010087.

R Core Team. 2023. R: A language and environment for statistical computing. https://www.R-project.org

R Studio Team. 2023. R Studio: Integrated development for R. https://posit.co

Radley, J. D. and Allen, P. 2012a. The Wealden (non-marine Lower Cretaceous) of the Weald sub-basin, southern England. *Proceedings of the Geologists' Association*, **123**, 245–318.

Radley, J. D. and Allen, P. 2012b. The Wealden (non-marine Lower Cretaceous) of the Wessex Sub-basin, southern England. *Proceedings of the Geologists' Association*, **123**, 319–373.

Rauhut, O. W. 2003. The interrelationships and evolution of basal theropod dinosaurs. *Special Papers in Palaeontology*, **69**, 1–213.

Rauhut, O. W. and Werner, C. 1995. First record of the family Dromaeosauridae (Dinosauria: Theropoda) in the Cretaceous of Gondwana (Wadi Milk Formation, northern Sudan). *Paläontologische Zeitschrift*, **69**, 475–489.

Rauhut, O. W., Milner, A. C. and Moore-Fay, S. 2010. Cranial osteology and phylogenetic position of the theropod dinosaur *Proceratosaurus bradleyi* (Woodward, 1910) from the Middle Jurassic of England. *Zoological Journal of the Linnean Society*, **158**, 155–195.

Raven, T. J., Barrett, P. M., Pond, S. B. and Maidment, S. C. 2020. Osteology and Taxonomy of British Wealden Supergroup (Berriasian–Aptian) ankylosaurs (Ornithischia, Ankylosauria). *Journal of Vertebrate Paleontology*, **40**, e1826956.

Ribeiro, T. B., Brito, P. M. M. and Gomes Da Costa Pereira, P. V. L. 2024. The predominance of teeth in the non-avian dinosaur record from Cretaceous Brazil: a review. *Historical Biology*, **36**, 2019–2034.

Sales, M. A. F. and Schultz, C. L. 2017. Spinosaur taxonomy and evolution of craniodental features: evidence from Brazil. *PLoS One*, **12**, e0187070.

Sales, M. A., Liparini, A., De Andrade, M. B., Aragão, P. R. and Schultz, C. L. 2017. The oldest South American occurrence of Spinosauridae (Dinosauria, Theropoda). *Journal of South American Earth Sciences*, **74**, 83–88.

Schindelin, J., Arganda-Carreras, I., Frise, E., Kaynig, V., Longair, M., Pietzsch, T., Preibisch, S., Rueden, C., Saalfeld, S. and Schmid, B. 2012. Fiji: an open-source platform for biological-image analysis. *Nature Methods*, **9**, 676–682.

Sereno, P. C. 1999. The evolution of dinosaurs. *Science*, **284**, 2137–2147.

Smith, J. B. and Dodson, P. 2003. A proposal for a standard terminology of anatomical notation and orientation in fossil vertebrate dentitions. *Journal of Vertebrate Paleontology*, **23**, 1–12.

Smith, J. B., Vann, D. R. and Dodson, P. 2005. Dental morphology and variation in theropod dinosaurs: implications for the taxonomic identification of isolated teeth. *The Anatomical Record*, **285**, 699–736.

Soto, M., Toriño, P. and Perea, D. 2020. *Ceratosaurus* (Theropoda, Ceratosauria) teeth from the Tacuarembó Formation (Late Jurassic, Uruguay). *Journal of South American Earth Sciences*, **103**, 102781.

Stromer, E. 1915. Ergebnisse der Forschungsreisen Prof. E. Stromers in den Wüsten Ägyptens. II. Wirbeltierreste der Baharîje Stufe (unterstes Cenoman). 3. Das Original des Theropoden *Spinosaurus aegyptiacus* nov. gen., nov. spec. *Abhandlungen der Königlich Bayerischen Akademie der Wissenschaften, Mathematisch-Physikalische Klasse Abhandlung*, **28**, 1–32.

Sweetman, S. C. 2004. The first record of velociraptorine dinosaurs (Saurischia, Theropoda) from the Wealden (Early Cretaceous, Barremian) of southern England. *Cretaceous Research*, **25**, 353–364.

Sweetman, S. C. 2013. Albuliform fish remains (Teleostei, Elopomorpha) from the Lower Cretaceous (Valanginian) Wadhurst Clay Formation of the Wealden Supergroup of southeast England. *Journal of Vertebrate Paleontology*, **33**, 1239–1243.

Topley, W. 1875. *The Geology of the Weald (parts of the Counties of Kent, Surrey, Sussex, and Hants)*. HM Stationery Office, London.

Turmine-Juhel, P., Wilks, R., Brockhurst, D., Austen, P. A., Duffin, C. J. and Benton, M. J. 2019. Microvertebrates from the Wadhurst Clay Formation (Lower Cretaceous) of Ashdown Brickworks, East Sussex, UK. *Proceedings of the Geologists' Association*, **130**, 752–769.

Turner, A. H., Makovicky, P. J. and Norell, M. A. 2012. A review of dromaeosaurid systematics and paravian phylogeny. *Bulletin of the American Museum of Natural History*, **2012**, 1–206.

Upchurch, P., Mannion, P. D. and Barrett, P. M. 2011. Sauropod Dinosaurs. 476–525. *In* Batten, D. J. (ed.) *English Wealden fossils*. The Palaeontological Association, Field Guides to Fossils, 14, 769 pp.

von Heune, F. 1914. Beiträge zur gesichte der Archosaurier [Contribution to the history of the archosaurs]. *Geologie und Paläontologie Abhandlungen*, **13** (7), 1–56.

von Huene, F. 1923. Carnivorous Saurischia in Europe since the Triassic. *Bulletin of the Geological Society of America*, **34**, 449–458.

Weishampel, D. B., Barrett, P., Coria, R. A., Le Loeuff, J., Xing, X. U., Xijin, Z., Sahni, A., Gomani, E. M. P. and Noto, C. R. 2004. Dinosaur distribution. 517–606. *In* Weishampel, D. B., Dodson, P. and Osmólska, H. (eds) *The Dinosauria*. University of California Press.

Williamson, T. E. and Brusatte, S. L. 2014. Small theropod teeth from the Late Cretaceous of the San Juan Basin, northwestern New Mexico and their implications for understanding latest Cretaceous dinosaur evolution. *PLoS One*, **9**, e93190.

Wills, S., Underwood, C. J. and Barrett, P. M. 2021. Learning to see the wood for the trees: machine learning, decision trees, and the classification of isolated theropod teeth. *Palaeontology*, **64**, 75–99.

Wills, S., Underwood, C. J. and Barrett, P. M. 2023. Machine learning confirms new records of maniraptoran theropods in Middle Jurassic UK microvertebrate faunas. *Papers in Palaeontology*, **9**, e1487.

Young, C. M., Hendrickx, C., Challands, T. J., Foffa, D., Ross, D. A., Butler, I. B. and Brusatte, S. L. 2019. New theropod dinosaur teeth from the Middle Jurassic of the Isle of Skye, Scotland. *Scottish Journal of Geology*, **55**, 7–19.